ATHESIS

FOR THE DEGREE OF DOCTOR OF PHILOSOPHY

Printing of Fine Resolution Patterns through Electrohydrodynamic (EHD) Patterning Technology

Khalid Rahman

Department of Mechatronics Engineering

GRADUATESCHOOL

JEJUNATIONALUNIVERSITY

2012.08

Printing of Fine Resolution Patterns through Electrohydrodynamic (EHD) Pattering Technology

Khalid Rahman

(Supervised by Professor Kyung-HyunChoi

and

co-supervised by Professor Ki-Rin Kwon)

A thesis submitted in partial fulfillment of the requirement for the degree of Doctor of Philosophy

2012.08

The thesis has been examined and approved.

....

Thesis director, Chul-Ung Kang, Professor,Department of Mechatronics Engineering

....

Yang-HoiDoh, Professor, Department of Electronics Engineering

....

Jin-HoBae, Professor,Department of Ocean System Engineering

....

Kyung-Hyun Choi, Professor, Department of Mechatronics Engineering

....

Piljoong Kang, Ph.D., Samsung Electro-MechanicsCo., Ltd.

....
Date

Department of Mechatronics Engineering
GRADUATESCHOOL
JEJUNATIONALUNIVERSITY
REPUBLIC OF KOREA

To

My Parents and Family

Acknowledgements

Abbreviations and notations

RFID	Radio Frequency Identification Tag
DNA	Deoxyribonucleic acid
CVD	Chemical Vapor Deposition
PVD	Physical Vapor Deposition
E-beam	Electronic Beam Evaporation
EHD	Electrohydrodynamic Patterning
DOD	Drop-on-Demand
DC	Direct Current
AC	Alternating Current
Cu	Copper
Ag	Silver
TFT	Thin Film Transistors
XRD	X-ray Diffraction
SEM	Scanning Electron Microscopy
AFM	Atomic Force Microscopy
σ_h	Hydrostatic Pressure
σ_e	Electrostatic Pressure
σ_s	Surface Tension
d_j	Jet Diameter
ρ	Density of Liquid
μ	Viscosity of Liquid
K	Electric Conductivity of Liquid
γ	Surface Tension
Q	Flow-rate
E	Electric Field
d_n	Nozzle diameter
$\varepsilon\varepsilon_0$	Permittivity of Liquid
ρ_E	Electrical Resistivity of Pattern
R	Resistance of Pattern
A	Cross-sectional Area of Pattern

t	Average thickness of Pattern
L	Pattern Length
d	Droplet Diameter
d_s	Distance between two Consecutive Droplets
V_s	Substrate Speed
f_d	Droplet Generation Frequency
V_{on}	Onset Voltage
r_c	Outer Radius of Capillary
h	Distance between Nozzle and Ground
θ	Half Cone-jet Angle
τ_c	Charge Relaxation Time
R_M	Resistance between the Tip of Nozzle and the Meniscus Tip
A_L	Cross-section Area of Liquid Volume between Nozzle Tip and Meniscus
C	Capacitance between Nozzle and Ground Plate
S_M	Surface Area of Meniscus
$f_{Rayleigh}$	Natural Frequency of Pendant Droplet
τ_H	Hydrodynamic Relaxation Time
I-V	Current Voltage Analysis of Pattern

Contents

List of Figures

List of Tables

Summary

In electronic industry the manufacturing of conductive patterning is necessary and ineluctable. Traditionally, lithography is widely used for fabrication of conductive patterns. However, lithographic process requires complicated equipment, is time consuming and the area throughput is limited. In order to reduce the material usage, decrease process time and enable large area fabrication, different fabrication technique is needed. Nonlithographic-direct fabrication methodsuch as inkjetand roll-to-roll printing (also known as printed electronics) are predominant examples with reasonable resolution and high throughput compared to lithography techniques.

Conventional inkjet printing techniques including (thermal and piezoelectric print-heads) are being applied in various applications in the field of printed electronics with modest functional resolution with the feature size of 15~30μm (approximate spherical minimum diameter of 15μm). However, in order to reach this resolution the surface to be printed on needs modifications and also these technologies have limitation to produce droplets smaller than the nozzle size. Moreover, these conventional patterning techniques also have limitation on the type of materials to be deposited in terms of the viscosity of the ink. However, the droplet diameter after printing on the substrate is typically two times larger than the ejected droplet diameter on flat surfaces. Electrohydrodynamic patterning is realized by applying strong electric energy at the tip of the nozzle on the meniscusto generate necessary liquid flow jetting and patterning on the substrate.

In this work, electrohydrodynamic patterning methods both continuous and drop-on-demand mode areexperimentally investigated in order to generate patterns with fine resolution on various substrates. Moreover, experimental guidelines are discussed in order to achieve the fine resolution using electrohydrodynamic patterning. Patterns are made by using different inks containing Silver and Copper nanoparticles with different concentrations on different kinds of substrates. In order to check the functionality, the patterns are characterized physically as well as electrically. This study will help in paving road for electrohydrodynamic patterning technology for the formation of submicron patterns for printed electronics applications.

1. Introduction

In electronic industry the manufacturing of conductive patterning is necessary and ineluctable. Traditionally, lithography is widely used for fabrication of the conductive patterns. However, lithographic processes require the complicated equipment, are time consuming and the area throughput is limited. In order to reduce the material usage, process time and large area fabrication, different fabrication technique is required. Non-lithographicdirect fabrication method(Pique and Chrisey 2001) such as inkjet(Gamota et. al. 2004) and roll-to-roll(Gans et. al. 2004) printing (also known as printed electronics) are predominant examples for reasonable resolution and high throughput as compared to lithography techniques. This direct fabrication technology can be further classified into two different technologies depending on the fabrication method as contact (gravure, offset or flexographic etc) and non-contact (inkjet) method. Non-contact inkjet printing method has moved beyond graphic printing as a versatile manufacturing method for functional and structural materials.

Commercially available inkjet printer can be divided into two modes based on the ejection of the fluid: Continuous, where jet emerges from the nozzle which breaks in stream of droplets or Drop-on-Demand, the droplet ejects from the nozzle orifice as required (Le 2003). Inkjet printing offers the advantages of low cost, large area throughput and high speed processing. The most prominent examples of inkjet printing includes the direct patterning of printed circuit board, conductive tracks for antenna of radio frequency identification tags (RFID) (Yang et. al. 2007), Photovoltaic (Jung et. al. 2010), thin film transistors (Arias et. al. 2004), micro arrays of the DNA (Goldmann and Gonzalez 2000) , biosensors, etc. In case of continuous inkjet printing, the deflector directs the stream of droplets into a waste collector or onto substrate, for start and stop of the printing. This wastage of the ink issue has been addressed by the introduction drop-on-demand inkjet printing (thermal and piezoelectric). In drop-on-demand, thermal or vibration pulse are used to eject the liquid droplet from the nozzle to the substrate. However, the current printing technologies have constrained due to limitation of the ink viscosity, clogging of

small size nozzles, generation of pattern smaller than the nozzle size and limitation of material to be deposited (Le 1998). In order address these limitations, many researchers are focusing on electrohydrodynamic inkjet printing (continuous and drop-on-demand) (Park et. al. 2007). Electrohydrodynamic jet printing uses electric field energy to eject the liquid from the nozzle instead of thermal or acoustic energy (Hartman 1998). Based on the applied electric field energy, the electrohydrodynamic jetting can be used for continuous patterning, drop-on-demand printing and thin film deposition (electrospray). Electrohydrodynamic drop-on-demand, jetting or atomization has numerous applications in inkjet printing technology (Wang et. al. 2009), thin film deposition (Jaworek 2007), bio-application (Park et. al. 2008) and mass spectrometry (Griss et. al. 2002), etc.

1.1 Competing Patterning Technologies

The patterning technologies for the conductive patterns on the substrates can be categorized in conventional and unconventional method. The conventional approach such as photolithography, CVD, PVD, thermal evaporation, E-beam etc. as shown in figure 1.1, needs different steps to fabricate the patterns on different kinds of substrate and also needs masks. These conventional methods have advantage on the feature size as compare to unconventional patterning technologies but have limitation in terms of cost-efficient, high material wastage, types of substrate, time required to make the features and also large area throughput.

(a)

(b)   (c)
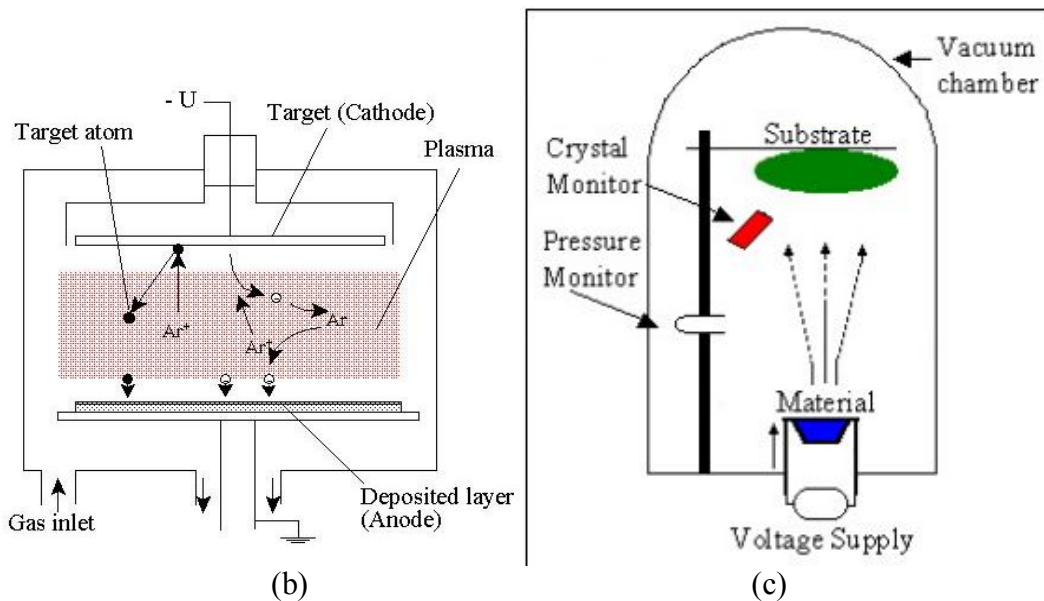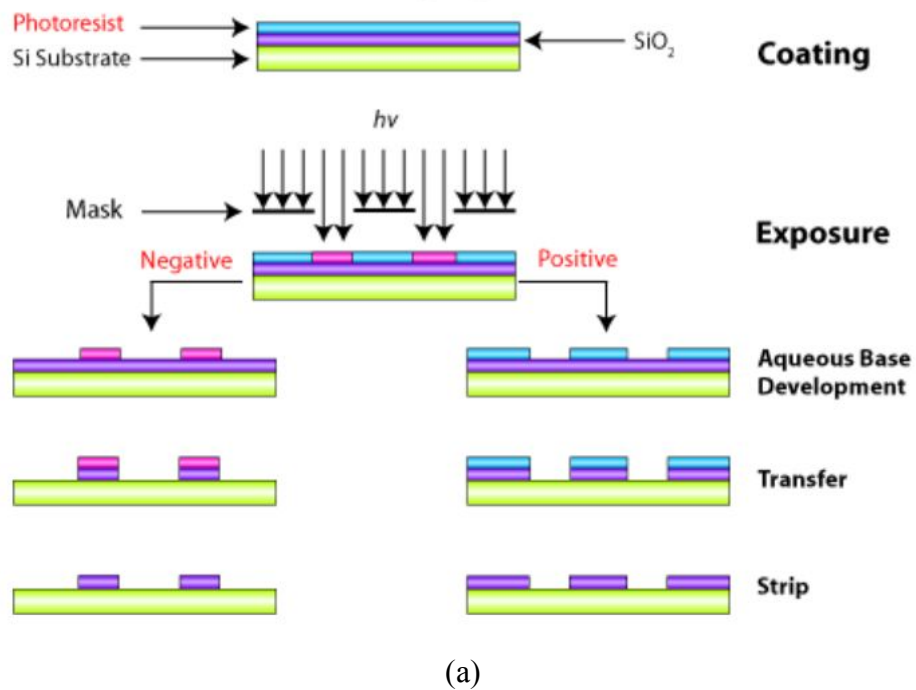
Figure 1.1Convention patterning technology (a) Photo-lithography, (b) Physical Vapor Deposition and (c) E-beam

The unconventional patterning technology, also known as printed electronics can be characterized into two types: contact and non-contact technology.

1.1.1 Contact Patterning Technologies

In contact patterning technologies (Gans et. al. 2004)the patterns are transferred on the different substrates by transferring the ink from the roller or mesh. These printing technologies are good for the mass production but have limitation with respect to patterning of the complex structures due to fixed pre-pattern structure of the rollers or mesh. The common types of contact printing are gravure, offset, flexographic, screen printing and micro-contact (soft lithography) printing as shown in figure 1.2.

| (a) | (b) |
| (c) | (d) |

(e)
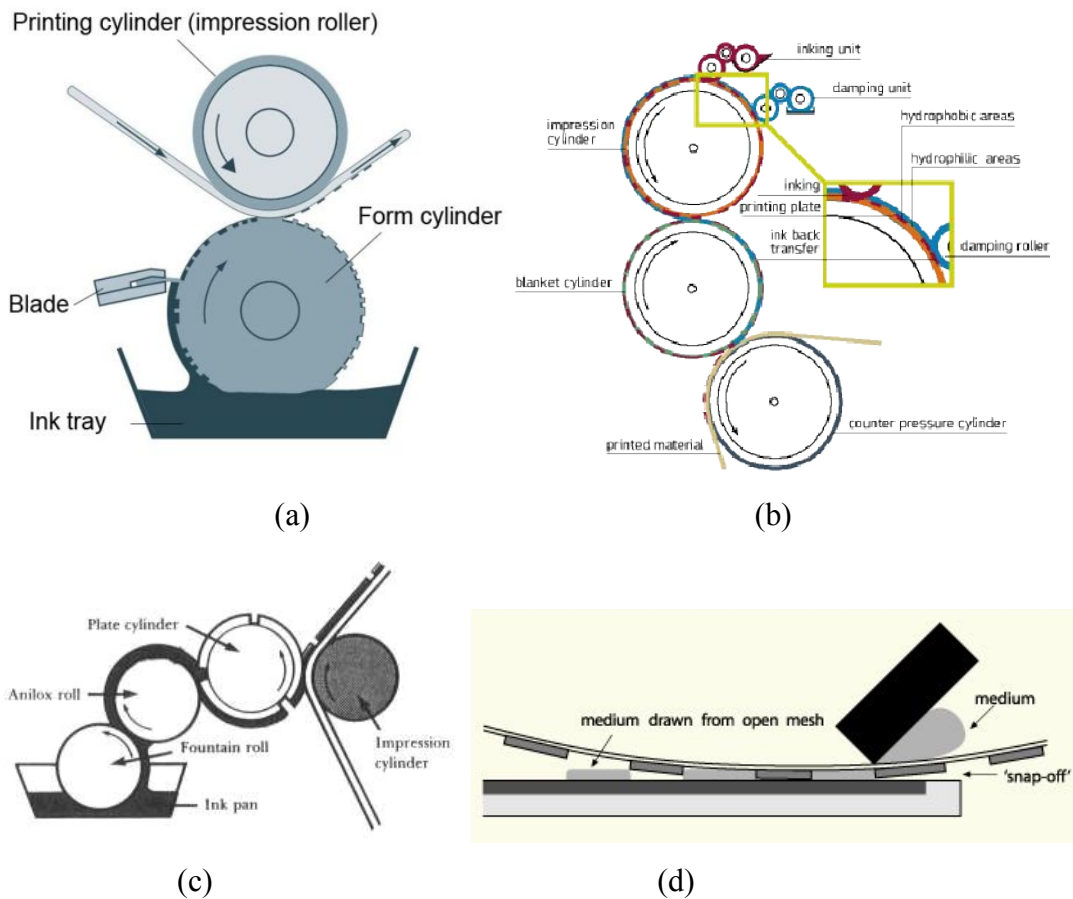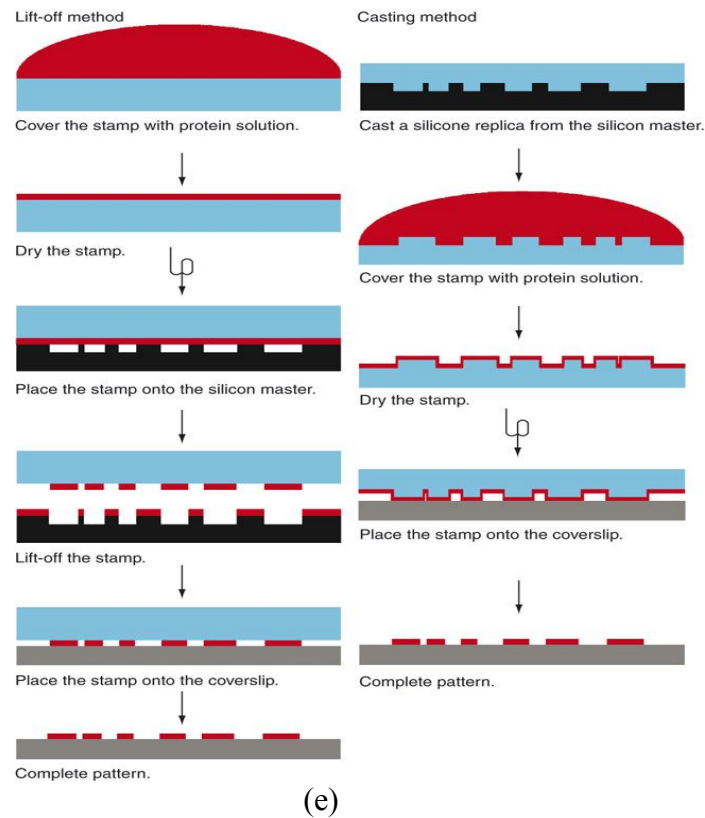
Figure 1.2Types of contact patterning technology (a) Gravure, (b) Offset,
(c) Flexographic, (d) Screen-printing and (e) Micro-contact

1.1.2 Non-contact Patterning Technologies

Non-contact pattering technologies (Le 2003) also known as inkjet (mask-less printing techniques) deposit the function materials directly on the substrate through droplets or confined jet of liquid. These technologies have more flexibility of making complex patterns on different substrates directly without involving the complex steps.

Commercially available inkjet printing consists of two major technologies based on the phenomena related to ejection of the droplets: continuous and drop-on-demand modeas shown in figure 1.3.
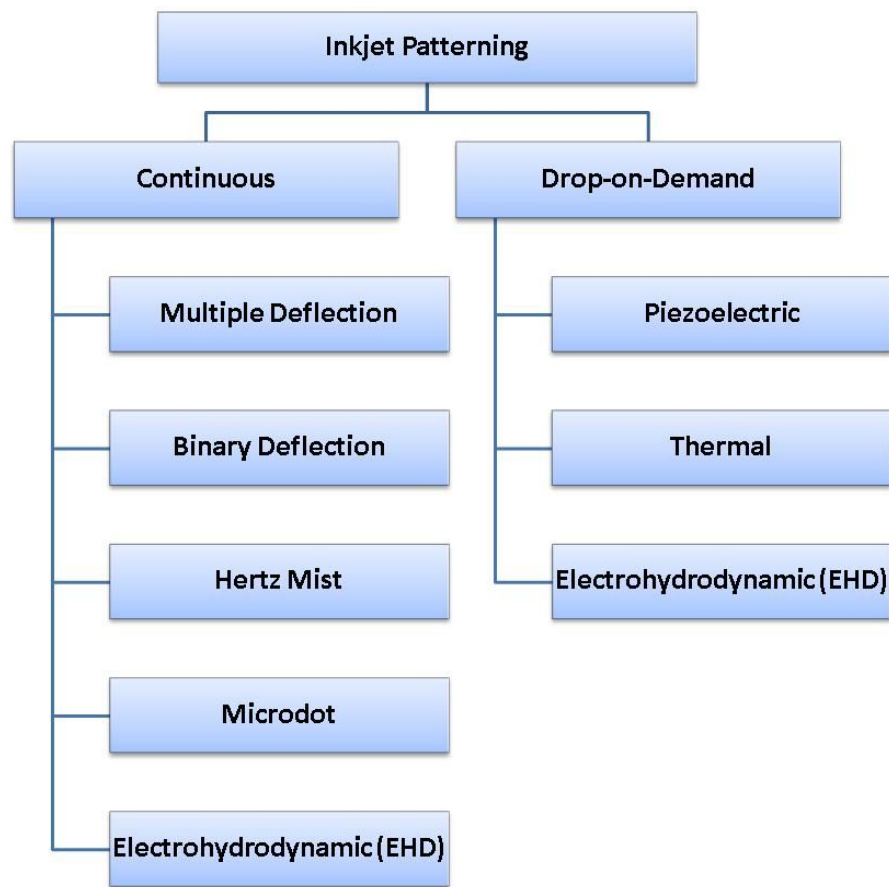
Figure 1.3Classification of inkjet printing technologies

Continuous inkjet technology permits very high-rate drop generation, one milliondrops per second or faster, but is expensive to manufacture and to operate. Twoclasses of continuous inkjet printers are available today. High-speed industrial printersare used for applications such as carton and product marking and addressingand personalizing direct mail. Proofing printers on the other hand offer the bestprint quality among non-photographic devices, but they are much slower. Althoughthe resolutions are not that high, the variable-sized dots make photographicquality possible.
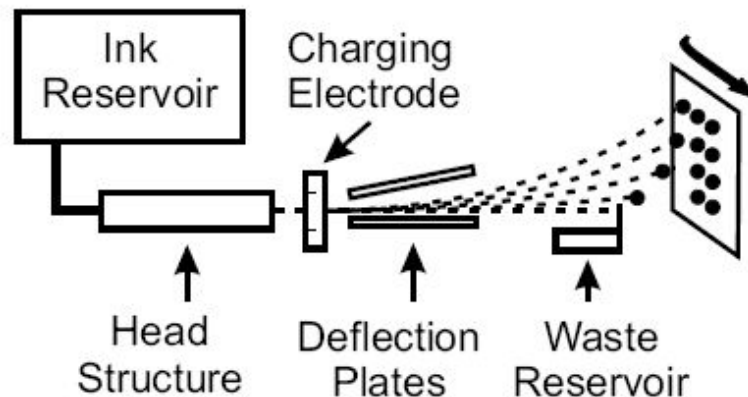
Figure 1.4Functional Principle of a Continuous Inkjet system

A simplified sketch of a typical continuous jet printing system is shown infigure 1.4. Ink under pressure is delivered from an ink reservoir via an input lineto a head structure. The head structure, containing a piezoelectric driver plate,is periodically constricted at its mechanical resonance frequency by means of anapplied electric field. By this method, an ink stream discharged from it breaks upinto a plurality of individual drops. A charging electrode applies charge to eachof the drops. The magnitude of the charge placed on individual drops is variableand determines the drop's ultimate paths. After the drops have exited the chargingelectrode, they pass between a pair of deflection plates, to which a fixed potentialis applied. Drops that are utilized for printing are deflected to a media to formcharacters while excess drops are directed to a gutter, which in turn directs thedrops to a waste reservoir

Thermal inkjet, sometimes referred to as bubble jet, is a drop-on-demand technology that uses electrical pulses applied to heating elements in contact with the fluid near the ejection aperture nozzle in order to vaporize a small amount of liquid to produce pressure impulses by the formation and collapse of gas bubbles, schematic of thermal inkjet system is shown in figure 1.5. The conversion of the electrical drive pulses to localized heating of the fluid is mediated by thin film resistors in intimate contact with the fluid. No direct electrical contact with the fluid itself is needed. This pressure pulse is used to eject a jet of fluid from a small orifice that, under correct drive level, will form into a single drop. This technique has the advantage of ease of integration into a dense print array inkjet print head, since the drive mechanism is

simply a resistor placed in contact with the fluid to be ejected. The two forms in common use areclassified by their fabrication technology as roof shooters and edge shooters. Roofshooters are fabricated by bonding an ejection orifice plate structure over the topof a wafer on which the fluid flow and heating elements are fabricated. Edgeshooters, in contrast, form their ejection apertures from channels etched longitudinallyinto the wafer.
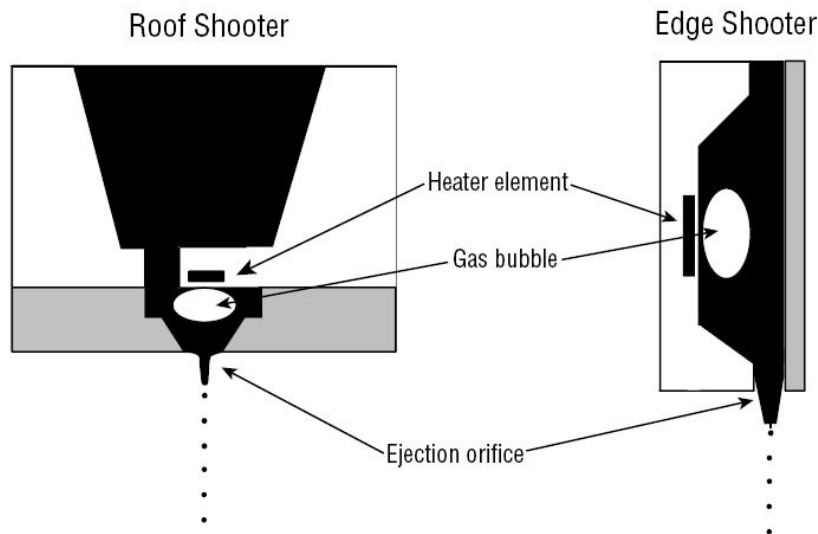
Figure 1.5Schematic of Roof Shooter and Edge Shooter Thermal Inkjet Printer

Piezoelectric inkjet printers harness the inverse piezoelectric effect (as shown in figure 1.6), which causescertain crystalline materials to change shape when a voltage is applied across them.A small electrical pulse makes the crystal contract slightly, squeezing ink out of thenozzle onto the media.Depending on the piezoelectric ceramics' deformation mode, the technology canbe classified into four main types: squeeze, bend, push, and shear. For squeezemode, radially polarized ceramic tubes are used. In both, bend- and push-modedesign, the electric field is generated between the electrodes parallel to the polarizationof the piezo-material. In a shear mode print-head, the electric field is designedto be perpendicular to the polarization of the piezo-ceramics.

(a)   (b)

(c)   (d)
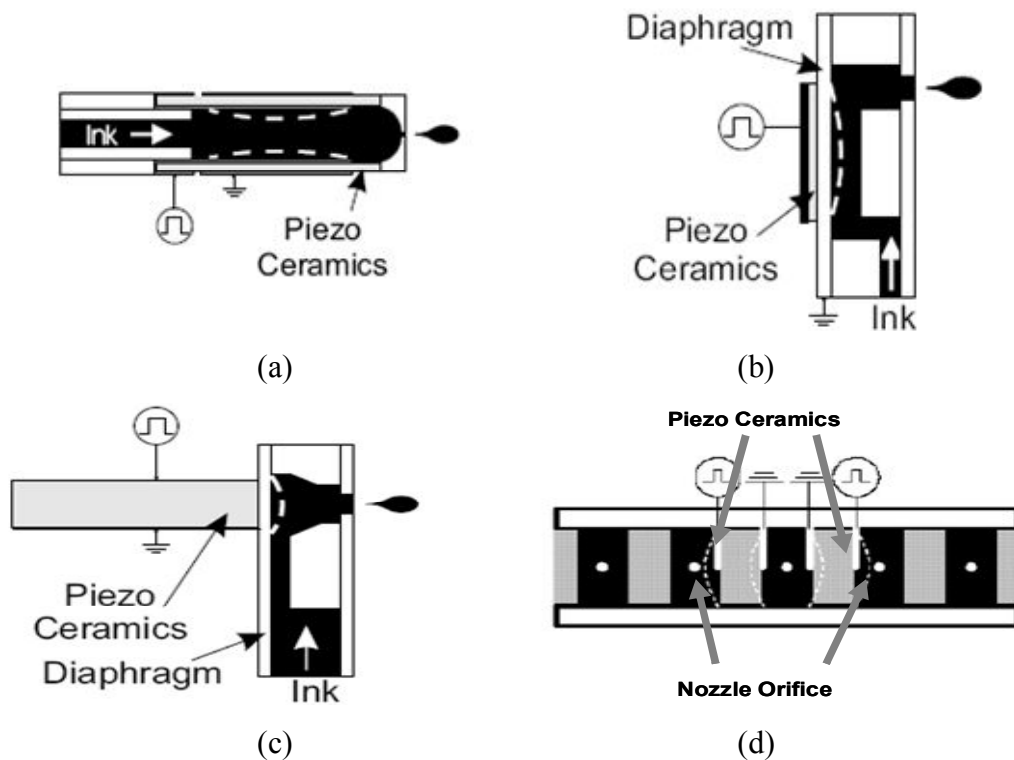
Figure 1.6Schematic of piezoelectric inkjet printer (a) Squeeze mode, (b) Bend mode, (c) Push mode and (d) Share mode

But these types of conventional DOD systems (thermal and piezoelectric) have limitations, such as thermal problems, nozzle size limitation, clogging and generation of the droplets smaller than the nozzle size etc.Droplet generation from thermal and piezoelectric inkjet requires sufficiently high kinetic energies and velocity (normally 1~20 m/sec) to overcome the interfacial energies that exist in and around the nozzle(Menard et. al. 2007). When the droplet strikes on non-absorbing substrate, it spreads outward due to its high kinetic energy and then recoils back due to its surface tension at the contact line between liquid layer and substrate, to reach final equilibrium state. Ejected droplets after impacting on substrate are in form of single droplet with well-defined diameter. Typical ejected droplet from thermal and piezoelectric inkjet system is having volume of 2-10 picoliters (spherical minimum diameter of approximately 15µm). However, the droplet diameter after printing on the substrate is typically two times larger than the ejected droplet diameter on flat surfaces.

1.3 Electrohydrodynamic Jet Patterning

Electrohydrodynamic patterning is performed by applying the strong electric energy at the tip of the nozzle on the meniscus, rather than thermal or acoustic energy, to generate the liquid flow for necessary jetting and patterning on the substrate. When the ink is supplied to the nozzle, a hemispherical meniscus pendent is formed at the tip of the nozzle in absence of electric field. With the application of the electric field between the nozzle filled with the ink and substrate (placed on top of ground electrode), mobile ions with same polarities accumulate at the surface of the liquid meniscus. Maxwell electrical stress is induced due to Coulombic repulsion forces between the ions causing the hemispherical meniscus to deform into liquid cone by overcoming the surface tension forces. This formation of the cone can be determined by the balance between the applied electrostatic forces and surface tension, and is known as Taylor cone or cone-jet. When the electrostatic forces exceed the certain limit of surface tension, single jet with very thin diameter can be ejected from the apex of the cone and then printed on the substrate. This mode of jetting can be used for patterning of a wide range of materials on various substrates. The diameter of the jets and droplets can be tuned by adjusting the process parameters (applied voltage, applied flow-rate and nozzle diameter) and also properties of the ink (conductivity, surface tension, viscosity and density). Depending on the application of the electrical forces (applied voltage) electrohydrodynamic patterning can be performed in continuous as well as drop-on-demand mode as shown in figure 1.7.
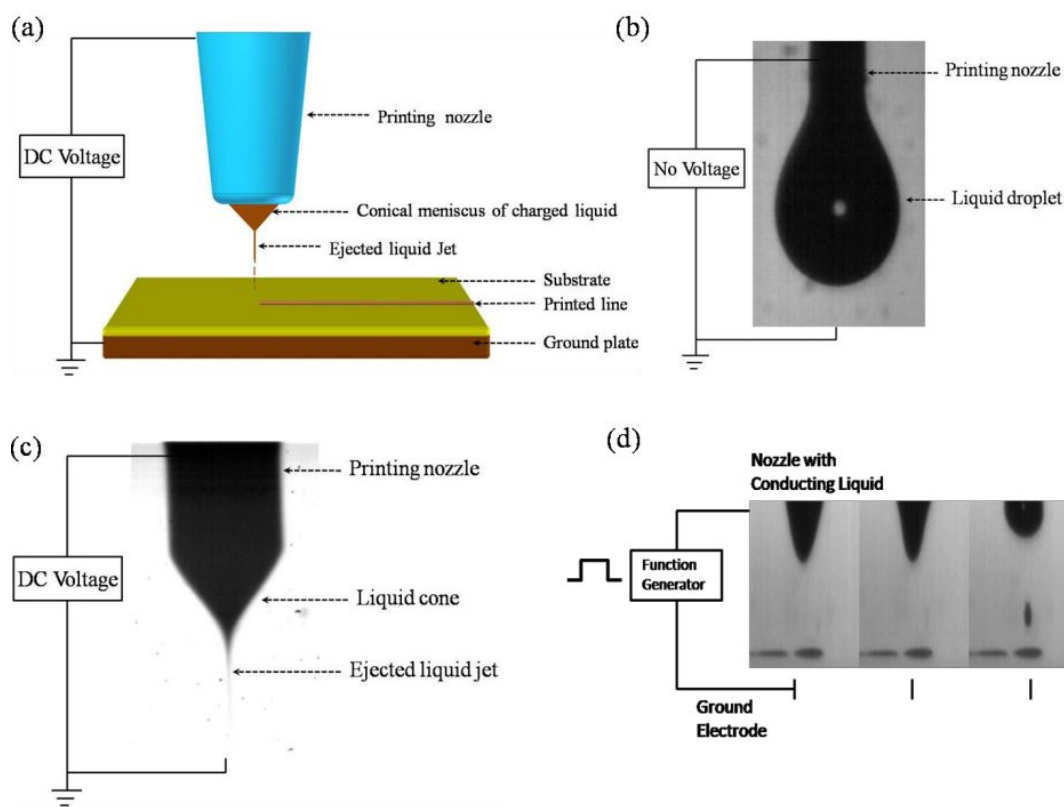
Figure 1.7 Methodology of EHD inkjet printing process (a) Schematic illustration of EHD inkjet printing technique, (b) When no electric potential is applied i.e. liquid is driven by pressure forces only, (c) Continuous cone-jet mode with applied DC voltage and (d) Drop-on-demand mode with pulsed voltage

1.4 Research Goal

Although conventional patterning techniques (thermal and piezoelectric) are being applied at various applications in the field of printed electronics with modest functional resolution with the feature size of 15~30μm. However, in order to reach this resolution, modification of the surface to be printed is needed and also these technologies have limitation to produce the droplets size smaller than the nozzle size. Moreover, these conventional patterning techniques also have limitation on the type of materials to be deposited in terms of the viscosity of the ink.

In order to achieve fine resolution patterns less than 15μm, electrohydrodynamic jet patterning technology has to be explored. In case of electrohydrodynamic patterning method, small size nozzle can be used, because electric field can overcome the

11

capillary pressure by pulling the liquid from the nozzle orifice rather than pushing from the nozzle opening as in case of the thermal and piezoelectric inkjet system. Also, electrohydrodynamic can generate extremely thin jets of diameter smaller than the nozzle diameter.

In this work, electrohydrodynamic patterning methods both continuous and drop-on-demand mode is experimentally investigated in order to generate the fine resolution patterns on various substrate. Moreover, experimental guidelines have been discussed in order to achieve the fine resolution patterns using electrohydrodynamic patterning. Patterns are made by using different inks containing Silver and Copper nanoparticles with different concentrations on different kinds of substrates. In order to check the functionality, the patterns were characterized physically as well as electrically. This study will help in paving the electrohydrodynamic patterning technology for the formation of submicron patterns for printed electronics applications.

This thesis consists of five chapters. Chapter 1 will give brief introduction to the different patterning technologies as well as the electrohydrodynamic pattering techniques.

Chapter 2 deals with the experimental study of electrohydrodynamic patterning in continuous cone-jet mode. Different modes of electrohydrodynamic jetting are also discussed in this chapter along with the effect of different operating parameters on the formation of the cone-jet. In the end of this chapter, results related to electrohydrodynamic patterning in continuous mode are discussed.

Chapter 3 explains the fundamental experimental study of the electrohydrodynamic patterning in drop-on-demand mode with the help of different operating parameters such as applied voltage, frequency and flow-rate. Effects on the patterns size with respect to operating parameters are also explained in this chapter.

In chapter 4, fine resolution patterning in continuous and drop-on-demand mode has been studied with the help of different inks and by using 60μm and less internal diameter glass capillary nozzles. The effects of the different operating parameters on the pattern size are explained in detail through experimental results.

Chapter 5 explains the detail phenomena of electrohydrodynamic jetting and also the effect of ink properties and operating parameters.

Finally, in chapter 6 the conclusionsof the thesis is given and future work is envisaged.

2. Continuous EHD Patterning

In electrohydrodynamic printing the liquid is pulled out of the nozzle rather than pushing out as in the case of conventional inkjet systems. When the liquid is supplied to nozzle without applying the electric field, a hemispherical meniscus is formed at the nozzle due to the surface tension at the interface between the liquid and air. When the electric field is applied between the liquid and the ground plate (located under the substrate), the ions with same polarity move and accumulate at surface of the meniscus. Due to ions accumulation, the Maxwell electrical stresses are induced by the Coulombic repulsion between ions. The surface of the liquid meniscus is mainly subjected to surface tension σ_s, hydrostatic pressure σ_h and electrostatic pressure σ_e. If the liquid is considered to be a pure conductor, then the electric field will be perpendicular to the liquid surface and no tangential stress component will be acting on the liquid surface. The liquid bulk will be neutral and the free charges will be confined in a very thin layer. This situation can be summarized in the following equations.

$$\sigma_h + \sigma_e + \sigma_s = 0 \tag{2.1}$$

Since the liquid is not a perfect conductor, the resultant electric stress on the liquid meniscus has two components, i.e. normal and tangential as shown in figure 2.1. This repulsion force (electrostatic force) when exceeds the certain limit deforms the hemispherical meniscus to a cone. This phenomenon is known as the cone-jet transition, which refers to the shape of meniscus (Poon 2002). There are different modes of electrohydrodynamic dripping or jetting phenomena depending upon the magnitude of the potential difference (electric field) across the electrodes. In electrohydrodynamic jetting, when liquid is pumped into the capillary in the absence of electric field, the liquid droplets are generated with the greater size as compared to that of the nozzle size. With the application of the DC voltage, the size of the droplet decreases, the dripping frequency increase which is known as micro-dripping, by further increasing the DC voltage, the meniscus deforms into a conical apex and very small jet is generated at the apex of the cone. This jet from the conical apex of the meniscus is also known as cone-jet; the diameter of the jet is very small as compared

to the nozzle diameter. Further increasing the voltage makes the cone-jet unstable and multiple jets are formed (Cloupeau and Foch 1994, Smith 1986, Jaworek 1999). Transition between micro-dripping to cone-jet formation depends on the liquid properties (density ρ, surface tension γ, viscosity μ, electrical conductivity and relative permittivity $\epsilon\epsilon_o$) as well as operating parameters (applied electric field E, flow-rate Q and nozzle diameter d_n) (Poon 2002, Hartmann 1998). In cone-jet mode the functional relationship for the jet diameter can be expressed as:

$$d_j = f(\rho, \mu, K, \gamma, \epsilon\epsilon_0, Q, E, d_n) \qquad (2.2)$$

For low viscosity liquid the jet diameter in cone-jet mode can be related as (Ganan and Barrero 1996):

$$d_j \sim 0.6 Q^{\frac{1}{2}} \left(\frac{\rho\epsilon_0}{\gamma K} \right)^{\frac{1}{6}} \qquad (2.3)$$

The above relationship shows that the jet diameter directly depends on the flow-rate and not on the applied voltage. In electrohydrodynamic printing the main parameter to control the pattern width is applied flow-rate for any given liquid and experimental setup. Electrohydrodynamic dripping, jetting or atomization has numerous applications in inkjet printing technology (Park et. al. 2007 and Poon et. al. 2008), thin film deposition (Jaworek et. al. 2009 and Muhammad et. al. 2011), bio-applications (Li et. al. 2009 and Raghunath et. al. 2009), mass spectrometry (Law et. al. 2010) and micro-thrusters (Krpoun and Shea 2009).

15
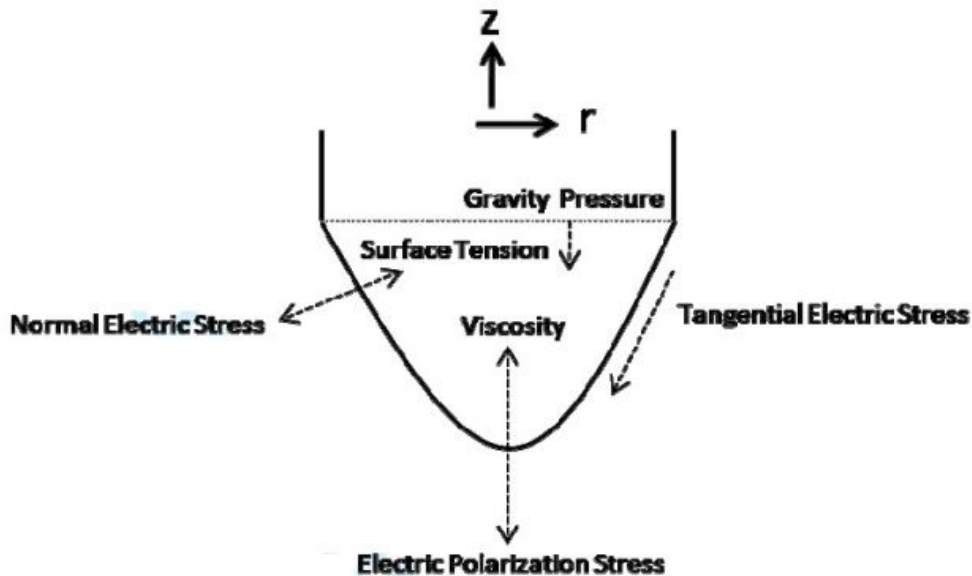
Figure 2.1 Stresses due to different forces on the liquid meniscus

For specific configuration and constant flow rate, there are different modes of electrohydrodynamic jetting as a function of applied voltage (Cloupeau and Foch 1994). It should be noted that not for all liquids each mode can occur, because of the properties of the liquid. The different modes of the electrohydrodynamic jetting are discussed as follows:

2.1 DrippingMode

In dripping mode, when the liquid is pumped in to the nozzle or capillary without applying the electric field, the droplets disintegrate from the orifice, the size of the droplets are larger than the size of the nozzle orifice. As the electric field is increased, the frequency of the droplet generation is also increased and size of the droplet decreases. At relative low flow rate, the droplet disintegrate in much smaller size as compare to the inner diameter of nozzle, this mode is known as micro-dripping mode, the frequency of the droplet increases with increase in applied electric field and size decreases. Depending on the liquid properties, increasing further electric potential, the spindle mode is observed. In spindle mode, the jet extends from the meniscus and breaks up into larger droplet and satellites droplets are also observed. Further increasing the applied voltage, with relative high flow-rate intermittent cone-jet mode occurs, causing the pulsating cone-jet modes due to the high space charges reduce the electric field on the liquid jet and causing relaxation of the cone-jet into hemispherical meniscus. The pulsation in the intermittent cone-jet mode increases with increase in the applied voltage.

2.2 Cone-jet Mode

Further increase in voltage, deforms the meniscus into cone and thin stable jet emerges from the apex of the jet. This mode is known as cone-jet mode. In cone-jet mode, an intact jet is used to fabricate the patterns on the surface of the substrates. The main advantage of cone-jet as compared to conventional method of ejection of the liquid is its large ratio between diameter of the nozzle and the jet. The typical jet

16

diameters are about two orders of magnitude smaller than that of nozzle; this enables patterning at very fine resolution. However, the cone-jet also has a shortcoming, it is very difficult to stabilize and control the trajectory of thin jet under an electric-field, and jet disintegrate into droplets and cause spray due to electrostatic repulsive forces between themselves.

2.3. Multi-jet Mode

If the applied voltage is further increased, the cone becomes smaller and smaller. With increasing the applied voltage, second jet emerges from the cone. With further increase in applied voltage, more and more jet emerges from the cone, this mode is called multi-jet mode.
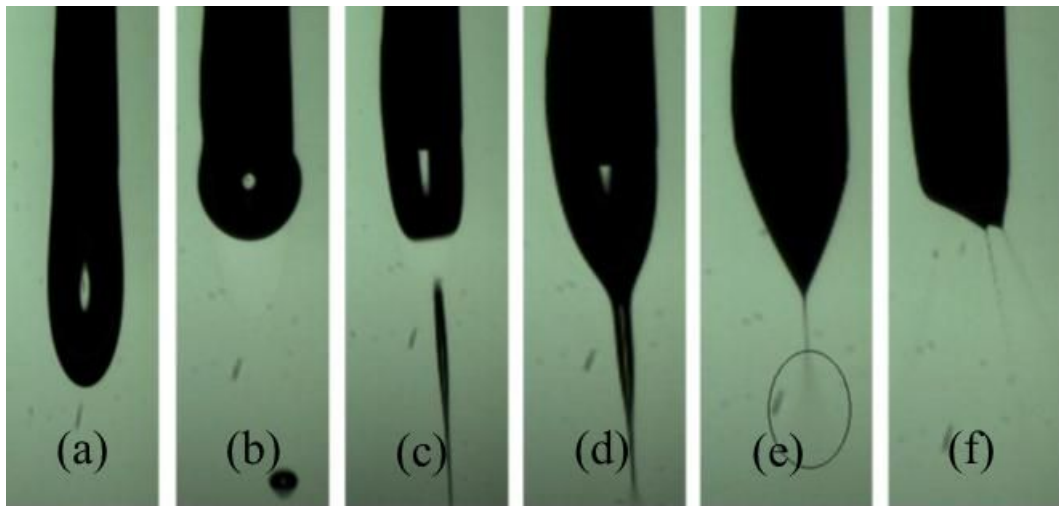
Figure 2.2 Modes of electrohydrodynamic jetting captured through high speed camera (a) dripping, (b) micro-dripping, (c) spindle mode, (d) pulsating cone jet, (e) stable cone jet, and (f) multi-jet mode

2.4 Parameters Affecting the Cone-jet

The parameters that influence the formation and transition of stable cone-jet mode can be divided in two groups. Operating parameters i.e. flow-rate, electric field and nozzle diameter, and liquid properties i.e. electric conductivity, viscosity and surface tension (Poon 2002).

17

2.4.1 Flow-rate

The flow-rate has a significant effect on the jet diameter and stability of the jet in cone-jet transition. It is the main parameters to control the jet diameter for the patterning process. The flow-rate also affects the applied potential requirement for development of cone-jet (operating envelop) and the resulting the shape of the cone-jet. In electrohydrodynamic jetting, flow-rate also affect the stability of the jet, at low flow-rate the jet is stable, whereas the high flow-rate in cone-jet region destabilize the jet resulting in shorter jet length. This is due to the amount of charge carrying at high flow-rate which destabilizes the jet. The typical effects of the flow-rate on stable cone-jet mode are shown in figure 2.3.

Flow-rate 75 ul/hr   Flow-rate 300 ul/hr   Flow-rate 500 ul/hr   Flow-rate 800 ul/hr
3.5 kV   3.4 kV   3.6 kV   3.7 kV
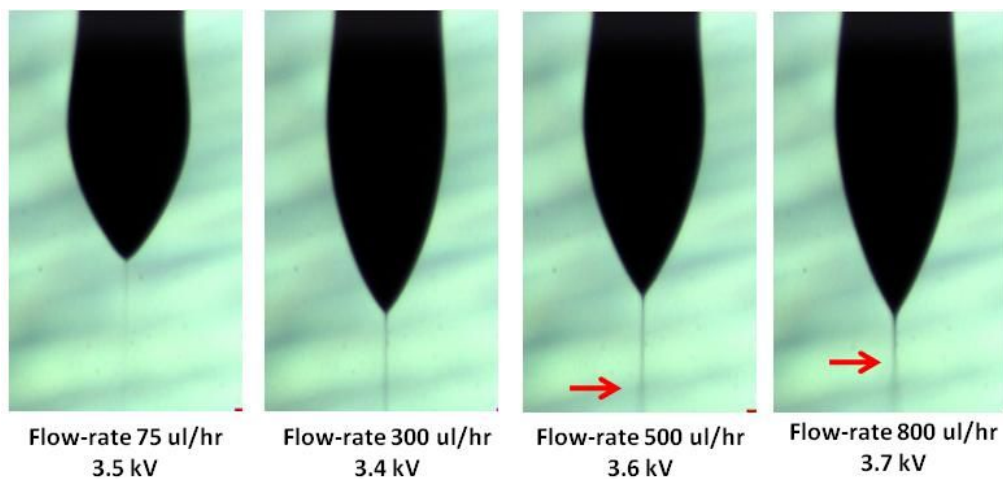
Figure 2.3Effect of flow rate on the cone-jet transition, as shown the jet diameter increases with increase in flow-rate. The red arrow indicates the jet break-up point.

2.4.2 Electric Field (Applied voltage)

Electric field affects the morphology of the cone, by increasing the electric field strength in steady cone-jet mode, the cone-jet recedes towards the nozzle. However, there is less effect on the jet diameter by increasing the applied voltage. At relatively low flow-rate and high electric field, the jet disintegrates into mist of small droplets and also known as electrospray atomization, this behavior is used for the thin film deposition of functional material. The typical shape of the cone at different applied voltage is shown in figure 2.4.
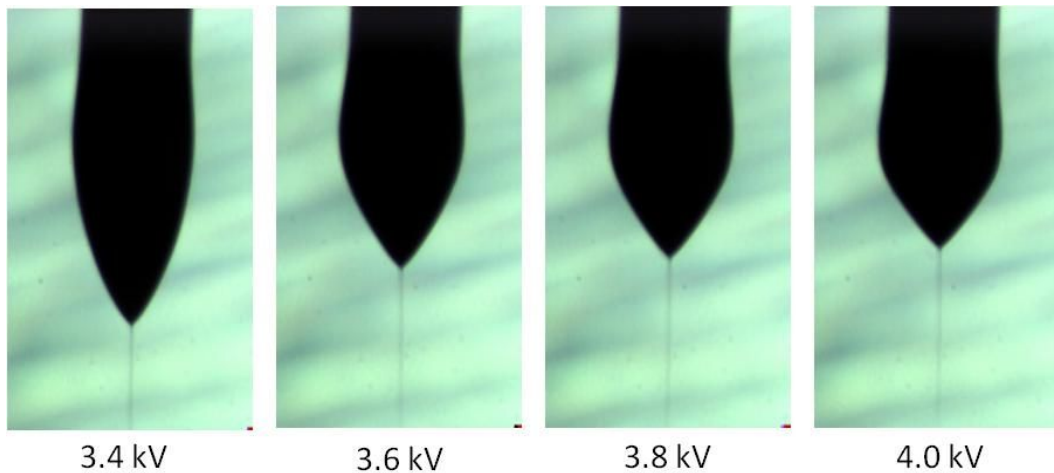
Figure 2.4Effect of the applied voltage on shape of the cone-jet at constant flow rate (200µl/hr)

2.4.3 Nozzle Diameter

Nozzle diameter has significant influence on the operating envelope of the stable cone-jet region. Smaller nozzle diameters extend the lower and higher value of flow-rate limit. The voltage requirement for the cone-jet also decreases with decrease in nozzle diameter for any given liquid.

2.4.4 Conductivity

The liquid conductivity affects both the shape of the liquid cone and stability of the jet, due to the amount of electric charge on the liquid surface and the jet produced is also very unstable because of high radial electric field. Highly conductive liquid deforms into sharp cone-jet shape. Liquid with very low conductivity do not deform into cone-jet by applying electric field, only dripping mode is observed. Liquids with intermediate conductivity range produce steady cone-jet.

2.4.5 Viscosity

The role of viscosity is in the stabilization of the jet and diameter of the jet produced. In high viscous liquid, the jet is stable for larger portion of the length but also produces the thicker diameter. This is due to charge mobility, which is reduced significantly in high viscosity liquid, and causes decrease in conductivity.

2.4.6 Surface Tension

The formation of the jet occurs when the electrical forces overcomes the surface tension on the apex of the meniscus. The required applied voltage will be increased with increase in surface tension of the liquid.

2.5 Operating Envelop

In order to perform the patterning of any liquid containing nanoparticles, the operating parameters of flow rate corresponding to applied voltage for stable cone-jet has to be determined. Starting with high flow rate formation of stable cone-jet is determined by applying different voltages. Then for each flow-rate, the range of applied voltage is investigated at which the stable cone-jet is observed. This creates an operating envelop of certain liquid in electric field and voltage domain. Based on the operating envelop, behavior of the jetting is observed and parameters for patterning are determined. Operating envelop along with different modes of electrohydrodynamic jetting of the liquid containing Ag nanoparticles is shown in figure 2.5.
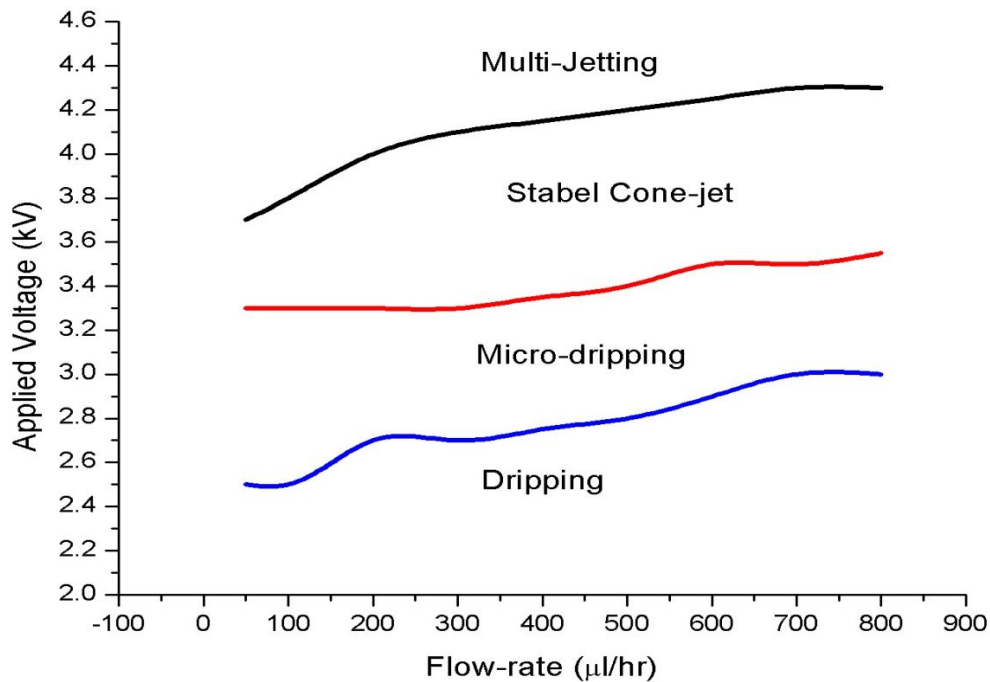
Figure 2.5 Operating envelop (stable con-jet region) along with different electrohydrodynamic jetting mode of ink containing copper nanoparticles, using metallic capillary of inner diameter 410μm, external diameter 720μm and capillary to ground distance is 2mm

2.6. EHDPatterning of Functional Materials

For the patterning of the functional materials, inks containing Cu and Ag nanoparticles were used for the patterning purpose.

2.6.1 Experimental Setup

For direct patterning through electrohydrodynamic printing, lab developed system was used. The equipment used for patterning is consistent of high voltage power supply, function generator, 5 channel voltage distributor, syringe-pump for ink supply, X-Y stage with motor controller, substrate holder, high-speed camera and nozzle holder with Z-axis controller, which are connected to National Instruments PXI-1042Q hardware system. This is controlled through lab made software based on LabView. Positive potential is applied to the nozzle head while ground is applied to the conductive plate. The substrate is place on the top of metallic ground plate. The schematic of experiment setup along with the actual system is shown in Figure 2.6.

제주대학교 중앙도서관
JEJU NATIONAL UNIVERSITY LIBRARY
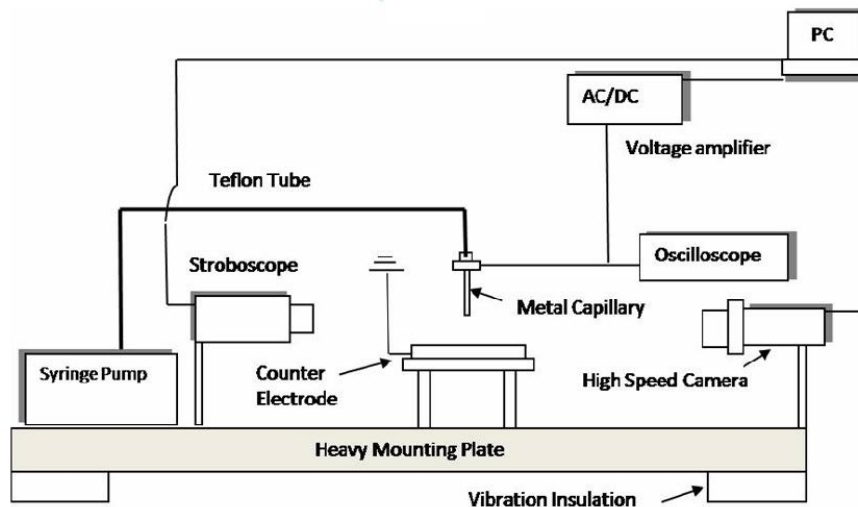
(a)
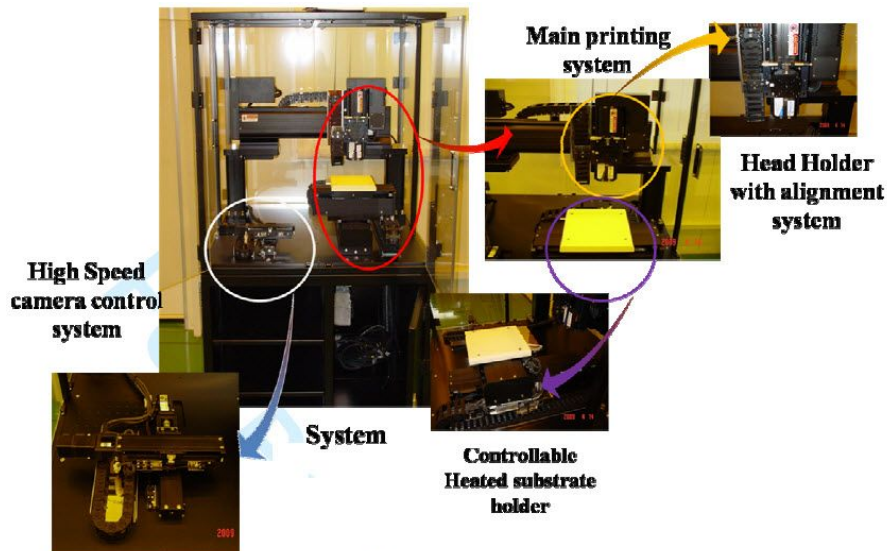
(b)

Figure 2.6(a) Schematic of lab developed system and (b) Photograph of the electrohydrodynamic inkjet system used for patterning

2.6.2 Patterning of Cu nanoparticles

For direct patterning of the Copper nanoparticles through electrohydrodynamic printing, lab developed system was used. Figure 2.6 represents the schematic diagram of the experiment system. The equipment used in deposition system consist of tapered glass capillary with electrode inserted in it, high voltage power supply, syringe pump for ink supply, X-Y stage motor control, substrate holder, high speed camera and nozzle holder with Z-axis control. The glass capillary tube of 1.5 mm

22

outer diameter and 750µm inner diameter was pulled and tapered-nozzle was formed, with sharp tip of 100µm inner diameter and 160µm outer diameter by using a micropipette puller (P-97, Sutter Instrument). The 0.65mm thick copper wire was inserted to provide an electric potential to ink in nozzle head while ground terminal was attached to the conductive plate kept at a distance of 1mm below the nozzle tip. The patterning was performed on 500µm glass substrate which was placed on the top of the ground plate. The ink containing 40 weight% copper nanoparticles with values of surface tension 36.9mN/m, viscosity 7.6cps, conductivity of $7.5e^{-3}$S/m and relative permittivity of 48.5 was used for experiments. The ink was obtained from Korea Research Institute of Chemical Technology (KRICT).

For electrohydrodynamic printing, stable and continuous cone-jet is required for patterning on the substrate. For stable cone-jet, the operating envelop (electric field and flow-rate domain) has to be investigated for any given liquid. However the lower and upper voltage limits of the stable cone-jet region vary with flow-rate and also depend on the ink properties such as conductivity and surface tension. A number of experiments were performed to find the lower and upper limit of flow-rate and voltage to establish the operating envelop of the copper nanoparticles ink. In stable cone-jet region (operating envelop) the stable cone-jet is the result of a balance between the forces i.e. surface tension, electrical stresses on the liquid interface, inertia (flow-rate), electrical stresses and viscous stresses. As the value of the flow-rate goes below the stable cone-jet region, the velocity of the liquid becomes insufficient to balance the forces required to generate stable cone-jet and causes disturbance in the process from stable cone-jet to normal droplet shape. As the flow-rate of the liquid increases, more electrical force is required to balance the effect to generate the stable-cone-jet. Below the lower limit, the pulsating phenomena is observed, which can be classified into dripping, micro-dripping and pulsating cone-jet mode depending on flow-rate and applied voltage. Above the upper limit of operating envelop the cone-jet deforms into number of small cones known as multi-jet mode. The jetting process was monitored through a high speed camera to ensure that the patterning was performed in stable cone-jet mode. The operating envelope for copper nanoparticles ink using 100µm nozzle is shown in figure 2.7. The

23

operating envelop is obtained by increment of 10μl/hr flow-rate and by applying different applied voltages at which stable cone-jet is observed. The minimum flow-rate at which stable cone-jet is observed is 20μl/hr. As shown in the figure at flow-rate 20μl/hr, the stable cone-jet mode is observed from 2.6 to 3.5kV, similarly at 100μl/hr, the cone-jet mode is observed from 4.0 to 4.5kV.
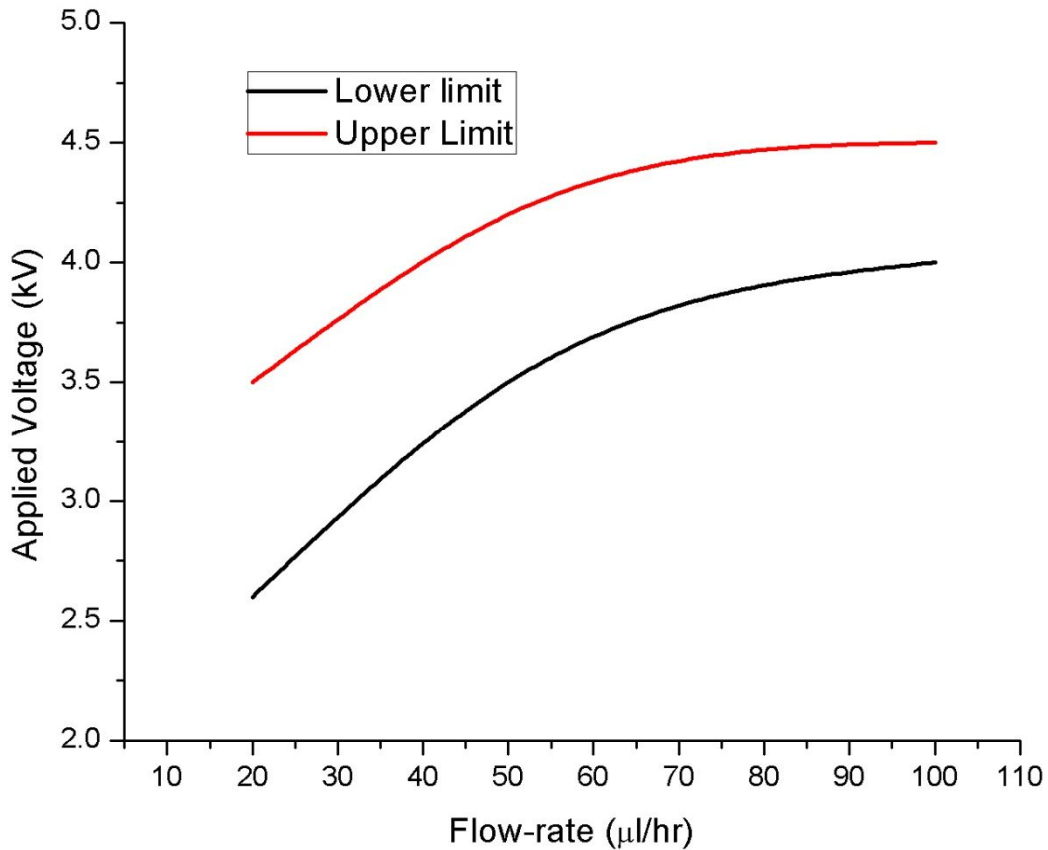
Figure 2.7Operating Envelope for the stable cone-jet

In order to perform patterning through electrohydrodynamic printing, the upper limit of voltage and low flow-rate of operating envelope was selected, because at low flow-rate the jet formed through cone-jet is more stable with larger length as compared to high flow-rate and small jet diameter can be achieved at low flow-rate. The patterning was performed on the glass substrate in cone-jet mode, the distance between the nozzle and substrate was kept at 500μm, and the speed of the substrate is kept at 25mm/sec. The pattern width with respect to flow-rate at upper limit of applied voltage in stable cone-jet region is shown in figure 2.8. The pattern width is increased at higher flow-rates this is due to the increase in the jet diameter in stable cone-jet mode with increase in flow-rate. The effect of the applied voltage on the

24

pattern width was also studied at 20, 60 and 100μl/hr flow-rate, by applying the different value of DC voltage which is investigated for the stable cone-jet.
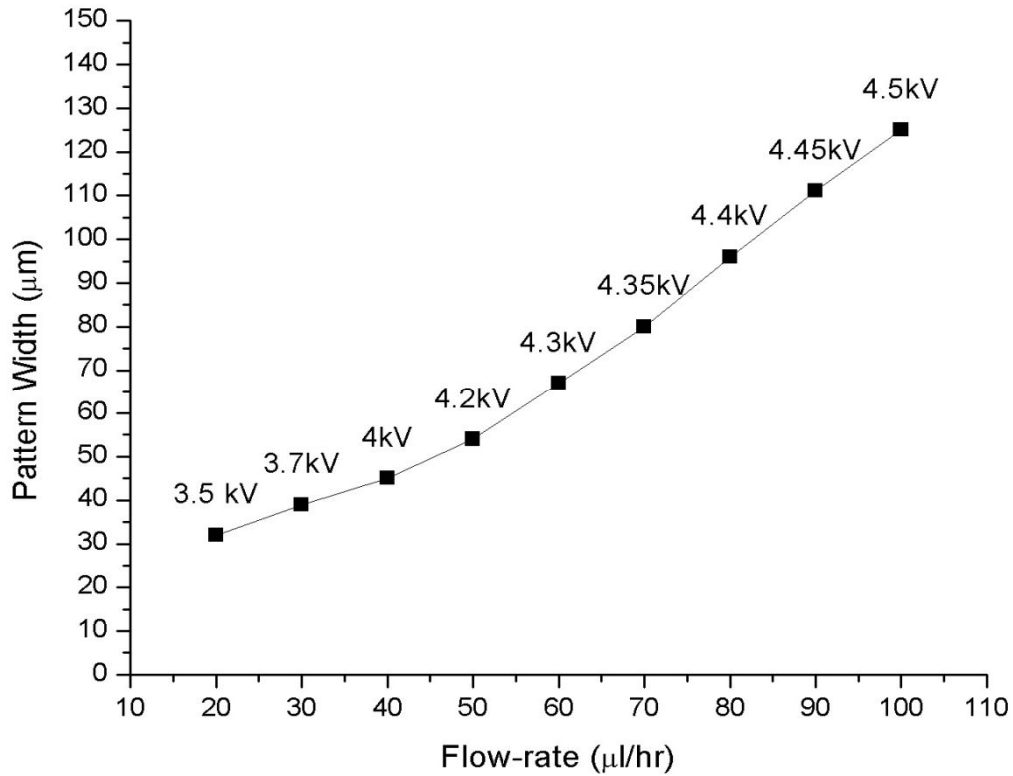
Figure 2.8Pattern width with respect to flow-rate along with upper limit of applied voltage

The graph at figure 2.9 shows pattern width with respect to change in applied voltage. As shown in the figure, at 20μl/hr the patterns width are 36, 34 and 32μm at applied voltage 2.6, 3 and 3.5kV respectively, and at 100μl/hr flow-rate the patterns widths are 132, 127, 125μm at applied voltage of 4, 4.25 and 4.5kV respectively. At 20μl/hr the effect of applied voltage on the pattern width is 4%, whereas at 100μl/h the effect of applied voltage on the pattern width is 7%. This shows that the effect of applied voltage on pattern width is not significant in comparison with the flow-rate effect. This shows that the flow-rate is the important parameter to control the pattern width in electrohydrodynamic printing. The minimum pattern achieved with electrohydrodynamic printing at flow-rate 20μl/hr and applied DC voltage of 2.6kV is 32μm with 2μm deviation. The minimum pattern width achieved is approximately 3.12 times smaller than nozzle internal diameter. The previously reported pattern

제주대학교 중앙도서관
JEJU NATIONAL UNIVERSITY LIBRARY

width is 450μm which was achieved with same nozzle size (Ganan 1996). By patterning in continuous con-jet mode,a minimum patternwidth of 14.1 times smaller than the previously reported pattern size is achieved by using 4.5 times smaller nozzle diameter, the pattern width achieved is 3.125 times smaller than the nozzle internal nozzle diameter, which is the main advantage of electrohydrodynamic jet printing in cone-jet mode as compared to other inkjet printing technologies.
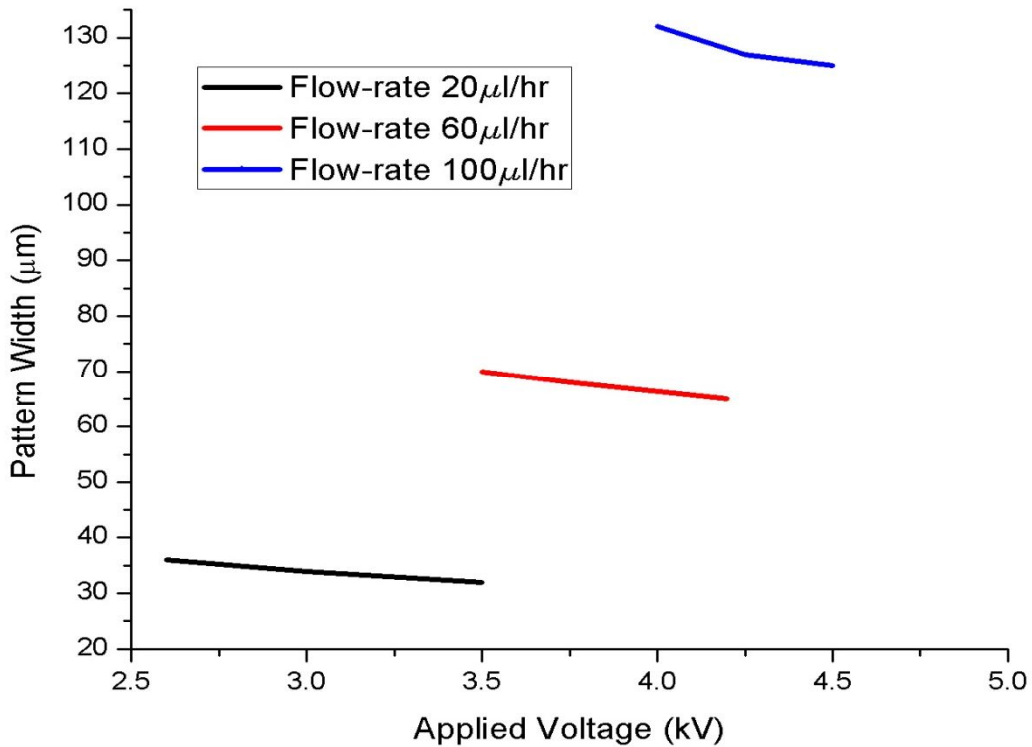
Figure 2.9Pattern width with respect to applied voltage at different flow-rate

After patterning, in order to avoid the oxidation of copper nanoparticles, the patterns are sintered in inert environment after injecting the N_2 gas in dry oven at 120°C for 30min. Figure 2.10(a) shows the pattern through electrohydrodynamic printing on glass substrate at 20μl/hr and applied DC voltage of 2.6kV, the width of the pattern is 32μm with good uniformity. Figure 2.10(b) shows the effect of flow-rate on the pattern width on glass substrate.

(a)

Increase in flow-rate
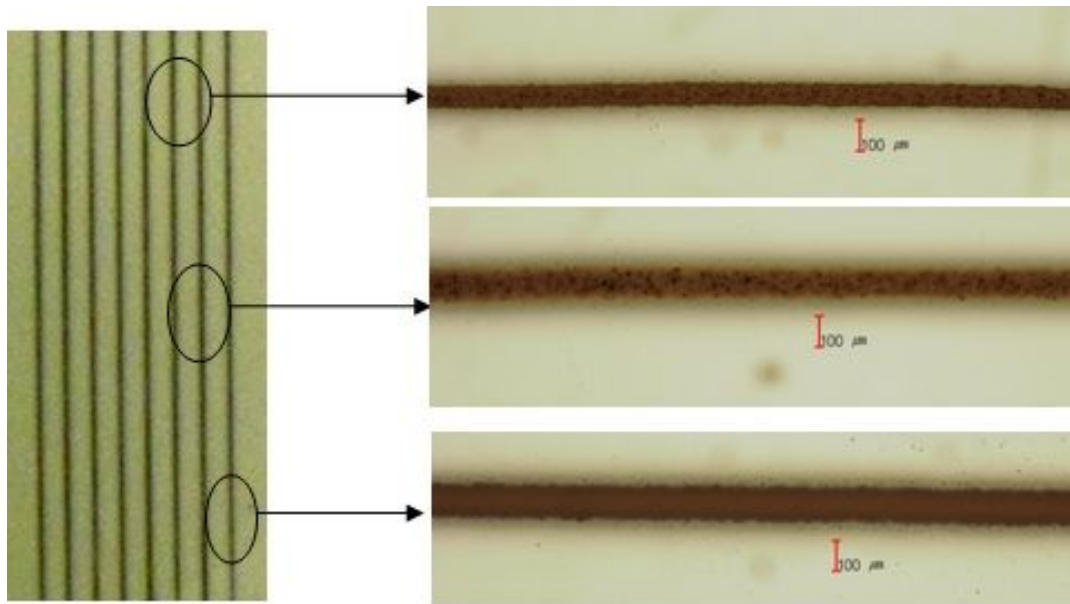
(b)

Figure 2.10(a) Microscopic image of the printed pattern of the copper nanoparticles at 20μl/hr and applied voltage is 2.8kV and (b) Pattern images of the copper nanoparticles on glass substrate through 60μm internal diameter glass capillary nozzle

Figure 2.11 shows the SEM image of the deposited copper nanoparticles after the sintering process. The SEM image shows that nanoparticles are properly interconnected, which helps in improving the electrical conductivity of the printed pattern. In order to characterize the chemical purity of the deposited patterns, XRD analysis was performed. Figure 2.12 shows the XRD spectrum of the deposited pattern, which confirms that the deposited material is copper and therefore the nanoparticles have remained inert during the deposition and sintering process.
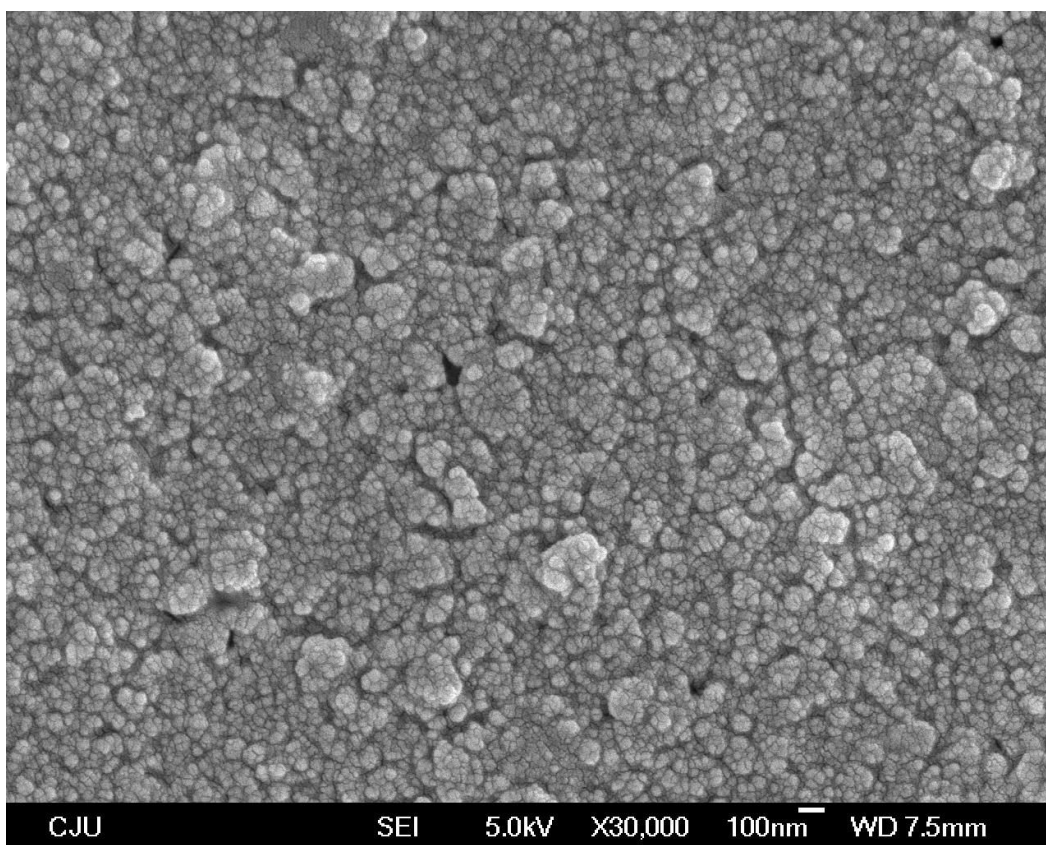
Figure 2.11SEM image of the printed pattern of copper nanoparticles
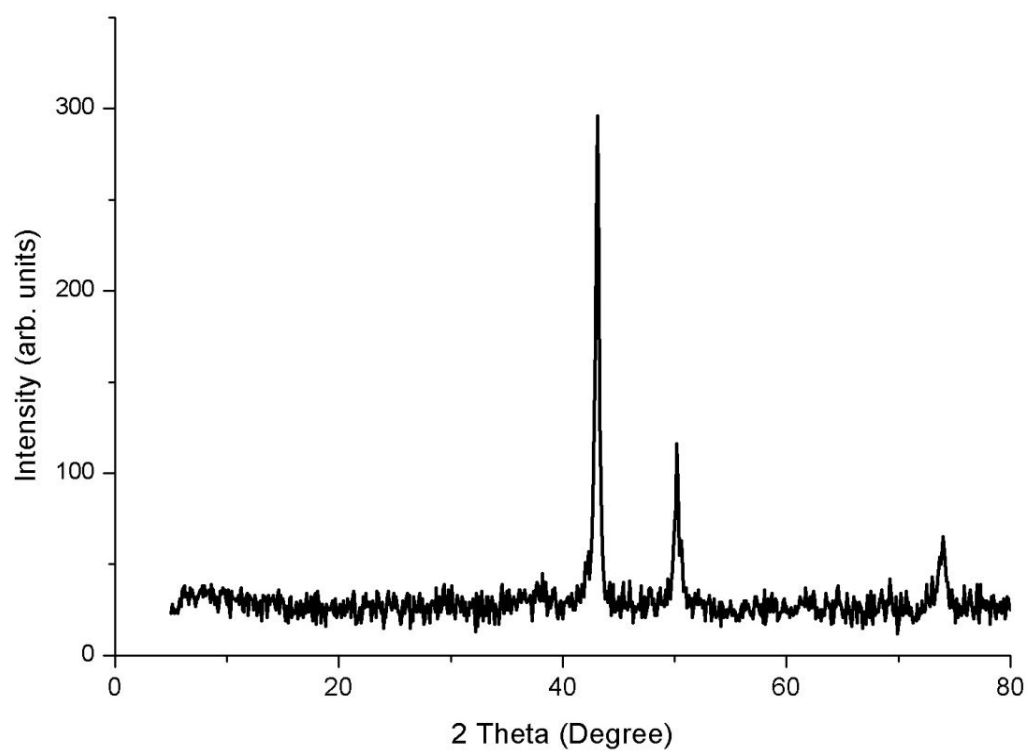
Figure 2.12 XRD spectrum analysis of printed pattern

For electrical characterization of the printed pattern, the resistivity is measured through 4-point probe method (DASOL ENG Model No. FPP-RS 8). The measured value of the 32, 67 and 125µm wide pattern are 6.8, 6.4 and 5.9µΩ.cm respectively, which is almost 4 times of the bulk copper. This shows that copper nanoparticles pattern through electrohydrodynamic printing can be used for the printed electronics applications such as TFT, RFID tags and collectors for solar cells.

2.6.3 Patterning of Ag nanoparticles

For continuous printing, commercial available NPK-2 ink containing 40% wt Ag nanoparticles is used. Initial patterning is performed by using metallic capillary of internal diameter of 210µm and outer diameter of 410µm. The distance between capillary and ground is kept 1.5mm. In order to perform the patterning, first operating envelop of the Ag ink was investigated. The operating envelop provide the lower and upper limit of applied voltage for generating the stable cone-jet with respect to applied flow-rate. The operating envelop for stable cone-jet is shown in figure 2.13.
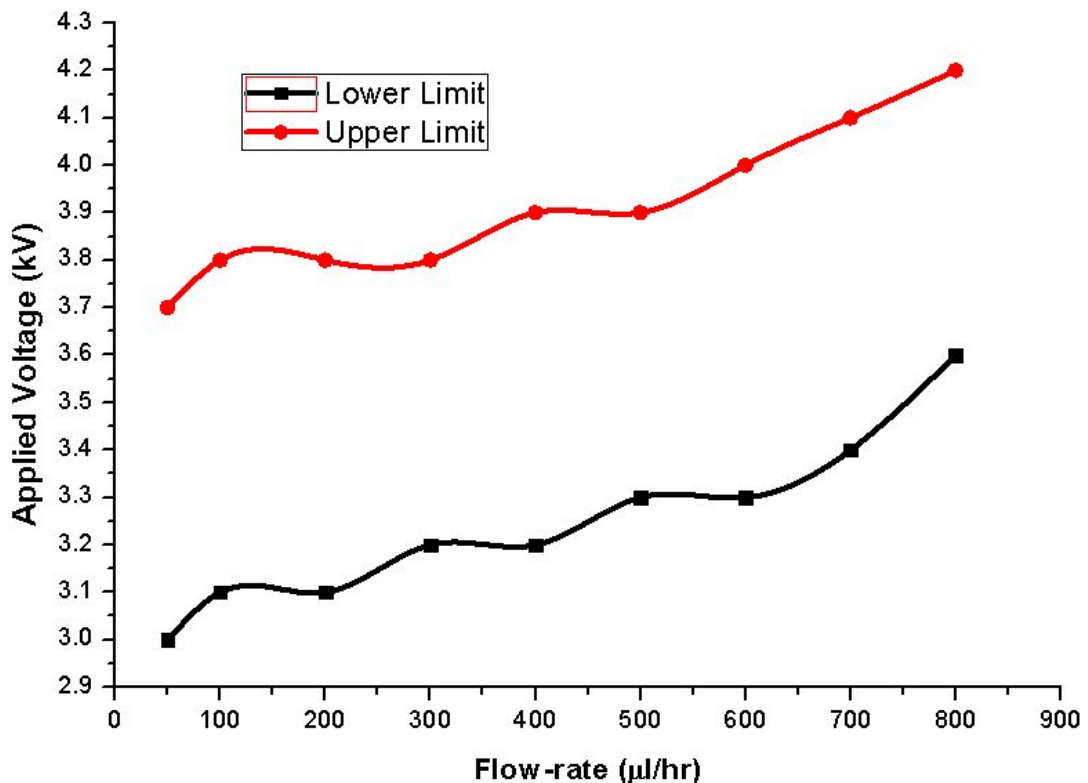
Figure 2.13Operating envelop of NPK-02 ink using 110µm capillary

29

The dependency of jet diameter emerging from the tip of the cone-jet was also measured using high speed camera with respect to flow-rate and applied voltage. It was noted that the jet diameter is more depended on the flow-rate as compared to applied voltage as shown in figure 2.14.
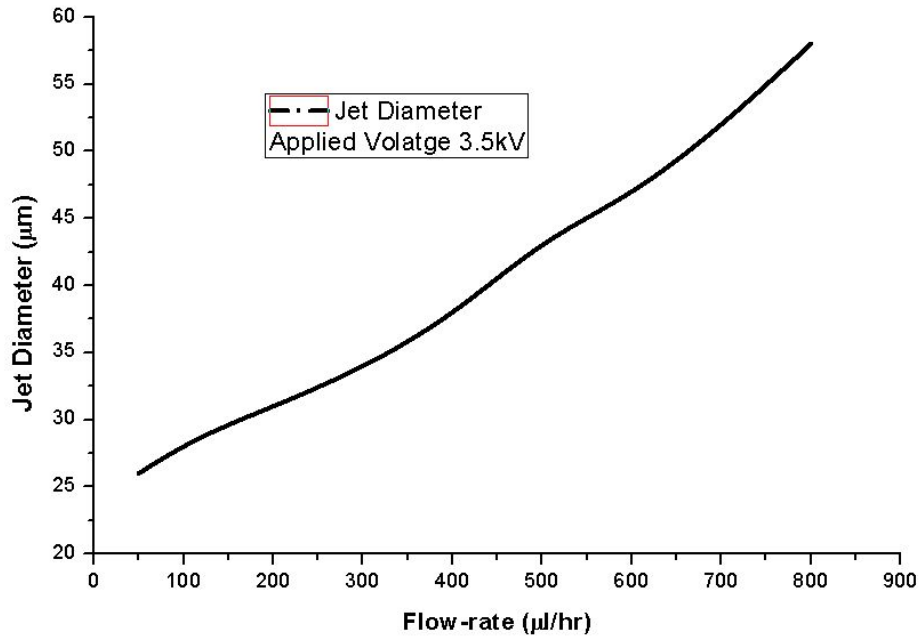
(a)
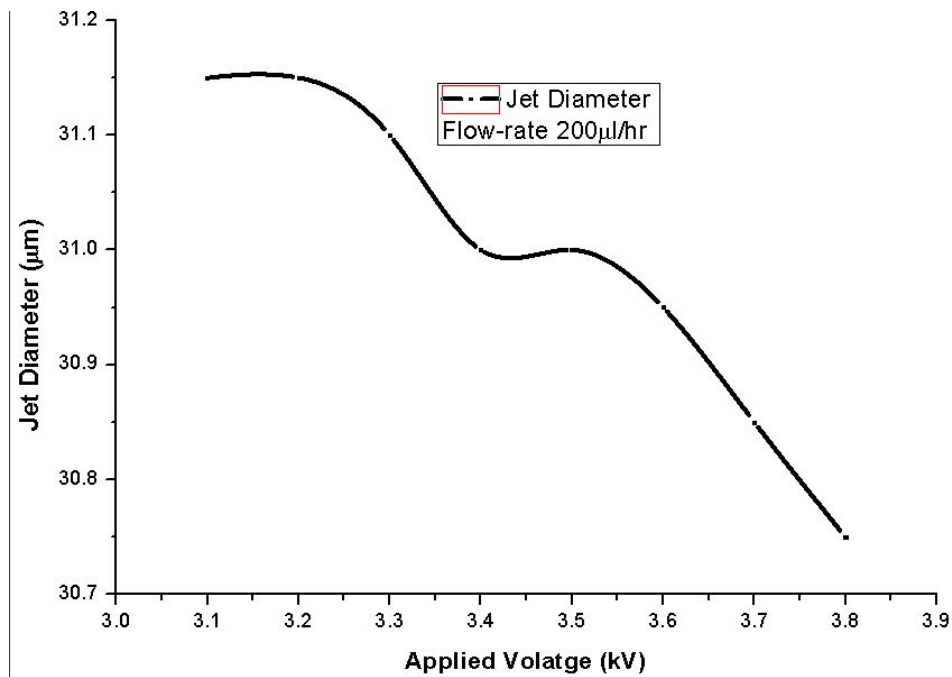
(b)

Figure 2.14 (a) Jet diameter with respect to applied flow-rate at 3.5kV and (b) effect of applied voltage on jet diameter at 200μl/hr

Patterning is performed on the glass substrate of 0.5mm thickness placed on the top of metallic ground plate by applying the upper limit of the applied voltage and corresponding applied flow-rate, which is investigated for stable cone-jet operating envelop, the speed of substrate is kept at 25mm/sec for all the experiment. In electrohydrodynamic printing the jet diameter is more dependent on the flow-rate, in a cone-jet region the diameter of the jet increases with increase in flow-rate. The applied voltage has minor effect on the diameter of the jet in cone-jet mode. After patterning, the samples are placed in dry oven for sintering at 150°C for 60min. After sintering the pattern width is measured with the help of digital microscope. The pattern width with respect to applied flow-rate is shown in graph at figure 2.15. As shown in the graph the pattern width increases with increase in the applied flow-rate. However, pattern at high flow-rate is irregular as compared to pattern at low flow-rate, because the length of the jet decreases with increase in flow-rate it causes destabilization to the jet in cone-jet mode. The minimum pattern width of 80µm is achieved after the sintering.
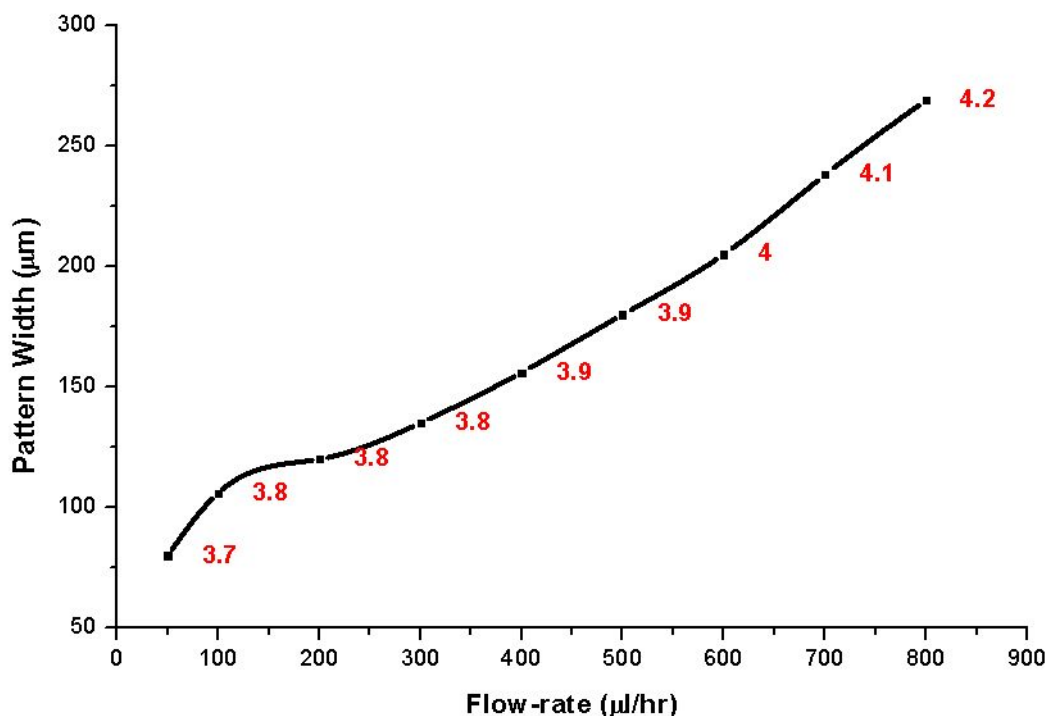
Figure 2.15 Pattern width of Ag nanoparticles after sintering with respect to flow-rate and applied voltage

The measured patterns widths are almost 4 times the size of the jet, because of the low substrate speed as compared to jet speed (in order of ~m/sec), which is major draw-back of patterning in continuous mode. In order to reduce the pattern size, high speed stage movement is required. The microscope images of the Ag nanoparticles patterns are shown in figure 2.16.
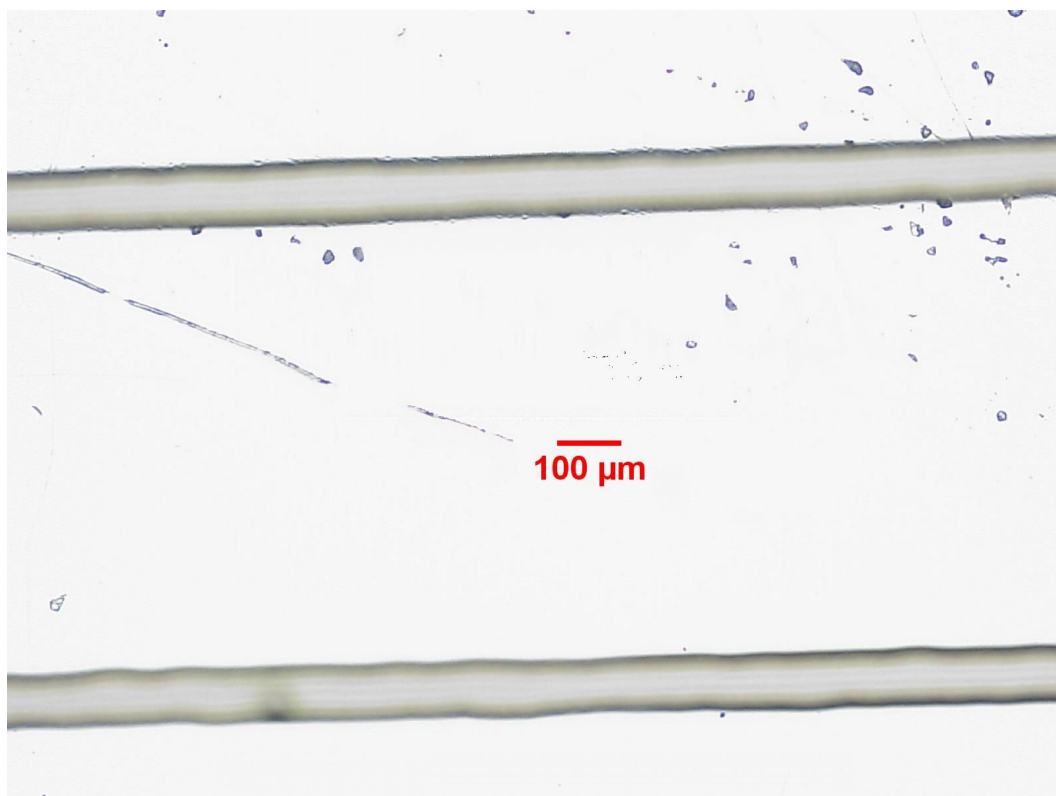
Figure 2.16Microscope image of the pattern printed through 110µm capillary by applying 3.7kV and flow-rate of 50µl/hr, size of the pattern is 80µm

3. DOD EHD Patterning

Inkjet systems based on thermal and piezoelectric system have been employed successfully in commercial application especially with regard to digital printing and printed electronics. But these types of conventional DOD systems (thermal and piezo) have limitations, such as thermal problems, nozzle size limitation, clogging and generation of the droplets smaller than the nozzle size etc(Le 1998). For the development of new kind of printing technology for printed electronics,a lot of research being done in the field of Electrohydrodynamic Patterning (Choi and Kim 2011, and Kim and Lee 2011). The main benefit of the electrohydrodynamic printing system is the generation of small droplet size then nozzle diameter at high frequency and overcoming the discrepancies in those conventional inkjet systems.

Among many other applications of electrohydrodynamic printing(Park et. al. 2007, Jaworek 2007, Vela et. al. 2006, Griss et. al. 2002, and Li et. al. 2008),a novel application is fabrication of micro patterns through DOD method for printed electronics(Choi et. al. 2008, Kawamoto 2007, and Wang and Stark 2010)and bio application(Kuil et. al. 2006, and Kim et. al. 2010).In electrohydrodynamic DOD patterning the pulsed voltage is applied to the capillary. When high pulsed voltage is applied, the meniscus deforms into the cone-jet producing a fine jet for very short period of time, after detachment of the jet it forms a droplet(Ishida et. al. 2008, Stachewica et. al. 2007, and Li 2007)and process is pulsating. The droplet size depends on the applied pulsed voltage as well as frequency of the applied voltage. In previous researches for DOD, the researchers applied simple square wave pulse voltage or by superimposing AC on applied DC voltage(Li and Zhang 2009, Balachandran et. al. 1992, Li 2007, and Kim et. al. 2008),in both the cases the pulse is square either with zero or bias-voltage.

This chapter presents the novel technique for electrohydrodynamic DOD printing by applying multi-step pulse voltage. Multi-step voltage is applied by super-imposing two square waves with same frequency but different duty cycle on each other. The

multi-step voltage is consist of bias-voltage "Va" for initialization of the meniscus; intermediate-voltage "Vb" for deformation of the meniscus into cone shape and ejection-voltage "Vc" for steady droplet generations. The applied voltage is in the form of two step functions, with "Va" consists of 25% of the pulse, Vb" consists 50% of the pulse and "Vc" consists 25% of the pulse as shown in figure 3.1. Initially experiments were performed on Ethanol by changing the value of "Va", "Vb" and "Vc', flow-rate and frequency of multi-step pulsed voltage. The DOD behavior was also compared with the applied square pulsed voltage.

Lab made system was used for the experiments; the schematic of setup used is shown in Figure 2.6 in chapter 2. The multi-step pulsed voltage was supplied by the high voltage power supply (Trek Model 10/40A) which was connected to NI' PXI-1042Q hardware system with function-generator. The multi-step voltage with positive polarity was applied to the metallic capillary of 210μm internal diameter and 410μm outer diameter. Ink was supplied to capillary through syringe pump. The behavior of the system was monitored with the help of high speed camera. The ground made of copper plate was used as counter electrode, which was mounted on moving stage; 0.5mm thick glass substrate was placed on top of ground plate. The distance between capillary and ground was kept at 1.5mm. Experimental setup consist of high voltage power supply, syringe pump, camera, moving stage and movement of head (to adjust the distance between capillary array and ground) were connected through NI's PXI-1042Q hardware system which was controlled with lab made software system based on LabView, the control panel for voltage control is shown in figure 3.1 The multistep pulse shape, applied voltage, frequency and duty cycle were control with the help of this customized software. To study the effect of multi-step voltage the experiments were performed on Ethanol by changing the multi-step voltage, flow-rate and frequency.
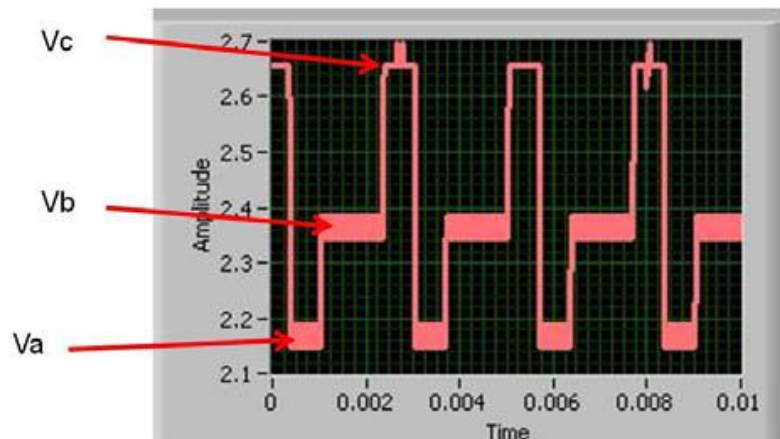
Figure 3.1Multistep pulsed voltage used for experiment

3.1 Study of Multi-step DOD phenomena

For the study of Multi-step DOD phenomena ethanol was used for theexperiments. In order to select the applied pulse voltages, theexperiments were performed by applying the DC voltage for upper andlower limit to achieve stable cone-jet region with respect to flow-rate. Theaverage lower value of applied DC voltage was 2.1kV and averageupper value of DC voltage was 3.2kV at which stable con-jet wasobserved.

3.1.1 Effect of pulsed voltage

To study the effect of the applied voltage in case of multi-stepvoltage for DOD purpose, number of experiments were performedby changing the value of "Va", "Vb" and "Vc", keeping the otheroperating parameters fixed, flow-rate 75μl/hr and frequency 150Hz.It was observed during the experiment that when the value of "Va"was kept very low such as 0 to 1kV, "Vb" kept at 2.5kV and "Vc" at3kV, the movement in the meniscus was more as compared to thecase where the value of bias-voltage "Va" was 1.75kV or higher asshown in figure 3.2. The phenomenon was more stable when the"Va" was closed to the stable cone-jet region. When the value of"Va" was close to stable cone-jet region, the forces requiredto deform into cone and extraction of droplet would also be less ascompared to low value of "Va", which

35

also minimize the motion ofmeniscus and the DOD process was more stable with high "Va".

However, the DOD also depends on the value of ejectionvoltage"Vc", if the value of "Vc" was very high; the jet will deformin to spray instead of single droplet or single event jetting. This alsocauses the spreading of the droplet on the substrate. For steady and controlled DOD printing, the value of "Va", "Vb" and "Vc" must beoptimized. The effective value of bias-voltage "Va" is close to lowerlimit of stable cone-jet, intermediate-voltage "Vb" should be closeto or middle of lower and upper limit of stable cone-jet andejection-voltage "Vc" must be closed to or at the upper limit ofstable cone-jet value. However, the value of "Vc" must beoptimized to avoid the high charge in the jet region to avoid thespray.
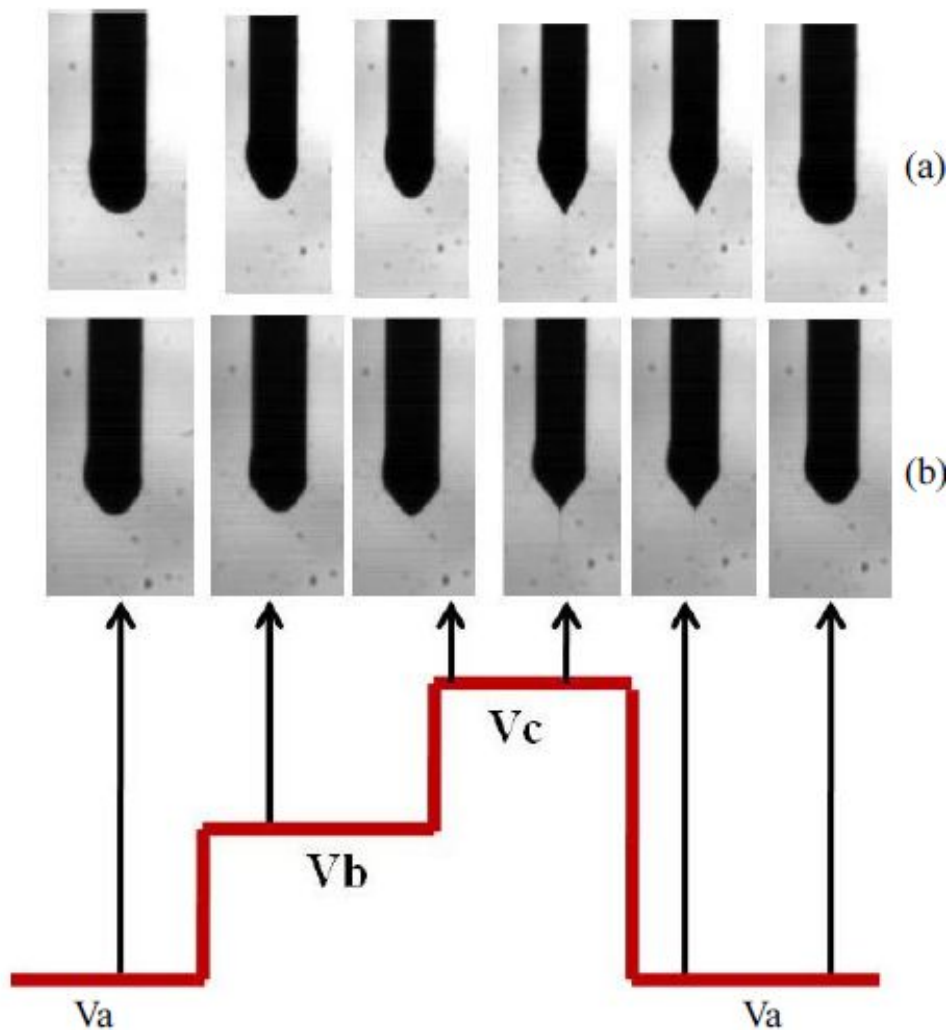
Figure 3.2Drop-on-demand ejection with respect to square pulse voltage and multistep voltage (a) Va=1kV, Vb=2.5kV, Vc=3kV and (b) Va=1.75kV, Vb=2.5kV, Vc=3kV

3.1.2. Effect of frequency and flow-rate

The effect of frequency and flow-rate on DOD phenomena was also studied by adjusting the bias-voltage Va=2kV, intermediate voltage Vb=2.5kV and ejection-voltage Vc=3kV and varying the flow-rate and frequency. The reason of selecting the values of "Va", "Vb" and "Vc" is because of stable cone-jet region, as "Va" was lower limit of stable cone-jet, "Vb" was middle value of stable cone-jet region and "Vc" was the upper limit of the stable cone-jet region. During the experiments it was observed that for low flow-rate the value of applied frequency was also low because at the higher frequency although the droplet size is decreased due to small pulse duration, the ejection of volume is also increased. Due to low flow-rate the DOD phenomena was difficult to achieve. The effect of frequency and flow-rate on DOD phenomena is shown in figure 3.3. At a given flow-rate, the DOD transforms into intermittent ejection; means that the behavior was not regular, the ejection occurs after 2 or more pulses, the number of non-ejection pulses increase with increase in the applied frequency of the step voltage. At high frequency the ejection of the droplet stops and there was only vibration in the meniscus. Theses vibrations and amplitude of the vibration is also increased with further increased in the applied frequency. At high frequency, behavior of the drop-generation at 250Hz and vibration at 325Hz of the meniscus, where applied multi-step pulse voltage Va=2kV, Vb=2.5kV and Vc=3kV and flow-rate was 75μl/hr is shown in figure 3.4. As shown in figure 3.4, at 250Hz frequency, the stable DOD phenomena could be observed due to sufficient time of the pulse to deform the meniscus and ejection of the droplet. Whereas, at 325Hz no ejection of droplets took place due to the short period of applied voltage pulse. The applied pulse time was not sufficient to deform the meniscus in cone and ejection of the droplet. For any given liquid the limitation in the frequency is due to the size of the meniscus generated through the capillary(Stachewicz et. al. 2009).The DOD frequency can be increased by decreasing the meniscus size by using smaller diameter nozzles.
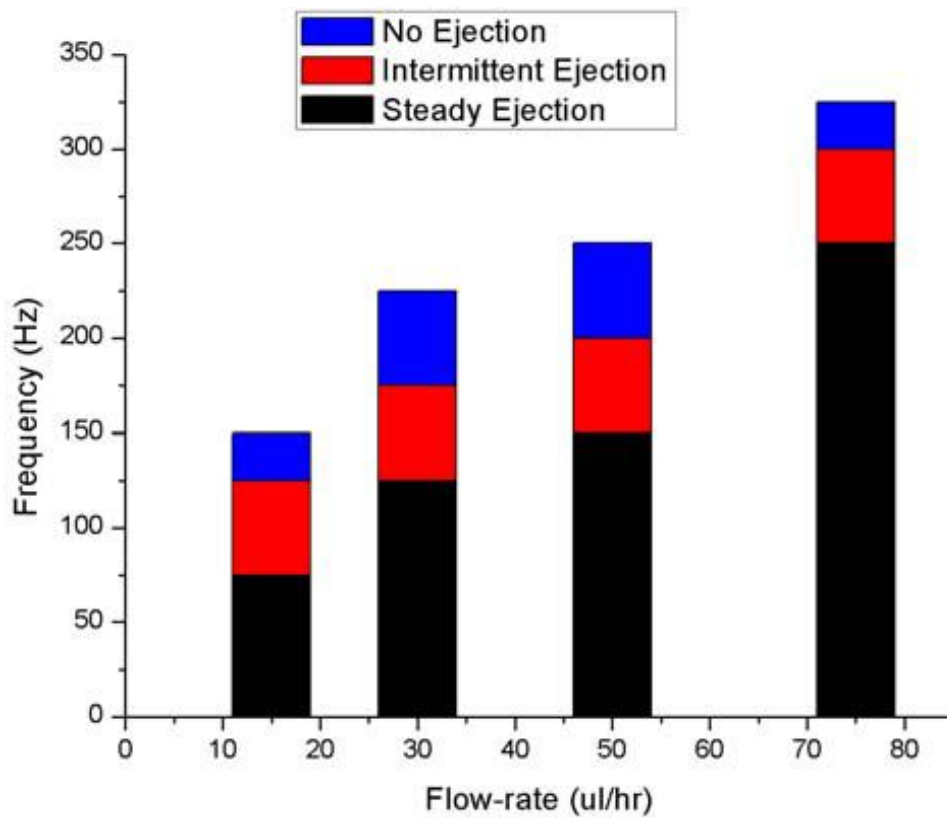
Figure 3.3Behavior of DOD phenomena at differences frequency and 30μl/hr, 50μl/hr and 75μl/hr of flow rate, respectively

(a)
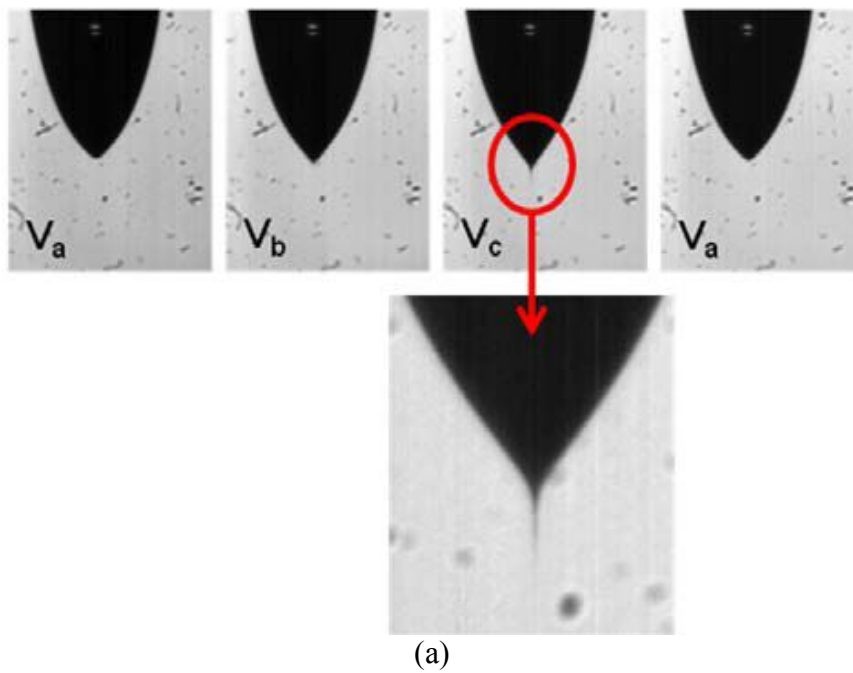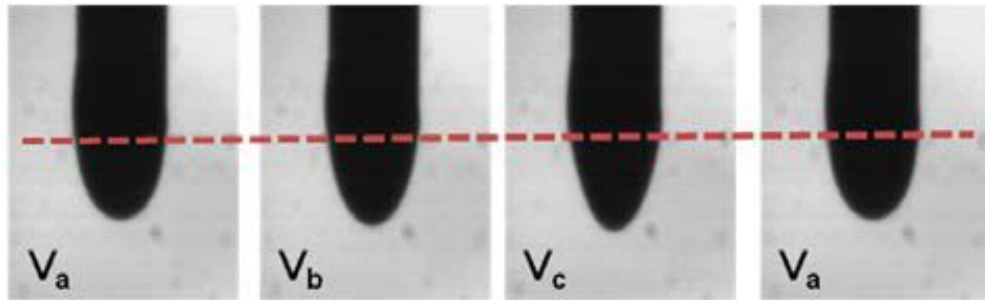
(b)

Figure 3.4The behavior ejection with Va=2kV, Vb=2.5kV and Vc=3kV and flow rate 75µl/hr (a) sequence of steady ejection at 250Hz, (b) at 300Hz only vibration in the meniscus as shown in the figure with reference to red dotted line

3.1.3 Comparison between Multi-step and Square-pulse DOD

The ejection behavior at 75µl/hr at 200Hz frequency by applying square voltage (Va=2kV and Vb=3kV) with 50% of Duty Cycle and multi-step voltage (Va=2kV, Vb=2.5kV and Vc=3kV) is shown in figure 3.5. The main benefit of the multi-step pulse voltage compared to the square pulse voltage is the times of application of bias voltage to ejection voltage. As shown in figure 3.5, in square voltage there was sudden change in applied voltage to ejection voltage, which causes disturbance in meniscus and instability in ejection phenomena. By multi-step pulse voltage there was intermediate voltage which ramp the effect of applied voltage, which avoids the sudden application of high voltage to the meniscus and also induced less vibration to the meniscus and hence results in stabilization of the ejection process. The other advantage of the multi-step pulse voltage is the related to high voltage switching hardware, in square the switching time is less as compared to multi-step pulse voltage due to intermediate voltage.
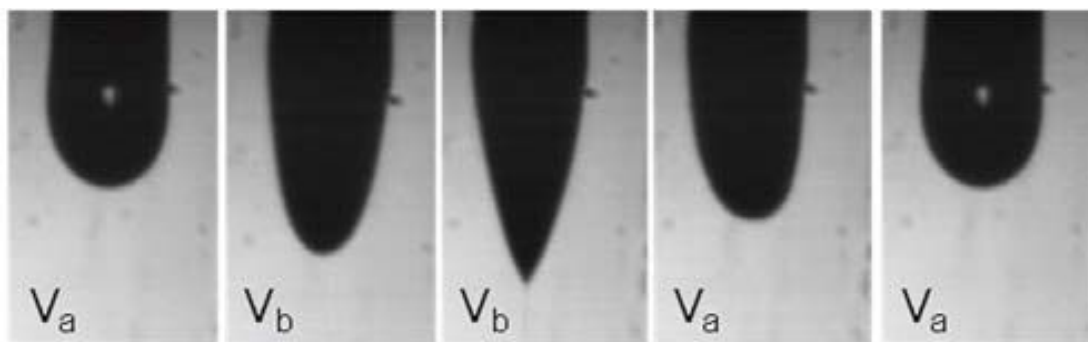
(a)
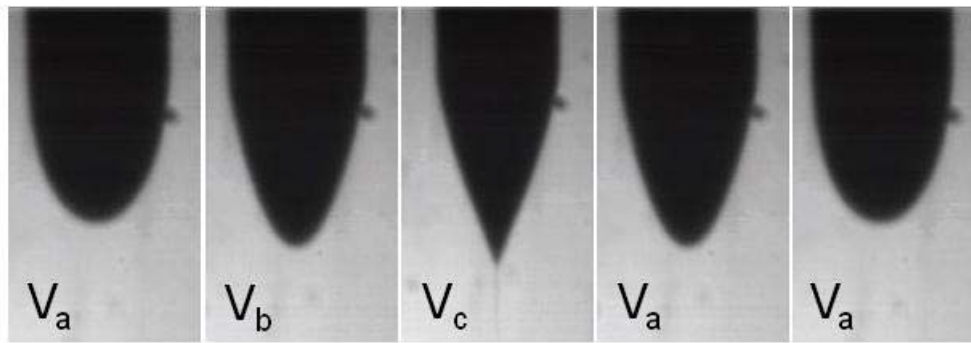
(b)

Figure 3.5The behavior ejection at flow-rate 75µl/hr and frequency200Hz, (a) Square wave Va=2kV and Vb=3kV with 50% Duty Cycle and (b) Multi-step voltage Va=2kV, Vb=2.5kV and Vc=3kV

3.2 DOD Patterning of Conductive tracks

For DOD printing, the commercially available inks with copper and silver nanoparticles are used. The properties of the inks are given in table 3.1. The patterning was performed on the glass substrate. After studying the multi-step DOD phenomena through ethanol following can be described as input parameters for DOD printing:

1. "Va" bias-voltage must be closed to the value of lower limit of stable cone-jet region.
2. "Vb" intermediate-voltage must be at middle range of stable cone-jet region.
3. "Vc" ejection-voltage must be closed to the value of upper limit of stable cone-jet region.
4. Determine the optimal value of "Va", "Vb" and "Vc" at low flow-rate and frequency at which the phenomena is stable.
5. After investigating the optimal value of "Va", "Vb" and "Vc", optimal frequency and frequency should be obtained.
6. Determine the optimal substrate speed based on the DOD frequency and droplet spacing on the substrate.

For DOD patterning on the glass substrate, a commercial inkcontaining silver nanoparticles was used. Initial experiments wereperformed to find lower and upper values for the applied DCvoltage at which stable cone-jet formed and corresponding flow-rate.The experiments revealed that the droplet diameter depends on multistep voltage and as well as on applied frequency. The Ohmic behavior of the pattern was measured through 4-point probe method which was linear and material characterization of deposited nanoparticles was performed through XRD after sintering. The goal of this study was to generate steady and controlled DOD ejection of the droplets through multi-step pulsed voltage.

Ink	Surface Tension (N/m)	Viscosity (Pa.s)	Conductivity (S/m)	Electric Permittivity	Weight %	Particle Size (nm)
Cu	3.69e-2	7.6e-3	7.5e-3	48.5	40	20
Ag	5e-3	39e-3	9.5e-6	40	40	50

Table 3.1Properties of Ag and Cu conductive ink used for patterning

3.2.1 DOD Patterning of Cu nanoparticles

The experimental set-up was developed in house. A stainless steel needle having a

normal edged exit (90^0 to the needle axis) with an internal diameter of 450μm and an

external diameter of 750μm was held in a holder made of acrylic. Copper plate was placed 800μm below the needle exitas ground/counter electrode. Glass having 500μm thickness was placed as a substrate on top ofground plate. The needle and the ground electrode were connected to a high voltage powersupply (10/40A Trek Model, USA). Forward multi-step waveform superimposed on biased DC voltage (shown in Fig1c) was supplied by this high voltage power supply. The needle inlet wasconnected to a syringe pump (PHD 2000 Infusion, Harvard Apparatus, USA). The behavior ofthe dripping was monitored with the help of a high speed camera (x3, 11X, 5000fps, Motion Pro,USA). High voltage power supply, syringe pump, high

speed camera, moving stage (forsubstrate motion) and movement of head holder (to adjust the distance between needle exit andground plate) were connected through a hardware system (PXI-1042Q, National Instruments,USA), controlled by a lab developed software based on LabVIEW. The multi-steppulse voltage, applied voltage, frequency and duty cycle were also controlled with the help of thiscustomized software.

Different sets of experiments have been performed by applying multi-step pulse voltage with externally applied electric field pulse frequencies of 10Hz, 25Hz, 50 Hz and 100 Hz and duty cycles of 50% and 75%. Fig. 3.6 shows the time sequential photographs of the motion of a droplet formed and ejected from the tip of the liquid meniscus compared with the multi-step pulsed voltage at 50 Hz frequency and 50 % duty cycle. Va represents the applied biased voltage, Vb correspond to the first step of multi-step voltage while Vc is the second step of the forward multi-step pulse voltage. When the forward multi-step pulse voltage is applied, the biased voltage Va provides the initial charging to the ink which develops the preliminary shape of meniscus at the tip of the nozzle. Once the first step of the multi-step pulse voltage (Vb) is triggered, the initial shape of meniscus deforms into a cone shape. Now at this stage the cone is fully developed and only a small triggering voltage pulse is required for the generation of droplet, for which the second step of multi-step pulse voltage (Vc) is applied. As a result of this triggering pulse Vc, a tiny droplet having a diameter of 110 ± 2 μm is detached from the apex of the meniscus and the other part of the liquid is retracted. The complete sequence of the droplet generation with respect to multi-step pulse voltage is shown in figure 3.6 for applied frequency of 50Hz. The appearance of the conical shape with a sharp apex and the generation of the small drop indicate that the Taylor cone is formed temporarily and periodically.
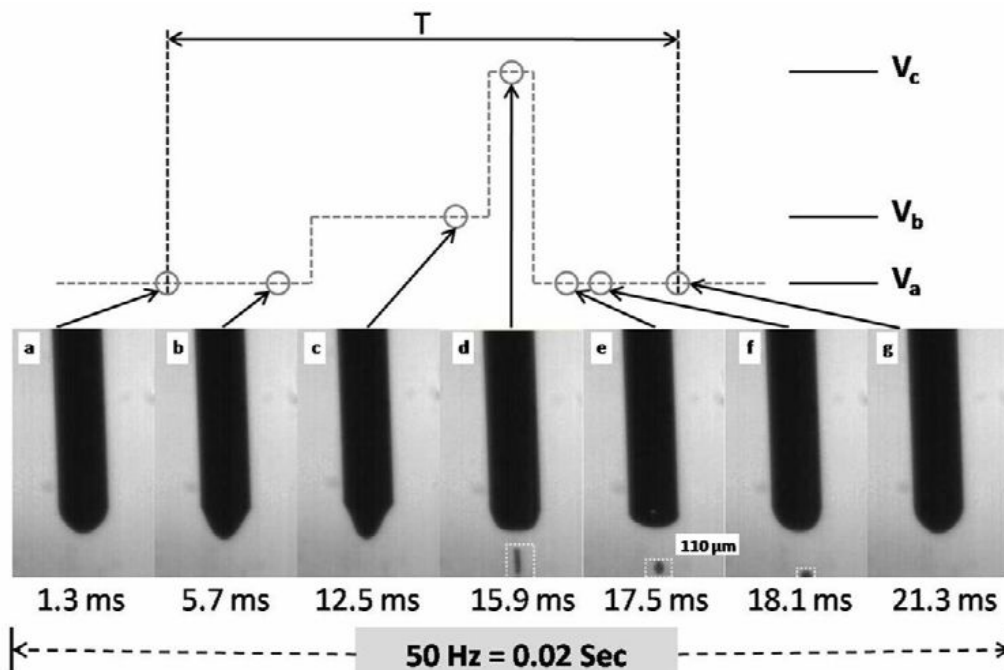
Figure 3.6Series of images of the meniscus deformation and drop generation with the forward multi step pulse signal at Va of 3.5kV, Vb of 4.5kV, Vc 5.0kV, duty cycle of 50% and frequency of 50Hz

Figure3.7 shows the static high zoom camera and microscopic images of printed dots and lines on the glass substrate by using EHD drop-on-demand ink jet printing technique. Patterning has been carried out at a constant flow rate and at pulse frequencies of 10 Hz, 25 Hz, 50 Hz, and 100 Hz with a constant linear motor speed (substrate speed) of 25 mm/s. Effect of biased and pulse voltages on droplet size has been analyzed by varying the biased and step voltages. Figure3.7(a) shows the deposited droplets which are generated at applied pulse of 50 Hz frequency with 50% duty cycle and at voltages Va, Vb and Vc of 2.5kV, 4.5kV (first pulse of 2kV) and 5.5kV (second pulse of 1.5kV) respectively. The average diameter size of droplets is 780 μm with standard deviation of 10μm. Comparatively smaller droplets have been generated by increasing the magnitude of biased voltage and decreasing the magnitude of step voltages. The deposited droplets in figure3.7(b) are generated at the same frequency and duty cycle as that of figure3.7(a) i.e. 25 Hz and 50% respectively but at low pulse voltages i.e. Va, Vb and Vc; 3.5kV, 4.5kV (first pulse of 1kV) and 5.0kV (second pulse of 0.5 kV) respectively. The average diameter size of deposited droplets is 500μm with a standard deviation of 10μm. The reason of this relatively smaller drop generation is that with low biased voltage and high pulsed

43

voltages, energy gain per unit area of the liquid and the tangential electric stress at the liquid meniscus increases more quickly than the normal electric stress. As a result, greater pulsed voltages (Vb and Vc) are more likely to produce a temporary jet rather than a dripping mode which generates relatively large sized droplets. Similarly figure3.7(c) shows the patterned droplets which are generated at applied pulse of 10 Hz frequency with 75% duty cycle and at voltages Va, Vb and Vc 3.5kV, 4.5kV(first pulse of 1kV) and 5.0kV(second pulse of 0.5 kV) respectively. The deposited droplets have an elliptical shape rather than round due to high duty cycle of the pulse voltage. High duty cycle (75%) increases the application time of the triggering pulse which results in a temporary jet rather than a droplet. Since the substrate speed is constant and relatively high than the speed of ejection of temporary jet which does not allow the temporary jet to accumulate to a large round shape drop on the substrate. As a result, temporary generated jet forms an oval shape drop after deposition on the substrate. Using this high duty cycle (75%) of pulsed voltage, conductive lines are patterned at applied pulse of 100 Hz frequency and at voltages Va, Vb and Vc of 3.5kV, 4.5kV (first pulse of 1kV) and 5kV (second pulse of 0.5 kV) respectively. The printed lines shown in Fig. 4d have an average size of 450μm with standard deviation of 10 μm. It can be concluded from the printed results shown in figure 3.7(d) that EHD drop-on-demand can also be used for printing of conductive lines for metallization in printed circuit boards and backplanes of printable transistors if the substrate speed and frequency of droplet generation get synchronized. Since the substrate i.e. glass has a hydrophilic surface therefore the deposited droplets were able to spread out resulting in large sized dot or width of a line than the original size of the generated droplet.

However, further research into tuning the operational conditions and treating the substrate is required to get a high resolution, precise and uniform pattern of copper colloidal ink by using forward multi-step waveform in drop-on-demand electrohydrodynamic inkjet printing.
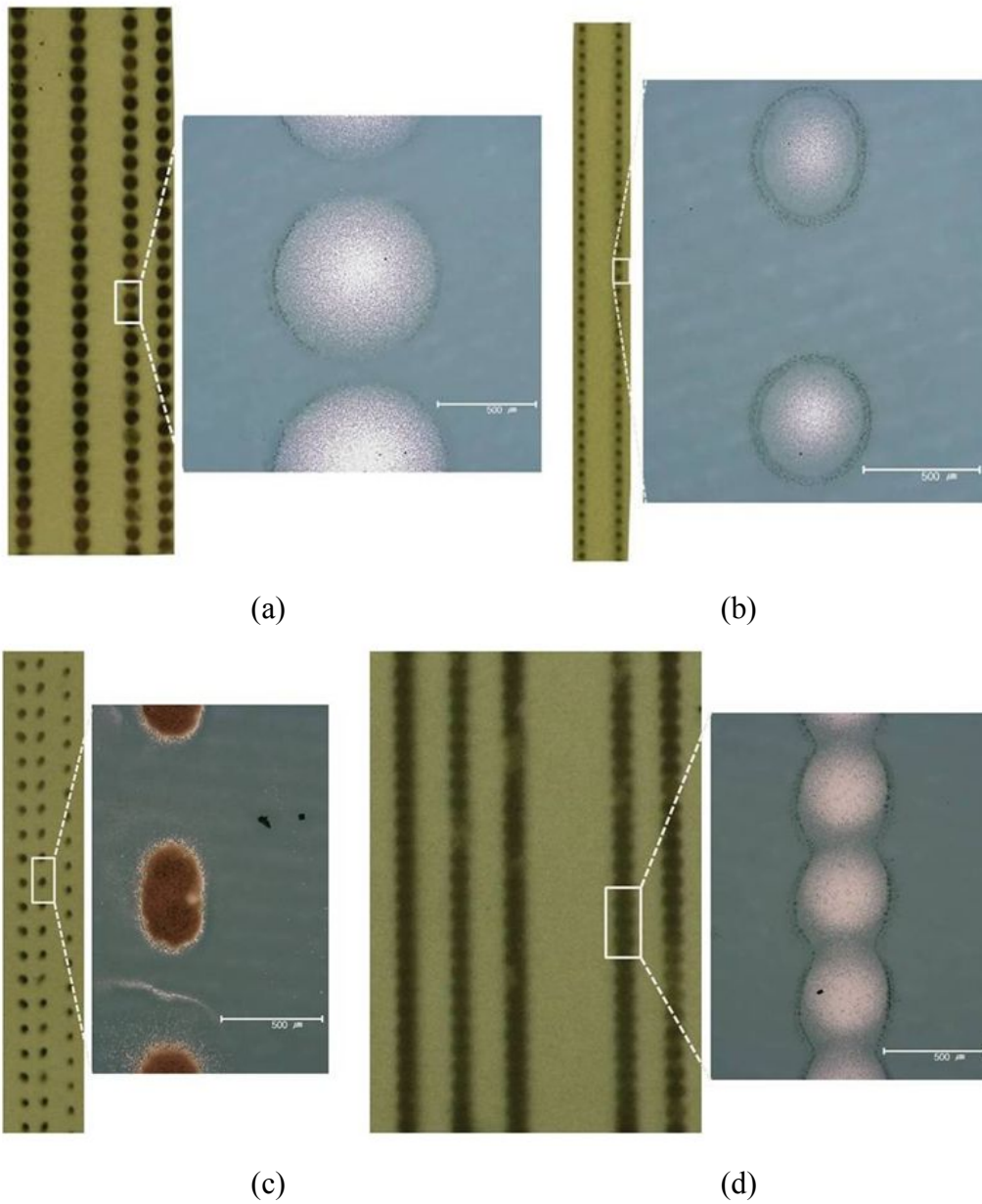
Figure 3.7 Color static camera and microscopic images of deposited droplets and line patterning resulted by drop-on-demand ejection at constant flow rate and constant substrate speed: (a) 50 kHz and 50% duty cycle, (b) 25 Hz and 50% duty cycle, (c) 10 Hz and 75% duty cycle and (d) the line pattern by drop-on-demand at 100 Hz and 75% duty cycle

3.2.2 DOD Patterning of Ag Nanoparticles

The experimental set-up was developed in house. A stainless steel needle having a

normal edged exit (90^0 to the needle axis) with an internal diameter of 210μm and an

external diameter of 410μm was held in a holder made of acrylic. Copper plate was placed 500μm below the needle exit as ground/counter electrode. Glass having 500μm thickness was placed as a substrate on top of ground plate. The needle and the ground electrode were connected to a high voltage power supply (10/40A Trek Model, USA). Forward multi-step waveform superimposed on biased DC voltage (shown in Fig1c) was supplied by this high voltage power supply. The needle inlet was connected to a syringe pump (PHD 2000 Infusion, Harvard Apparatus, USA). The behavior of the dripping was monitored with the help of a high speed camera (x3, 11X, 5000fps, Motion Pro, USA). High voltage power supply, syringe pump, high speed camera, moving stage (for substrate motion) and movement of head holder (to adjust the distance between needle exit and ground plate) were connected through a hardware system (PXI-1042Q, National Instruments, USA), controlled by a lab developed software based on LabVIEW. The forward multi-step waveform, applied voltage, frequency and duty cycle were also controlled with the help of this customized software.

The numbers of experiments were performed by changing the value of "Va", "Vb" and "Vc". The frequency of the multi-step voltage was at 50 Hz and with flow-rate 75μl/hr. The droplet diameter on the substrate at different multi-step voltage is shown in table 3.2. As shown in table 1, in Case-1 the droplet diameter was larger due to spray because at high voltage the droplet carries more charge. As in Case-5 and 6 the droplet diameter was smaller due to more stable phenomena. The microscopic image of the printed droplet on glass substrate after sintering for Case-1 and Case-6 is shown in figure 3.8.

Case	V_a(kV)	V_b (kV)	V_c (kV)	Approx. Droplet Diameter (μm)

1	0	2	4.1	200
2	1	2	4.1	189
3	2	3	4	160
4	3	3.5	4	126
5	3	3.2	3.7	106
6	3.2	3.5	3.8	82

Table 3.2Droplet Diameter at different applied multi-step voltage
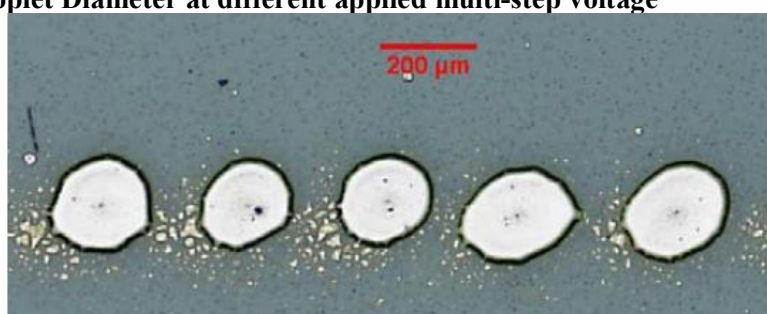
(a)
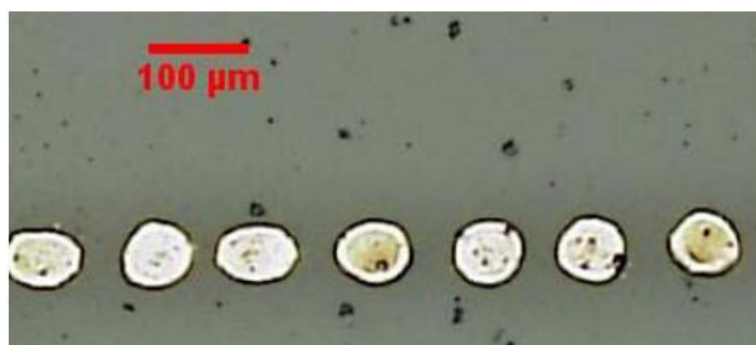
(b)

Figure 3.8 (a) Case-1 and droplet diameter approximately 200μm and (b) case-6 and droplet diameter approximately 82μm

In order to analyze the effect of frequency on the DOD pattering, the experiments were performed by changing the applied frequency. The applied multi-step voltage was kept as Case-6 (Va=3.2kV, Vb= 3.5kV and Vc=3.8kV) and flow-rate 75μl/hr. The measured droplet diameter on the glass substrate against the frequency is shown in graph at figure 3.9. The droplet diameter decreased from 120μm to 40μm as the frequency increases from 10Hz to 350Hz. The maximum applied frequency at which the DOD phenomenon was observed for the silver ink was 350Hz of applied frequency. This was due to short pulse times at high frequency, the voltage required to generate the jet is applied in shorter time i.e. jetting time decreases due to which

droplet diameter decreases at higher frequencies. Figure 3.10 shows the microscopic images of the droplets after sintering by applying 10Hz and 350Hz frequency. The result also indicates the size of the droplets was much smaller than the nozzle size which is the main advantage of electrohydrodynamic DOD technique.
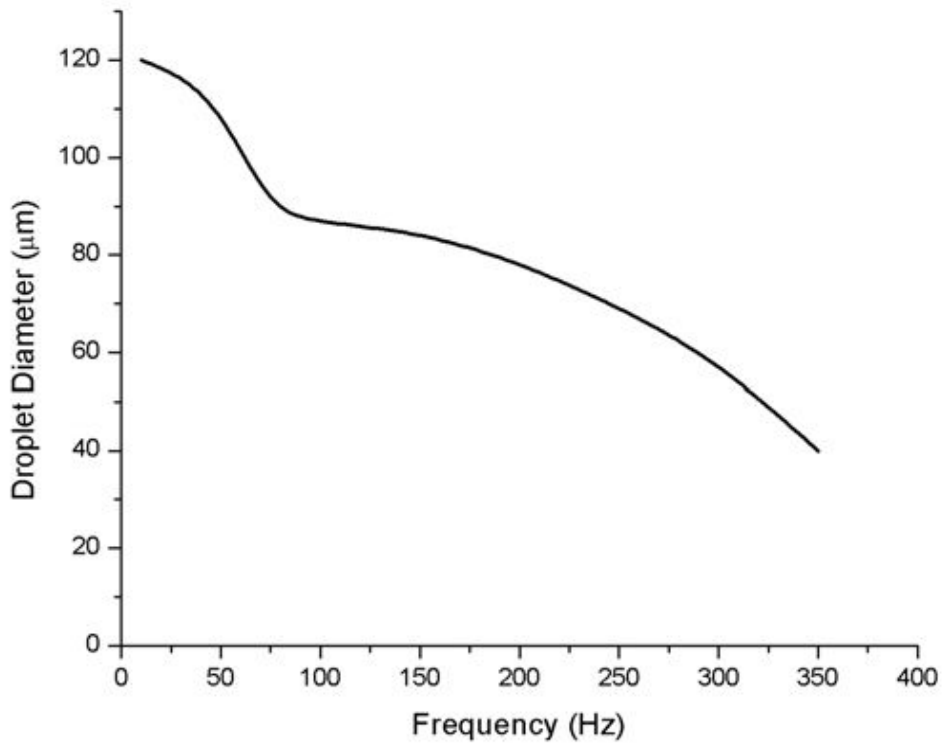
Figure 3.9 Droplet diameter vs. applied frequency
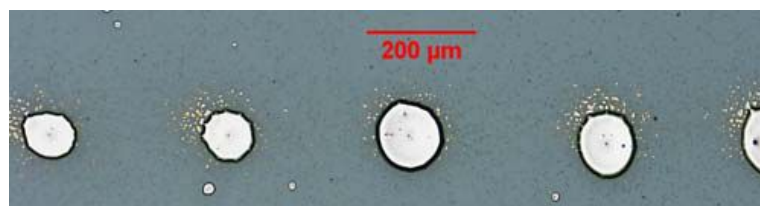
(a)
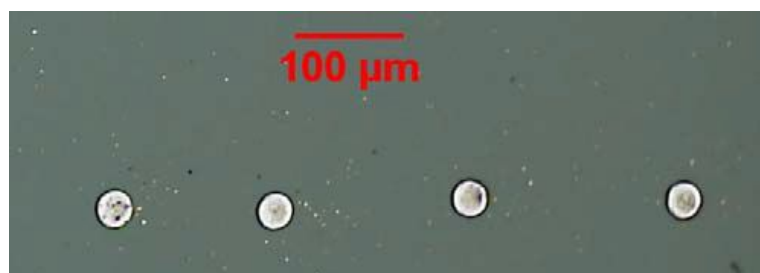
(b)

Figure 3.10Microscopic images of the sintered droplet by applying Va=3.2kV, Vb=3.5kV, Vc=3.8kV and flow-rate 75μl/hr (a) applied frequency 10Hz and diameter approximately 120μm (b) applied frequency 350Hz and droplet diameter approximately 40μm

The pattern line was formed after synchronizing the substrate speed with the DOD frequency by analyzing the droplet spacing on the substrate. The sequential images of the DOD line patterning with respect to applied multi-step pulse voltage at Va=3.2kV, Vb=3.5kV, Vc=3.8kV, flow-rate 75μl/hr and frequency 100Hz along with the pattern line are shown in figure 3.11. The pattern size shown was approximately 95μm, the line pattern size was greater thanthe droplet size (87μm) and this was due to the over lapping of the droplets to create the line pattern.
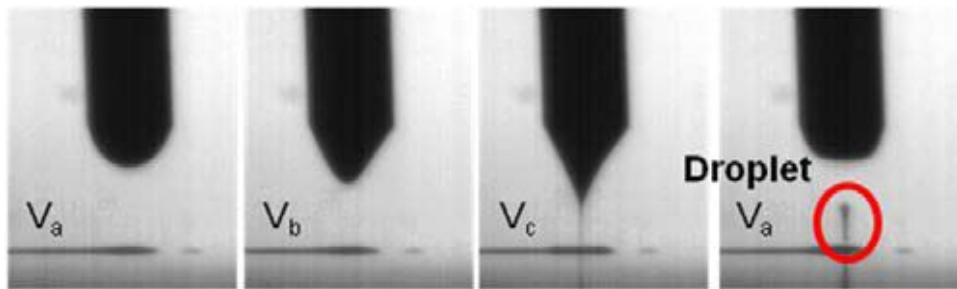
(a)
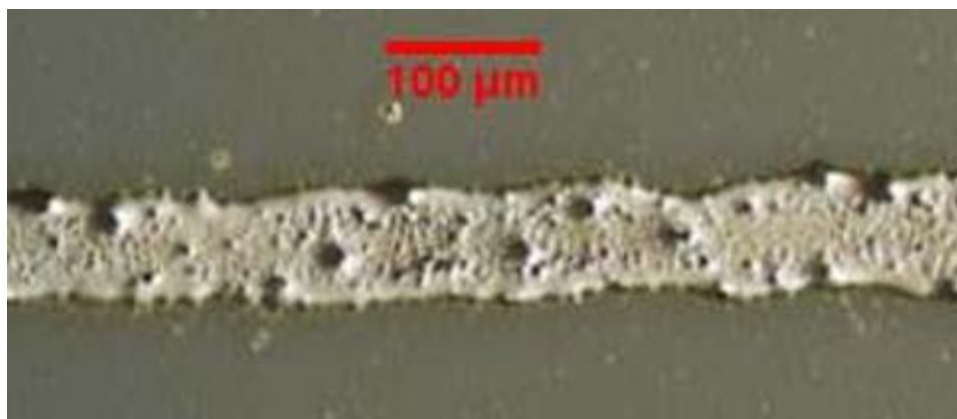
(b)

Figure 3.11 (a) Sequential images of the DOD pattern on the glass substrate with respect to applied multi-step pulsed voltage and (b) microscopic image of the line pattern after sintering process

Figure 3.12 shows the XRD spectrum of the printed line pattern on the glass substrate. The XRD spectrum peaks shows only the existence of the silver, which confirms that the deposited material was consisted of silver nanoparticles
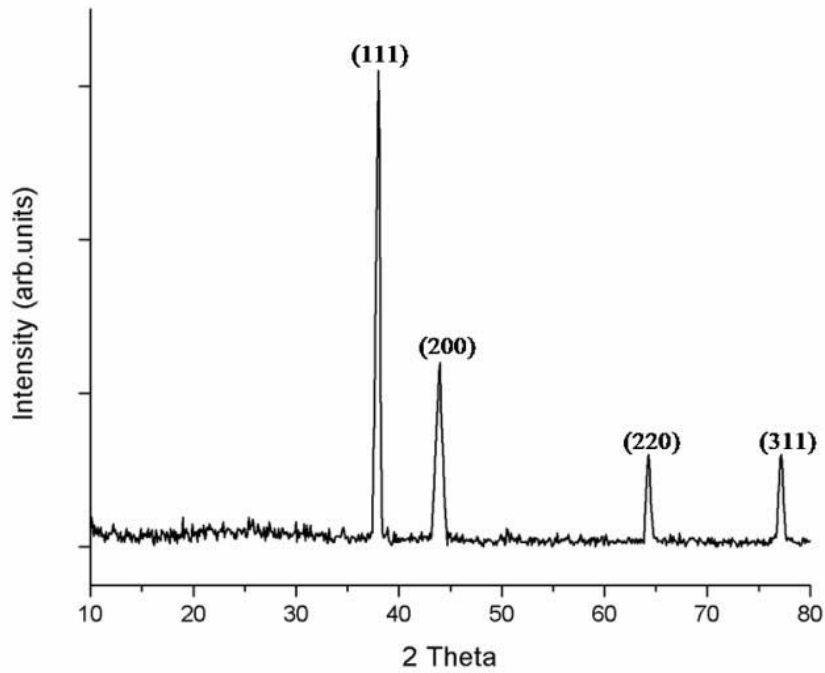
Figure 3.12XRD spectrum of the line pattern

The resistance of the pattern line was measured by 4-point probe method by measuring the voltage drop ΔV across 2mm long segment of the line pattern by applying the different current intensity of 10μA, 20μA, 50μA, 75μA and 100μA. The pattern line showed the linear ohmic behavior with resistance of 0.39Ω. I-V curve obtain through 4-point measurement is shown in figure 3.13.
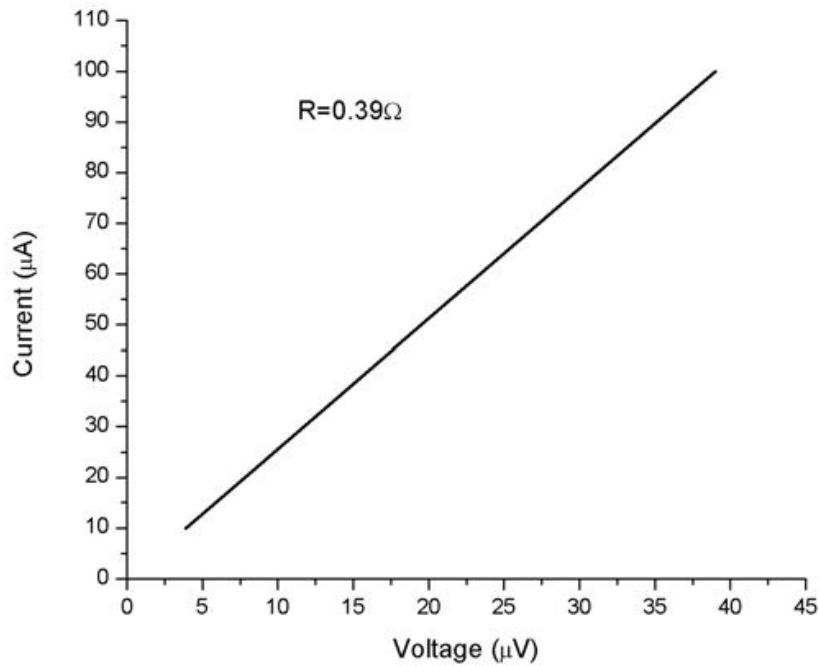
Figure 3.13I-V curve of the pattern line

The chapter presents the novel technique of electrohydrodynamic DOD by applying multi-step voltage. The results show that electrohydrodynamic DOD phenomena could be achieved through multi-step voltage, which provides stable and controlled process as compared to square pulse voltage. The experimental data shows that, the multi-step voltage at optimal values gives stable DOD jetting. The low value of bias-voltage causes more movement in meniscus, and also require higher value of ejection-voltage, due to this the phenomenon was not smooth. The other effect on the DOD phenomena is due to frequency and flow-rate.

4. Fine Resolution Electrohydrodynamic Patterning

There has been advancement in the field of inkjet printing beyond the conventional digital graphic arts printing. Inkjet printing has been widely used to deposit various functional materials for fabrication of devices or device components in printed electronicsand bio-applications etc. The inkjet based deposition has various advantages as follows(Forrest 2004, Gans et. al. 2004, and Parashkov et. al. 2005):

1. Purely additive process, functional materials can be deposited only where they are needed.
2. Can deposit various kinds of materials: inorganic, organic and biomaterials that are incompatible with established patterning technologies such as photolithography.
3. Applicable to large are area and various kinds of substrates
4. Low operating cost.

Conventional inkjet printing systems use thermal or acoustic energy to push the liquid from the nozzle for droplet generation(Parashkov et. al. 2005). But these conventional inkjet printing systems have certain limitations, such as, thermal problem due to heating and cannot produce droplets smaller than nozzle diameter apart from the limitation of materials to be deposited(Szczech et. al. 2002). In case of aqueous inks the drop size is twice the droplet diameter ejected from the nozzle.The conventional inkjet printing methods can typically produce the pattern size of 20-30µm(Ling and Bao 2004, Calvert 2001, Sanaur et. al. 2006, and Cheng et. al. 2005). In order to achieve these resolutions or to minimize the feature size through conventional inkjet printing, substrate modification/treatment is necessarily required to modify the droplet and substrate interaction or printing on pre-patterned or textured substrates to restrict the pattern size. For example, many researchers have predefined in order to assist the feature through lithography or by modifying the surface wetting morphology of the substrates by controlling the flow of the droplets as they landed on the substrate(Sirringhaus et. al. 2000, Wang et. al. 2006, and

Stutzmann et. al. 2003). These methods help in controlling the gap between the printed features in sub or micron levels. However, these methods do not contribute to the fine resolution of the pattern features and also require separate patterning system and processing steps to define the assist features.

In order to reduce the pattern size, many researchers are focusing on the electrohydrodynamic jet based printing method. Electrohydrodynamic jet printing (Park et. al. 2007)uses electric field by overcoming the surface tension to pull the liquid from the nozzle opening to deposit the material on the substrate rather than pushing the liquid as in case of conventional inkjet printing. Due to pull of the liquid, electrohydrodynamic printing can produce smaller size patterns as compared to the nozzle diameter. Depending on the applied electric field (DC or pulse voltage), electrohydrodynamic jet printing can be continuous or drop-on-demand. Both continuous and drop-on-demand mode can produce micro or even nano-size patterns. This chapter explains the fine resolution patterning of the conductive materials using electrohydrodynamic patterning technology in continuous as well as drop-on-demand mode on untreated substrate.

4.1 Fine-resolution pattern through continuous EHD

Electrohydrodynamic printing is performed by applying high voltage on meniscus of the liquid containing the nanoparticles in the cone-jet mode. In electrohydrodynamic jetting high voltage is applied to the liquid in the nozzle, which causes the mobility in ions, which then accumulate at the meniscus of the liquid at nozzle outlet. When the Columbic repulsive forces due to ions in liquid meniscus exceed a certain limit of the liquid surface tension force, the meniscus is deformed into a conical apex(Poon 2002). Depending on liquid properties and applied conditions, different modes of dripping and jetting can be observed. When liquid is pumped into a capillary in the absence of electric field, liquid droplets break-off and fall away. The size of the droplets is larger than the nozzle size, this mode is known as dripping mode. With the application of the voltage, the size of the droplets decreases and the dripping frequency increases which is known as micro-dripping. Increasing further the applied

potential the intermittent cone-jet is formed, where the meniscus is followed by ejection of droplets, this mode is also known as a pulsating cone-jet. With a further increase in the potential difference, a stable cone-jet emerges from the apex of the cone. This cone-jet is of major interest because of a large neck-down ratio between the jet and nozzle diameter(Poon 2002). Further increase in the voltage makes the cone-jet unstable and multiple jets emerge from the nozzle orifice, which is known as the multi-jet mode. This transition of stable cone-jet formation depends on liquid properties (surface tension, viscosity, electrical conductivity and dielectric constant) as well as operating parameters (applied electric field, flow-rate and nozzle diameter)(Poon 2002). For any given liquid, the most important parameters for controlling the behavior and stability of cone-jet are the flow rate and electric field (applied voltage).

For printing of conductive patterns, most researchers have focused on the ink containing silver or gold particles because of high functional performance(Fuller et. al. 2002, Perelaer et. al. 2009, Lee et. al. 2006, and Nur et. al. 2002). However, these materials are expensive to be used for mass production. Copper is another attractive alternative material because of its low cost and the same functional performance as that of silver and gold. The patterning of copper nanoparticles performed through inkjet technology has been reported previously(Park et. al. 2007, Kang et. al. 2010, Kim et. al. 2011, and Jeong at. Al. 2011).

This section presents the low-cost, fine-resolution printing of conductive copper patterns on silicon substrate. The colloidal solution containing copper nanoparticles is deposited through electrohydrodynamic printing technology. Conductive copper tracks of different width are printed by varying the operating conditions (applied voltage and flow rate) and controlling the jet diameter. The minimum pattern width achieved was approximately 12μm with the average thickness of 82nm across the width after the sintering process. The achieved pattern width is five times smaller than the capillary used for patterning. The morphology and purity of the printed copper tracks were analyzed through scanning electron microscopy (SEM), atomic force microscopy (AFM) and x-ray diffraction (XRD). The current–voltage (I–V)

characteristic of the printed copper tracks showed linear Ohmic behavior and exhibited resistivity ranging from $5.98 \times 10^{-8}\,\Omega/\text{m}$ to $2.42 \times 10^{-7}\,\Omega/\text{m}$.

4.1.1 Experimental setup

For fine-resolution patterning through electrohydrodynamic jetting, a lab-developed system was used. The system used for printing consisted of a tapered glass capillary, a glass capillary holder mounted on the motorized Z stage, a high voltage power supply, a syringe pump for ink supply, $X\text{–}Y$ stage with a motor controller for substrate movement and a high-speed camera for the observation of the jetting behavior. For patterning, a 60μm internal diameter tapered glass capillary was used; the tapered glass capillary was formed by pulling a glass tube of 750μm internal diameter and 1.5mm external diameter by using a micropipette puller (P-97, Shutter Instrument). The 500μm diameter copper wire was inserted into the glass capillary to apply the positive electric potential to the ink containing copper nanoparticles. A 1mm thick highly doped, 20mm × 20mm p-type silicon substrate was used by making the printing side nonconductive through a thermal oxidation process (SiO_2 layer), and the thickness of the SiO_2 layer was 300nm. The silicon substrate was placed on the metallic ground plate mounted on the motorized X–Y stage. The ink containing 30 wt% of 40nm copper nanoparticles with value of surface tension of 41.4mN/m, viscosity 4.5mPa.s, conductivity of 14.2mS/cm and relativity permittivity of 57.5 was used for experiments, which was obtained from Korea Research Institute of Chemical Technology (KRICT). A schematic of the electrohydrodynamic printing experiments system with the actual experiment system used for fine-resolution patterns is shown in figure 4.1.

After sintering of the printed copper patterns at 250°C for 30 minutes, the chemical composition was investigated by XRD (RIGAKU D/Max 2200 PC). The width of the patterns was measured through the digital microscope (Olympus BX51M), morphological features of the patterns were evaluated by the three-dimensional analysis with the help of AFM (EM4SYS AFM-100). The structural integrity of the copper nanoparticlesin the pattern after sintering was confirmed through SEM (JEOL

JSM-7600F). The electrical characterization was performed by measuring the I–V curve (Agilent B1500A).
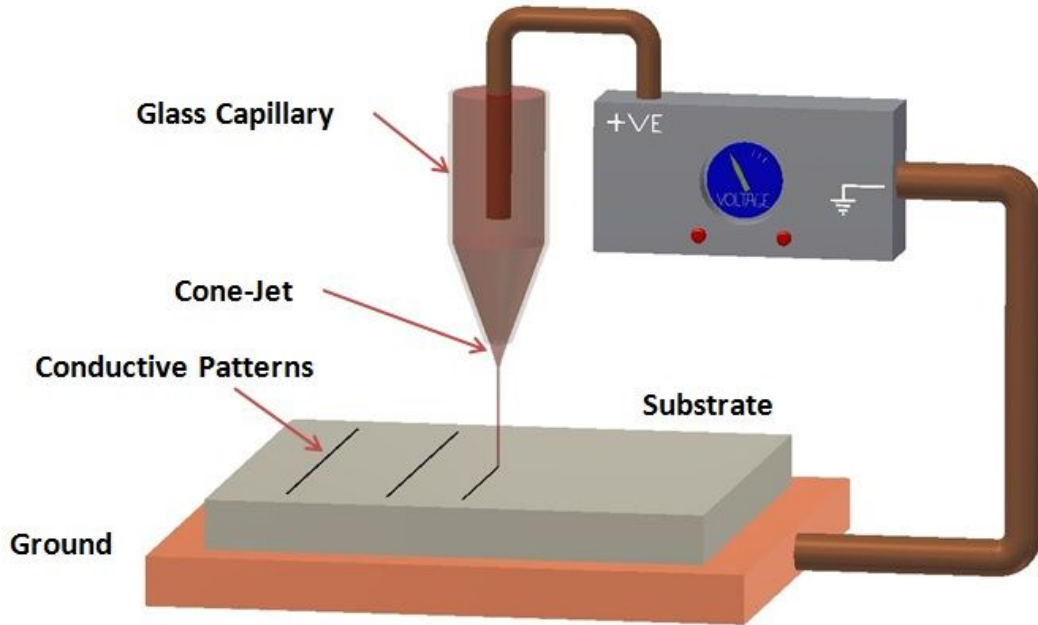
(a)
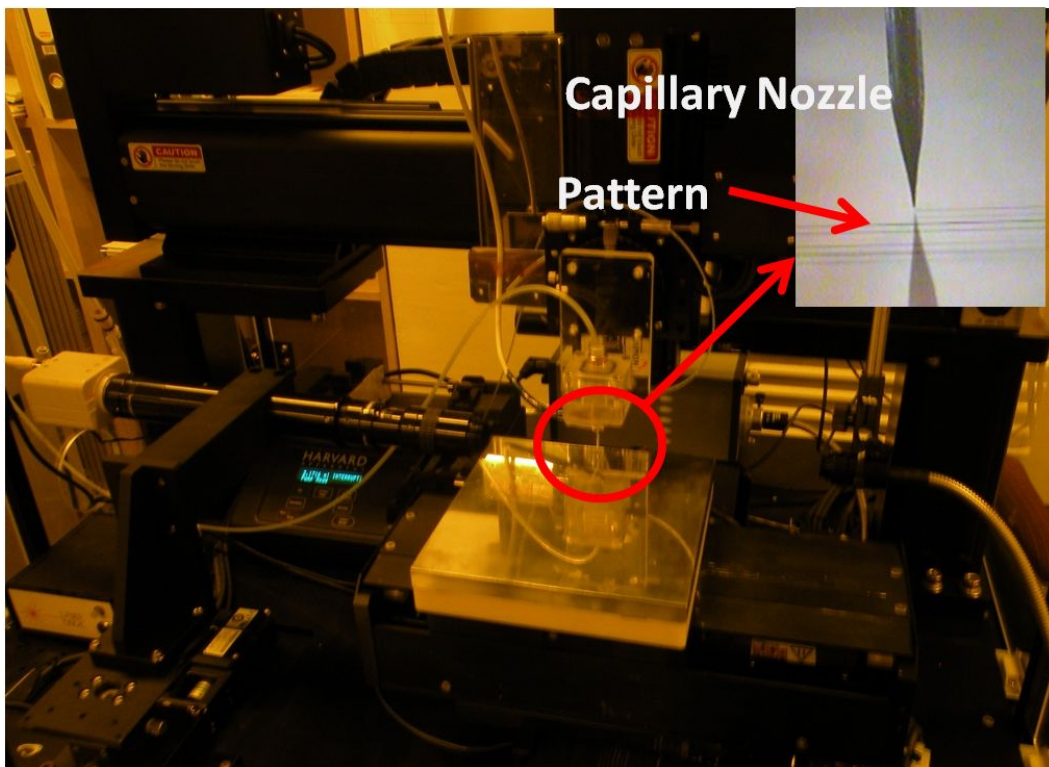
(b)

Figure 4.1(a) Schematic of the experimental electrohydrodynamic jet printing setup. (b) Lab-developed system used for electrohydrodynamic jet printing, inserted image showing the printing process on the substrate

4.1.2 Electrohydrodynamic patterning of copper nanoparticles

For printing of fine-resolution patterns through electrohydrodynamic jetting a stable and continuous cone-jet mode is required for any given ink containing nanoparticles. The reason of printing in stable cone-jet mode is due to formation of very stable micron size jet from the apex of the cone(poon 2002). For the generation of a stable cone-jet, the operating envelop (applied voltage and flow-rate domain) has to be investigated for ink containing copper nanoparticles. The lower and upper voltage limits of the stable cone-jet region vary with the flow rate and they also depend on the ink properties such as surface tension and conductivity. A number of experiments were performed to find the operating envelop, i.e. lower and upper limits of the applied voltage by varying the flow rate by using a 60μm internal diameter glass capillary by the increment of 5μl/h flow rate and varying the applied voltage, as the distancebetween the nozzle and ground plate was kept at 1.5mmand placing a 1mm thick silicon substrate between the nozzleand ground. The dripping or jetting behavior was observed byusing a high-speed camera.

The operating envelop of the ink containing coppernanoparticles is shown in the graph in figure 4.2. As shownin the graph, the minimum flow rate at which the stable cone-jetwas observed was 5μl/h withthe applied voltage rangeof 0.8~1.28kV. The stable cone-jet region was investigatedtill the applied flow rate of 50μl/h at an applied voltagerange of 1.1~1.53kV. The stable cone-jet is the resultant ofa balance between surface tension forces, applied electricalforces, inertial forces and viscous forces. When the flow rateis below the stable cone-jet region, the velocity of liquidis insufficient to balance the forces required to generate thestable cone-jet at any given applied voltage. At a higher flowrate, more electric potential is required to create the balancebetween the forces to generate the stable cone-jet region. Inelectrohydrodynamic jetting, below the operating range of thestable cone-jet, pulsating phenomena were observed, whichcan be classified as a dripping or a pulsating cone-jet dependingon the applied voltage. When the applied voltage exceeds theupper limit of the stable cone, the cone-jet deforms into a number of small jets which is known as a multi-jet mode. High-speed camera images of

dripping behavior at 25μl/h with an applied voltage of 0.75kV and a stable cone-jet at 25μl/h with an applied voltage of 1.3 kV are shown in figure 4.3.
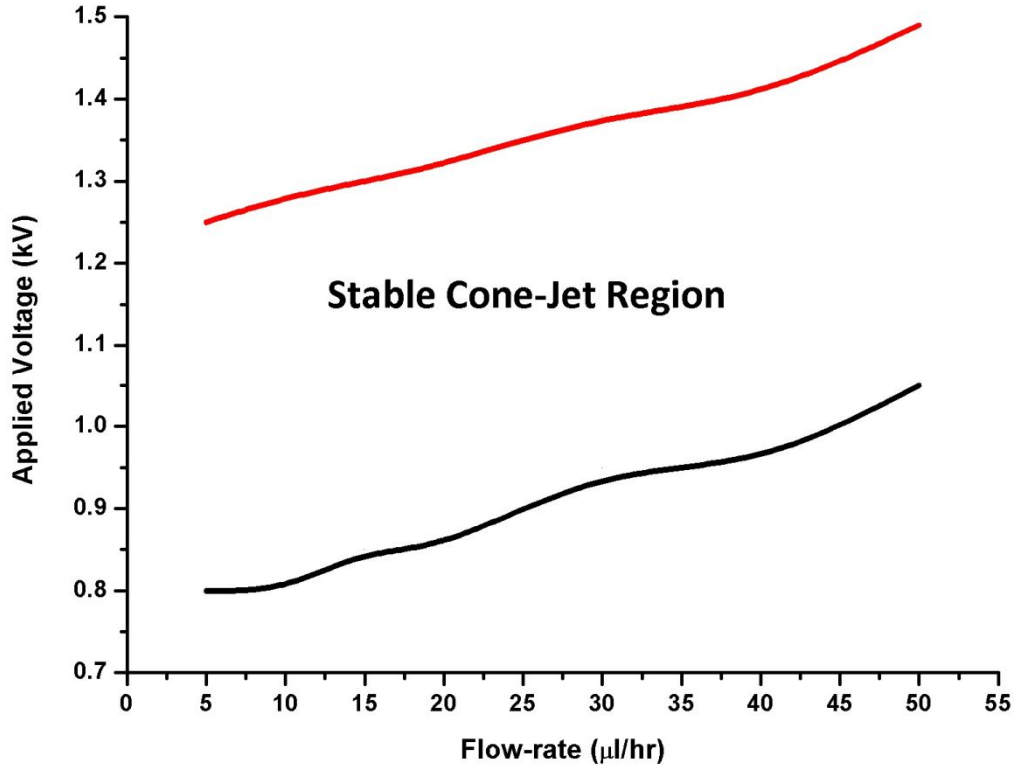
Figure 4.2Operating envelope for the stable cone-jet with upper and lower limit of the applied voltage at corresponding flow rate
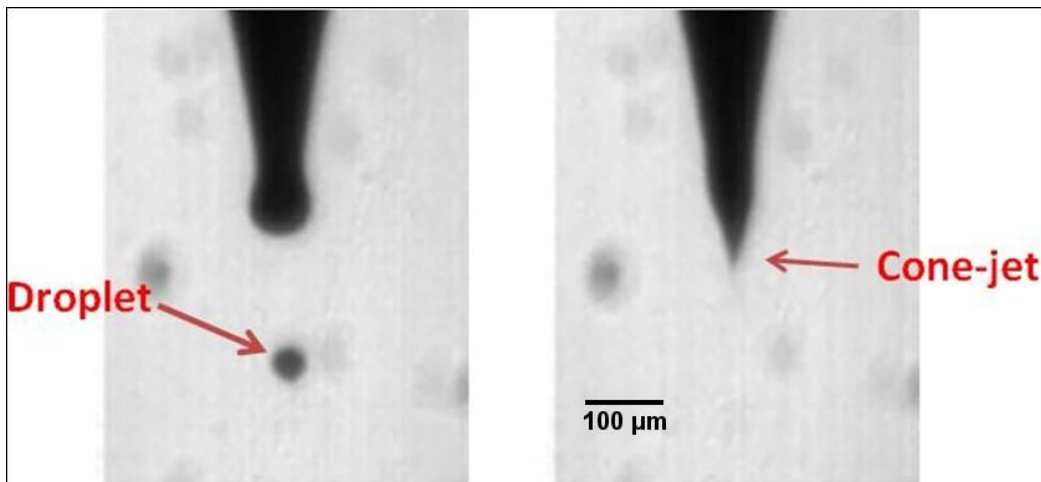
Figure 4.3Dripping behavior at an applied voltage of 0.75kV (left) and stable cone-jet at an applied voltage of 1.3kV (right), whereas the applied flow rate of 25μl/h using 60μm tapered capillary

After investigating the stable con-jet region, 15mm long patterns were printed on the silicon substrate in the cone-jet mode by applying upper limits of voltages in the operating envelop at the corresponding flow rate. For patterning of copper nanoparticles, the distance between the nozzle andsubstrate was kept at $500\mu m$, and the speed of the substrate was kept at 25mm/s by depositing the single layer for each experiment under different operating conditions (flow-rate and applied potential). Patterning through the cone-jet mode required pinning of a micron size jet on the surface of the substrate, whereas in conventional drop-on-demand printing (piezoelectric and thermal), patterning is performed by overlapping the ejected droplets. In order to ensure the stable pinning of the jet on the substrate and by avoiding the liquid bridge between the nozzle and substrate instead of cone-jet formation, the nozzle-to-substrate distance was kept at $500\mu m$ after studying the jetting behavior through a high-speed camera. The variation in pattern width with respect to the flow rate at the upper limit of the applied voltage in the stable cone-jet region is shown in figure 4.4. As shown in the graph, as the flow rate is increased the pattern width also increased. This difference in the pattern width is due to the difference in the jet diameter, as in electrohydrodynamic jetting the jet diameter strongly depends on the flow rate for any given liquid(Poon 2002). The minimum pattern width achieved during the experiment is approximately 12µm, which is 5 times smaller than the nozzle inner diameter. The effect of the applied voltage was also studied by measuring the pattern width by varying the applied voltage from the lower limit to the upper limit of the operating envelop at 5, 25 and 50µl/h as mentioned in table 4.1. As shown in the table the effect of the applied voltage on the pattern is negligible ascompared to the effect of the flow rate(Poon 2002). The literature of electrohydrodynamic jetting in the con-jet mode also suggested that the jet diameter is highly dependent on the flow rate, in some cases 2 order of magnitude (depending on liquid properties), whereas a typical change in jet diameters is less than 7% within the operating envelop of the steady cone-jet(Poon 2002). This shows that the main parameter to control the pattern width in electrohydrodynamic printing in the cone-jet mode is the flow rate rather than the applied voltage.
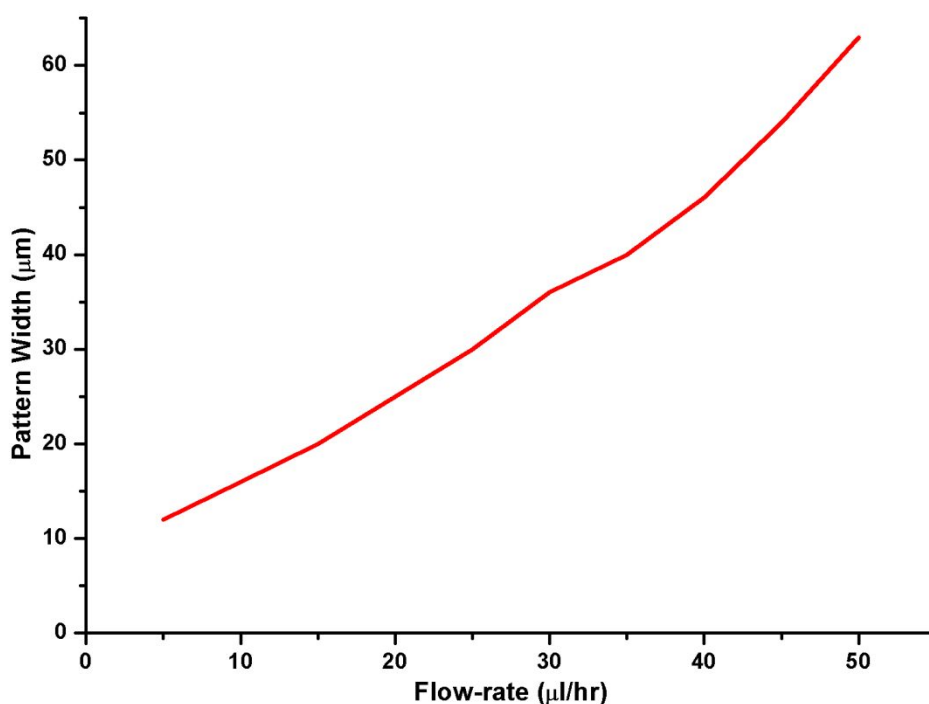
Figure 4.4Pattern width with respect to flow rate by applying upper limit of the applied voltage

Flow-rate (μl/hr)	Applied Voltage (kV)	Pattern Width (μm)
5	0.8	12.5
	1.04	12.5
	1.28	12
25	0.93	31
	1.15	30.5
	1.36	30
50	1.1	64
	1.31	63.5
	1.53	63

Table 4.1Pattern width with respect to the applied voltage at a different flow rate

After patterning of copper nanoparticles on silicon substrates, the patterns were sintered in a dry oven at 250°C for 30 minutes. Figure 4.5(*a*) shows the microscopic image of the patterns width of 30 and 63μm through electrohydrodynamic printing at the flow rates of 25 and 50μl/h by applying the applied voltages of 1.36 and 1.53kV, respectively. Figure 4.5(b) shows the microscopic image of the consecutive patterns of 12μm through 60μm capillary at a flow rate of 5μl/h by applying 1.28kV.As shown in the microscopic images of printed patterns through electrohydrodynamic

제주대학교 중앙도서관
JEJU NATIONAL UNIVERSITY LIBRARY

printing in the cone-jet mode, the patterns are uniform in size and also have smooth edges, which is the basic requirement for patterning of the conductive tracks.
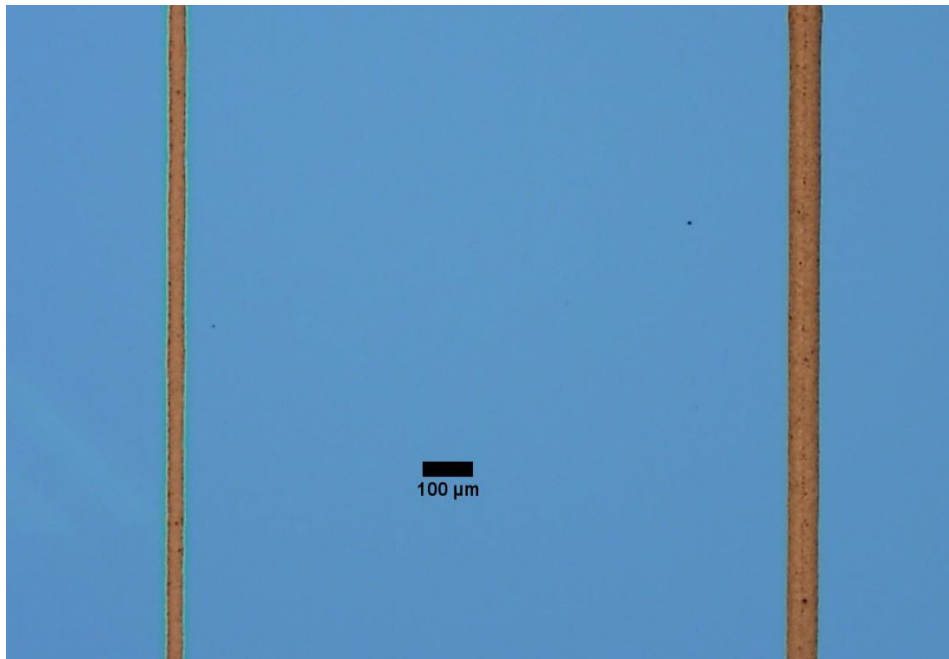
(a)
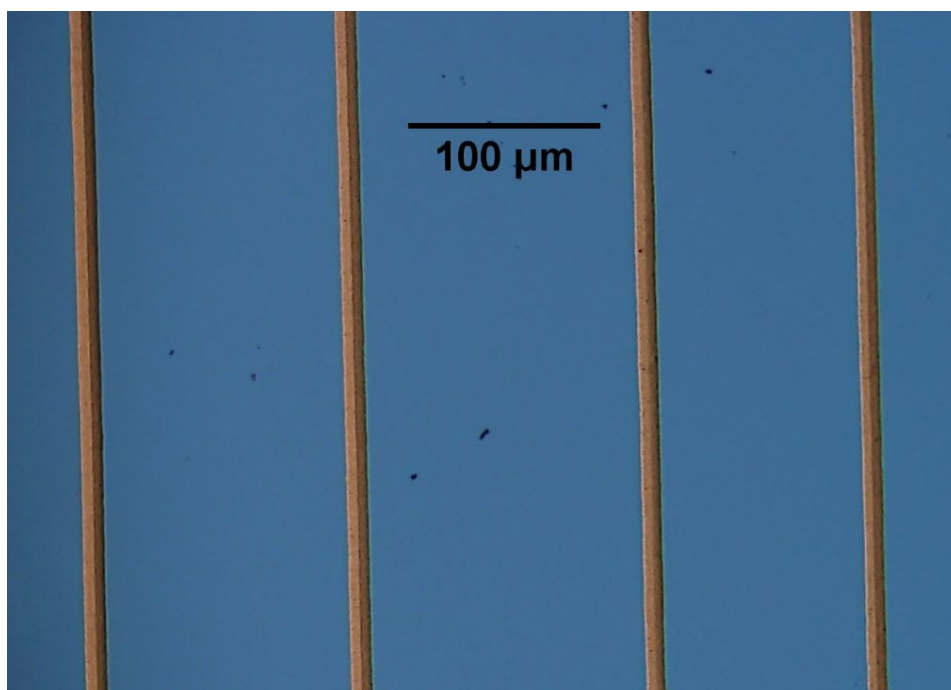
(b)

Figure 4.5(a) Microscope image showing the effect of flow rate on the printed pattern width; pattern on the left is 30μm in width and printed at 25μl/h and applying 1.36kV of applied voltage, whereas the pattern on the right side of figure is 63μm in width and printed at 50 μl/h and applying 1.53kV, and (b) Consecutive printed pattern of 12μm width at a flow rate of 5μl/h and applied voltage 1.28kV

4.1.3 Characterization

In order to investigate the composition of the copper particles after patterning, the XRD analysis was conducted. Figure 4.6shows the XRD spectrum of the chemical element measured from the surface of the pattern after sintering. The XRD spectrum confirmed that patterns deposited through electrohydrodynamic printing technology showed pure crystalline copper characteristics peaks without any copper oxide as a secondary phase.
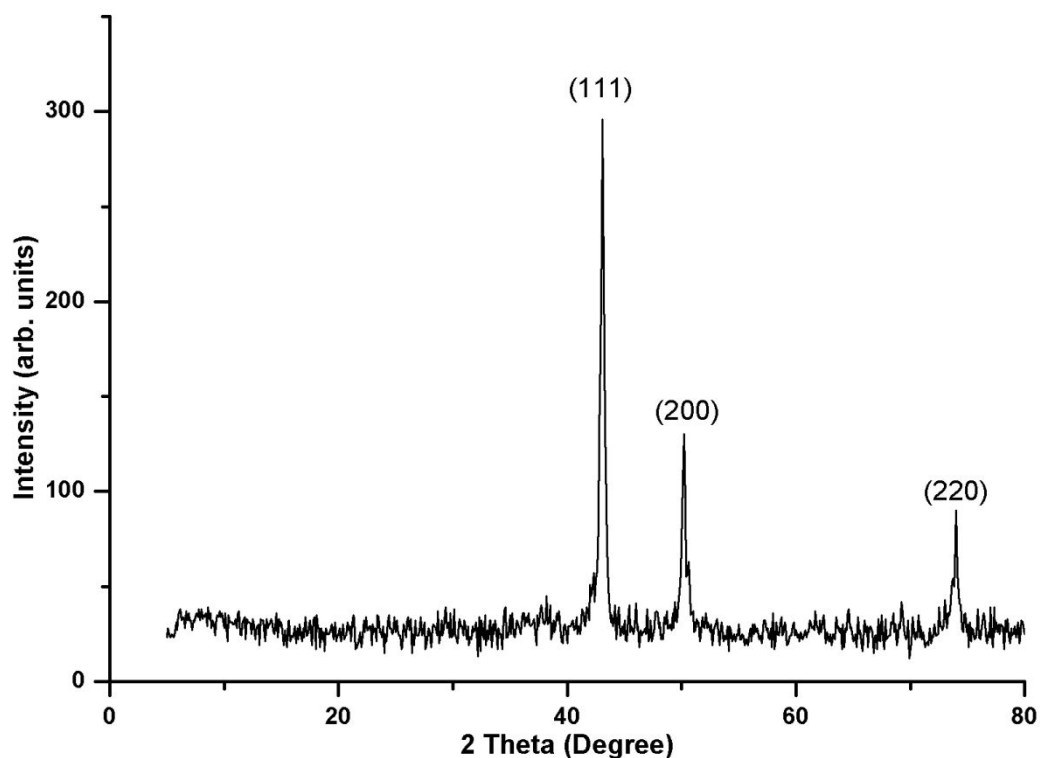
Figure 4.6XRD spectrum of the printed pattern of copper nanoparticles after sintering at 250°C for 30 minutes

In order to evaluate the morphological feature, three-dimensional analyses were performed with the help of AFM and also thicknesses of the patterns were measured. Figure 4.7shows the AFM data of the 12 and 63μm pattern widths printed on the silicon substrate. As shown in the figure, the maximum height of the 12μmthick pattern was 148nmand for the 63μm pattern the measured thickness was approximately 425nm. AFM results show uniform patterns with a smooth surface but also contained several hillocks which causes non-symmetry at different cross section

of the patterns(Chen et. al. 1996). These hillocks are due to the strong electric field between the nozzle and the substrate, which occurs because of preferential landing of the droplets on the substrate. These hillocks cause an increase in the surface roughness of patterns; however, this can be avoided by altering the electric filed, concentration of the nanoparticles and modifying the properties of liquid.
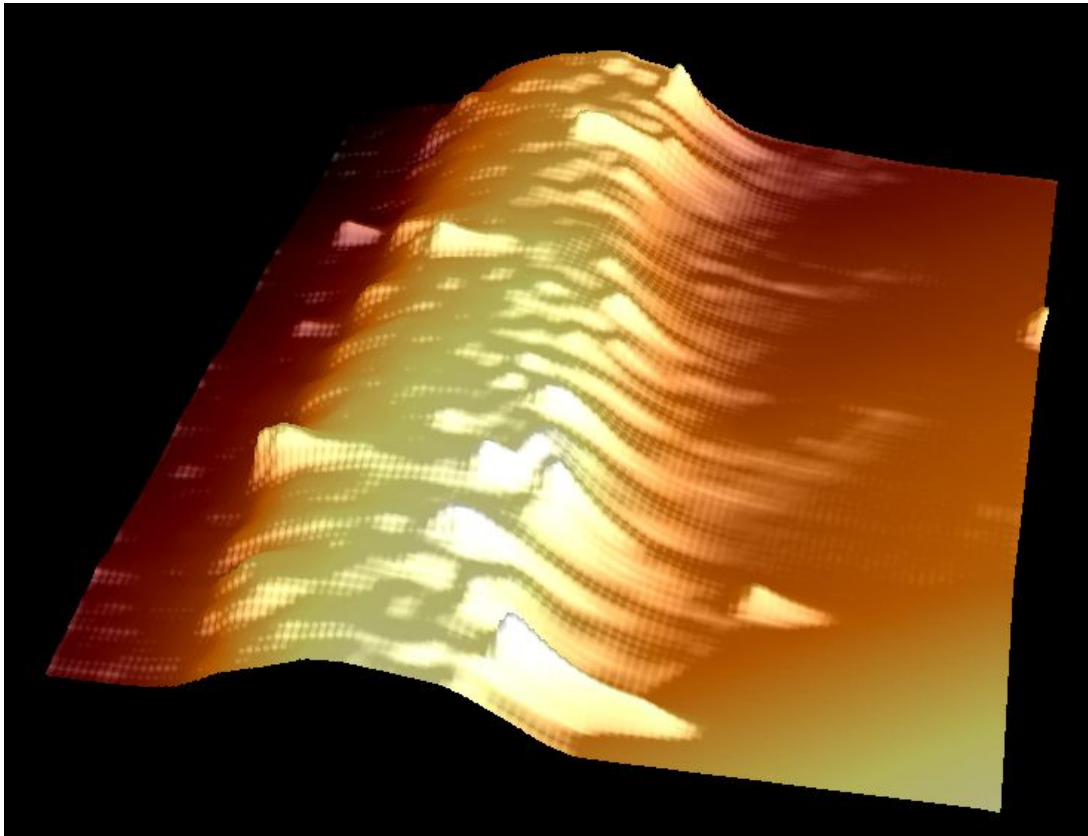
(a)
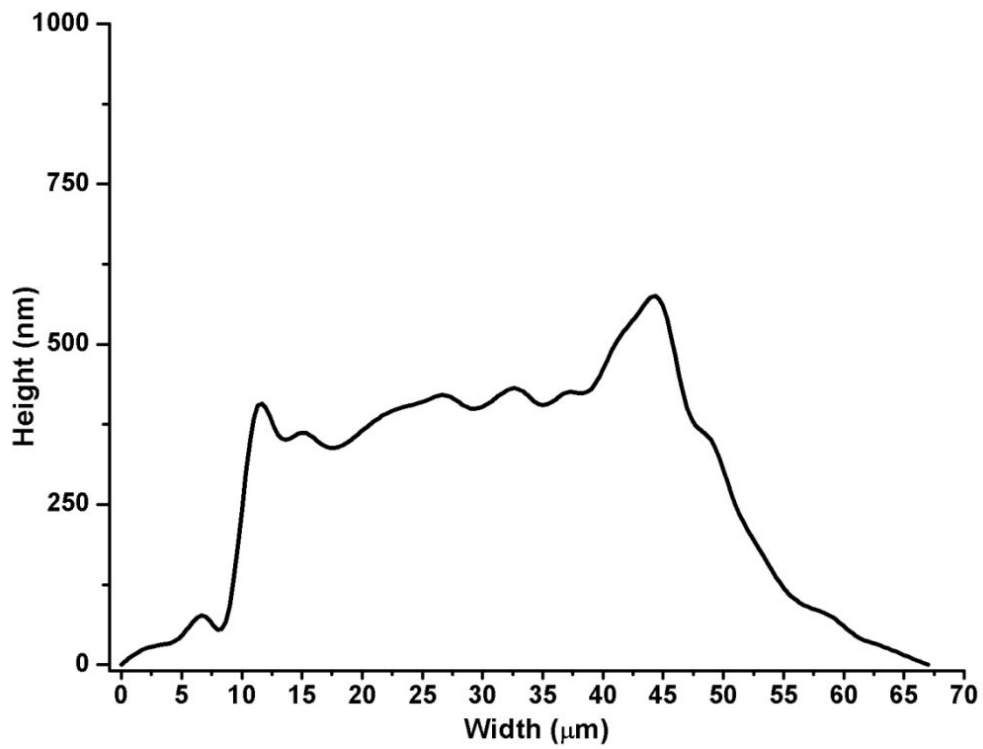
(b)
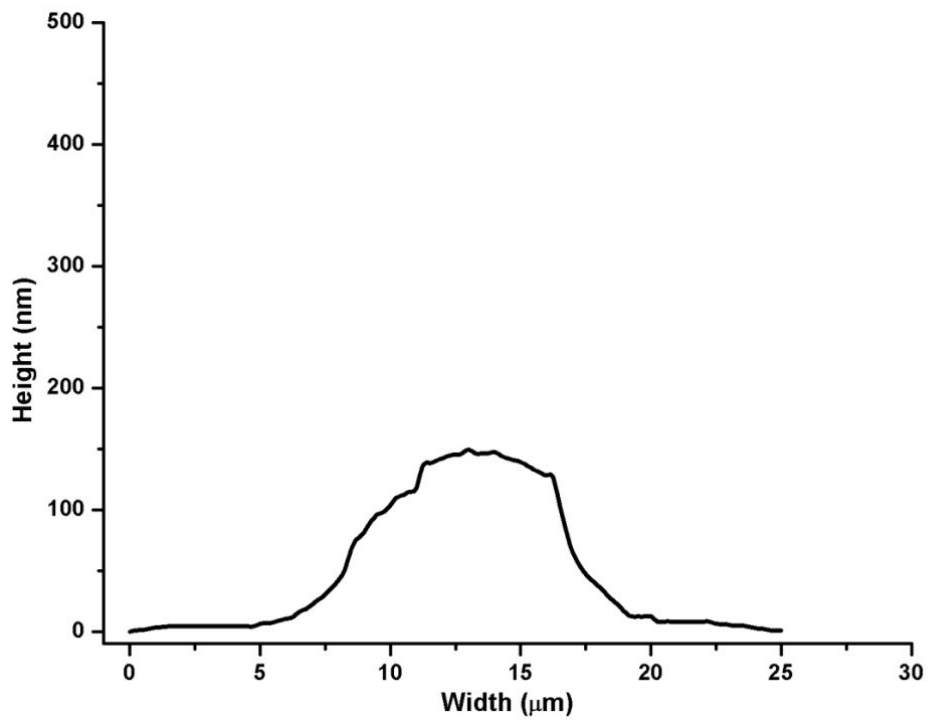
(b)

Figure 4.7(a) A 3D AFM image of the 63μm pattern. (b) Cross-sectional measured height of 450 nm for the 63μm pattern with an average thickness of 290.7nm. (c) Cross-sectional measured height of 148nm for the 12μm pattern with an average thickness of 82.3nm

In order to check the interconnectivity of the nanoparticles SEM analysis was performed. Figure 4.8 shows the SEM image of the 60μm printed pattern after the sintering process. As shown in the SEM image, the nanoparticles were interconnected three dimensionally; this favorably affects the electrical conductivity of copper patterns.
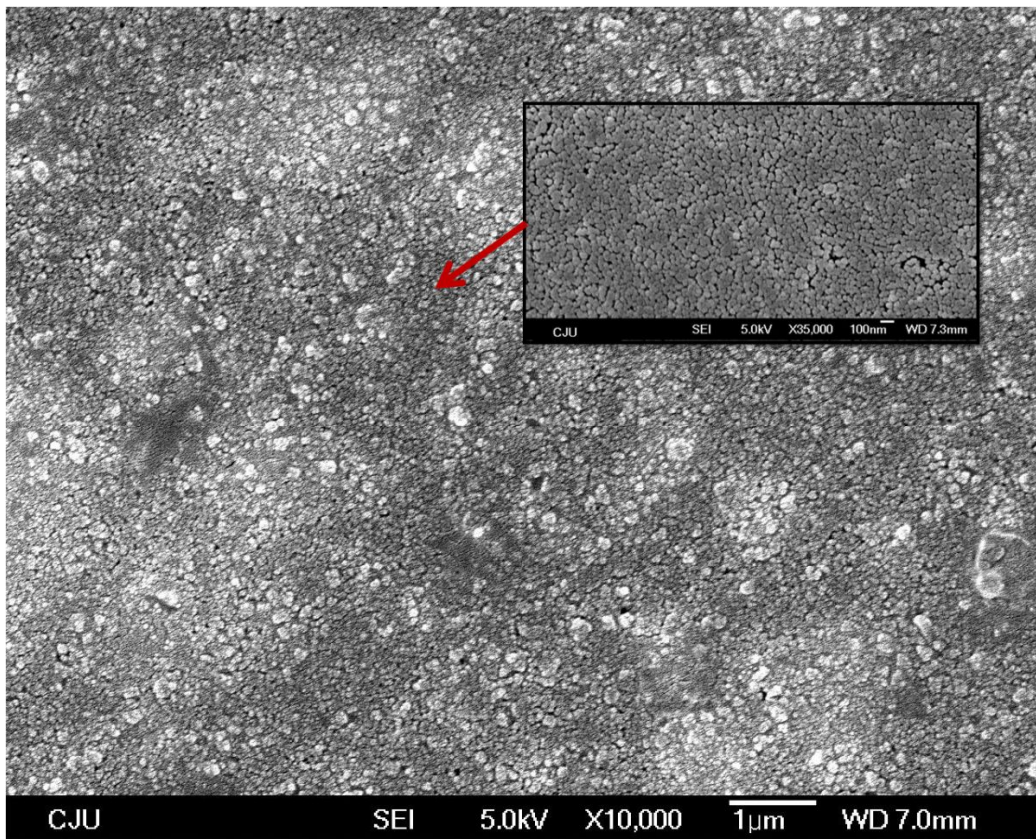
Figure 4.8SEM image of the printed copper tracks deposited by electrohydrodynamic jet printing showing the interconnection of copper nanoparticles after sintering process

In order to evaluate the electrical functionality of the conductive pattern the resistivity 'ρ_E' of the patterns and the resistance 'R' was measured with the help of I–V curve data by contacting two probes on sintered copper patterns. Five measurements were taken at each point at four different locations of the 15mm long pattern by measuring potential drop across 2mm length by applying current of different values. Figure 4.9shows I–V characteristics of the 12, 30 and 63μm copper patterns of five samples each by plotting the average value. Each patterns showed a good linear Ohmic behavior with approximately 5% error in the measured value. The

electrical resistivity ρ_E of the printed copper patterns were calculated by using the formula '$\rho_E = R.A/L$', where 'R' is the resistance of the pattern calculated with the help of average I–V curve data, 'A' cross-sectional area of the printed pattern and 'L' is the length of the pattern. The cross-sectional area 'A' of the patterns was calculated through 'A = w × t', where 'w' is width of the pattern and 't' is the average thickness of the pattern, measured through a microscopic image and AFM analysis respectively. 't' is calculated by averaging the thickness at ten equally spaced points along the width of the printed patterns. The electrical resistivity of the printed patterns is shown in table 4.2, whereas the bulk resistivity of the copper is $1.7 \times 10^{-8} \Omega/m$. The measured resistivity was approximately 3.5–14 times higher than the bulk resistivity with the error range of approximately −7% to 10%, due to the calculation using the average thickness of the patterns and also development of void or cracks resulting from formation of the coarse network of intermingled copper nanoparticles in the patterns during the sintering process. The reported results indicate that patterning of copper nanoparticles through electrohydrodynamic printing can be used for the printed electronics application for the fabrication of RFIDs and conductive tracks for TFT(Yin et. al. 2010).

(a)

66
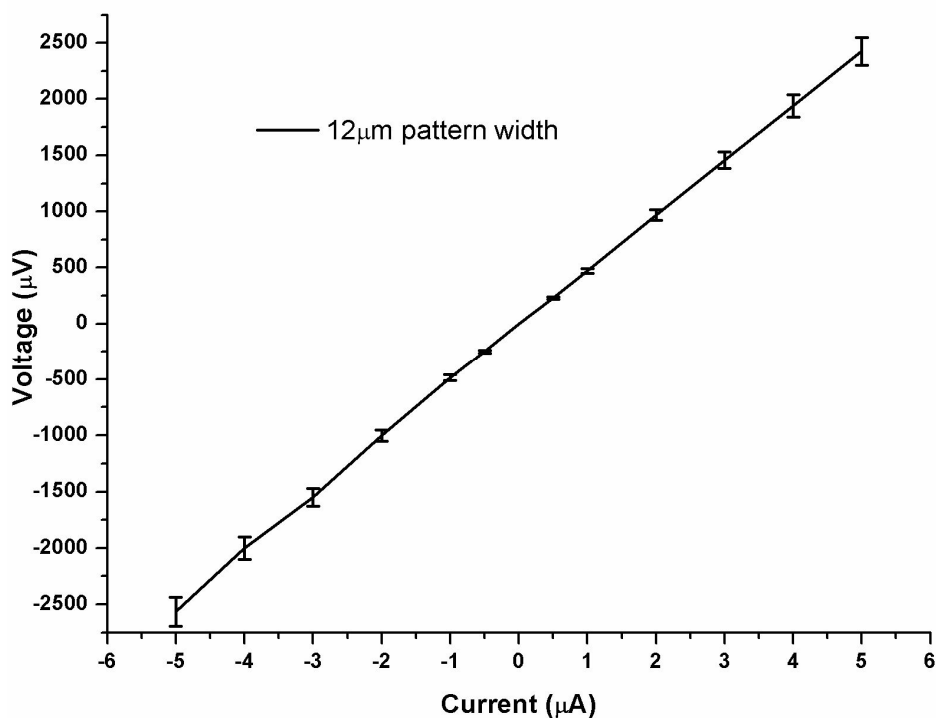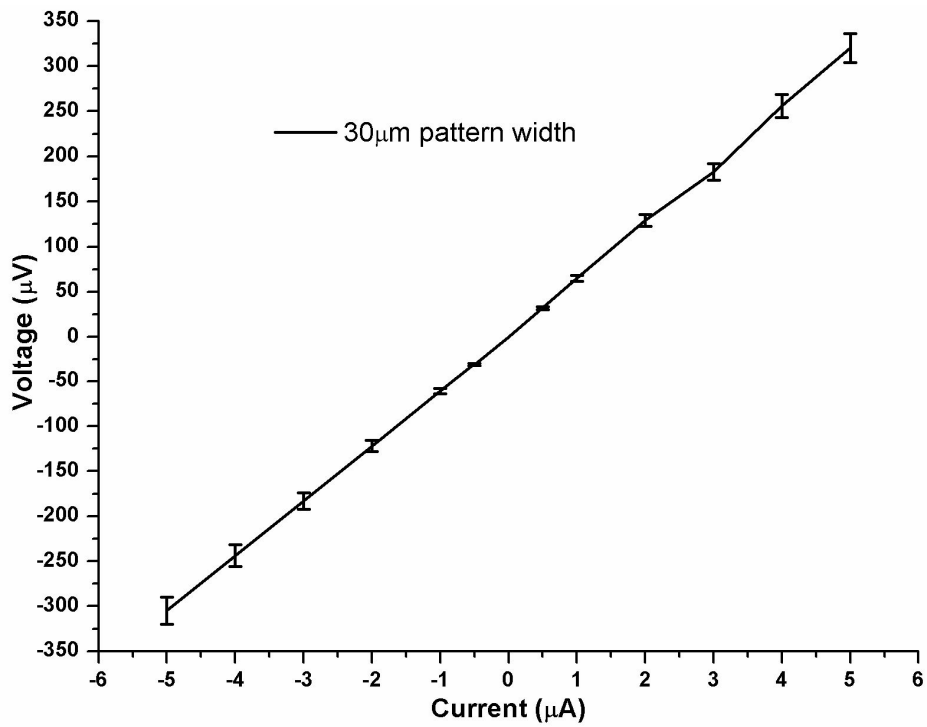
(b)
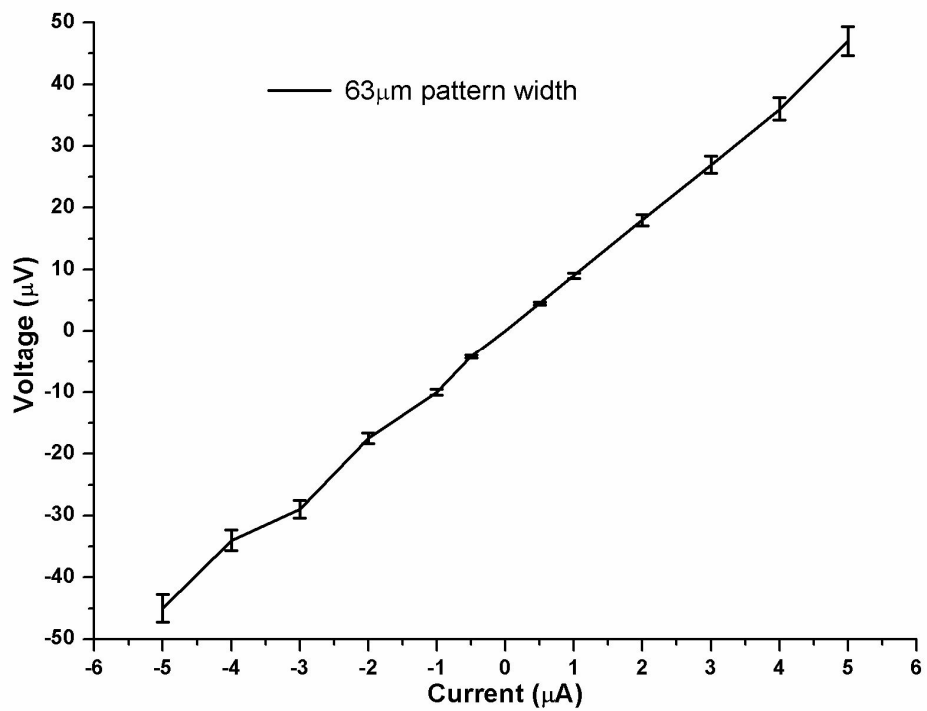
(c)

Figure 4.9I-V curves of printed patterns showing the Ohmic behavior plotted by taking an average value of measured data showing 5% of approximate error (a) I-V curves for 12μm pattern, (b) I–V curves for 30μm pattern, and (c) I-V curves for 63μm pattern

Length	Width	Average	Average	Resistivity	% Error

(mm)	(µm)	Thickness (nm)	Resistance (Ω)	(Ω.m)	Resistivity
2	12	82.3	490.7	2.42e-7	-6.2% to 4.6%
2	30	179.8	62.4	1.68e-7	-4.5% to 6.2%
2	63	290.7	9.05	5.98e-8	-7.8% to 9.8%

Table 4.2Resistivity of the different printed tracks

4.2 DOD EHD Fine Resolution Patterning of Ag

There has been advancement in the field of inkjet printing beyond the conventional digital graphic arts printing(Chrisey 2000). Inkjet printing has been widely used to deposit various functional materials for fabrication of devices or device components in printed electronics(Gans et. al. 2004, Szczech et. al. 2002, and Shimoda et. al. 2006)and bio-applications (Bietsch et. al. 2004)etc. The inkjet based deposition has various advantages in flexibility of patterns to deposit, less material wastage and can be scalable for large area fabrication. Conventional inkjet printing systems use thermal or acoustic energy to push the liquid from the nozzle for droplet generation. But these conventional inkjet printing systems have certain limitations, such as, thermal problem due to heating and cannot produce droplets smaller than nozzle diameter apart from the limitation of materials to be deposited(Calvert 2001). The conventional inkjet printing methods can typically produce the pattern size of 20-30µm(Derby 2010). In order to achieve these resolutions or to minimize the feature size through conventional inkjet printing, substrate modification/treatment is necessarily required to modify the droplet and substrate interaction or printing on pre-patterned or textured substrates to restrict the pattern size. In case of aqueous inks the drop size is twice the droplet diameter ejected from the nozzle(Cheng et. al. 2005).

In order to reduce the pattern size, many researchers are focusing on the electrohydrodynamic jet based printing method. Electrohydrodynamic jet printing uses electric field by overcoming the surface tension to pull the liquid from the nozzle opening to deposit the material on the substrate rather than pushing the liquid as in case of conventional inkjet printing(Park et. al. 2007).Due to pull of the liquid,

electrohydrodynamic printing can produce smaller size patterns as compared to the nozzle diameter. Depending on the applied electric field (DC or pulse voltage), electrohydrodynamic jet printing can be continuous (Poon et. al. 2008, Bisht et. al. 2011, and Khan et. al. 2011)or drop-on-demand(Huneiti et. et. al. 1996, Juraschek andRollgen 1998, and Kim et. al. 2008). Both continuous and drop-on-demand mode can produce micro or even nano-size patterns. Many researchers have focused on the continuous mode of electrohydrodynamic jet printing through stable cone-jet mode for the patterning purpose using various materials in electronics(Lee et. al. 2006) and bio-applications(Ahmad et. al. 2008). However, this micro or nano size high speed jet is difficult to stabilize(Hohman et. al. 2011). Moreover, a stable impinging of the jet is required to form continuous patterns on the substrate. Researchers have suggested different methods(Korkut et. al. 2008)and nozzle shapes(Kim et. al. 2010) for stabilization of the jet. Moreover, patterns through continuous jet mode may break or become irregular with beads like structure due to capillary forces or evaporation of the solvent or concentration of the suspension particles(Korkut et. al. 2008).

In order to address these issues, deposition through drop-on-demand mode has been suggested by applying the pulse voltage. Park et al. (Park et. al. 2007) reported high resolution electrohydrodynamic jet printing at sub-micron level using gold coated glass capillaries. Electrohydrodynamic drop-on-demand printing is performed by applying the pulsed voltage to the liquid and has been employed in electronics(Park et. al. 2007) and bio-applications(Park et. al. 2008). Li (Li 2007)] has studied drop-on-demand phenomena through meniscus deformation by applying the pulsed voltage. Stachewicz et al. (Stachewicz et al. 2009)explained the drop-on-demand behavior using relaxation times and operating conditions. Lei et al.(Lei et al. 2011) explained the dependency of the droplet deposition frequency with respect to flow-rate, applied voltage and duty cycle using polymeric solution. For direct patterning of the conductive tracks, Choi et al. (Choi et al. 2008)demonstrated the droplet deposition of the silver nanoparticles by applying pulse voltage; however, the deposited droplet was larger than the nozzle size. Park et al. (Park et al. 2007)has demonstrated the printing of less than 10μm patterns of PEDOT:PSS on 300nm

layers of SiO_2 on conductive Si substrate. Wang et al. (Wang et al. 2010)deposited Au and Ag nanoparticles on conductive silicon with feature size of less than $10\mu m$ and $35\mu m$ by controlling through pulse voltage. Kim et al. and Rahman et al. (Kim et al. 2011, and Rahman et al. 2011)deposited ink containing Cu and Ag nanoparticles respectively on thick glass substrate by applying forward multistep wave form or multistep pulse voltage. For the requirement of printed electronics device fabrication, conductive patterns or active materials have to be deposited on glass and thick polymer substrates. But this is the one of the major limitation of electrohydrodynamic jet printing in continuous mode due to charge carried by electrified jet, which affects the stability of the jet and also resolution of the printed patterns(Poon 2002). The electrohydrodynamic printing in drop-on-demand mode is more suitable choice for patterning on the thick substrate, because of event based formation of the cone-jet, which help in more stable printing process and can produce smaller diameter droplet then the nozzle size. However, fine resolution of Ag patterns less than $10\mu m$ on thick substrate has not been reported previously.

This section presents the direct fabrication of less than $10\mu m$ Ag patterns on $500\mu m$ thick glass substrate by applying the pulse voltage with the frequency of 250Hz using $10\mu m$ internal diameter glass capillary. The deposition frequency is studied by deposition position of the droplet on glass substrate and substrate speed. The effect on droplet size is studied with respect to operating parameters (applied voltage, duty cycle and pressure). The droplet size is measured after the sintering process. Continuous patterns are printed by sufficient overlapping of the deposited droplets by adjusting the substrate speed. The electrical functionality of continuous patterns is measured through I-V curve.

4.2.1 Experimental setup

Figure 4.10 shows the schematic of the experimental setup used for electrohydrodynamic jet printing. Glass capillary with internal diameter of $10\mu m$ (World Precision Instruments) was connected with ink reservoir which was mounted on manual z-stage to adjust the gap between nozzle and substrate. For ink supply to the nozzle tip, ink reservoir was connected with the pressure regulator by

maintaining the steady and constant flow-rate through compressed air. The pulsed voltage was applied through a metallic wire which was inserted in a glass capillary and connected with a high voltage power amplifier (Trek 610E) and controlled with multi-function signal synthesizer (HP 33120A). The droplets and patterns were deposited on 500µm thick 10cm x 10cm glass substrate without any surface treatment, placed on the top of ground electrode plate. The ground plate was mounted on X-Y motorized stage (SURUGA SEIKI DS102) to control the substrate speed during the patterning process. The nozzle to glass substrate distance was set at 250µm for deposition of Ag nanoparticles. The actual experiment setup used for fine resolution drop-on-demand patterning is shown in figure 4.11. For patterning, commercially available Ag nanoparticles ink (Harima Silver Nanopaste NPS-JL) with 55 wt% was used to be ejected from the glass capillary. The deposition process on the substrate was observed with high speed camera (Motion Pro X3). After sintering the printed droplets and patterns at $150^{O}C$ for 60 minutes, dimensions were measured through a digital microscope (Olympus BX51M) and electrical characterizations were performed by measuring I-V curve (Agilent B1500A).
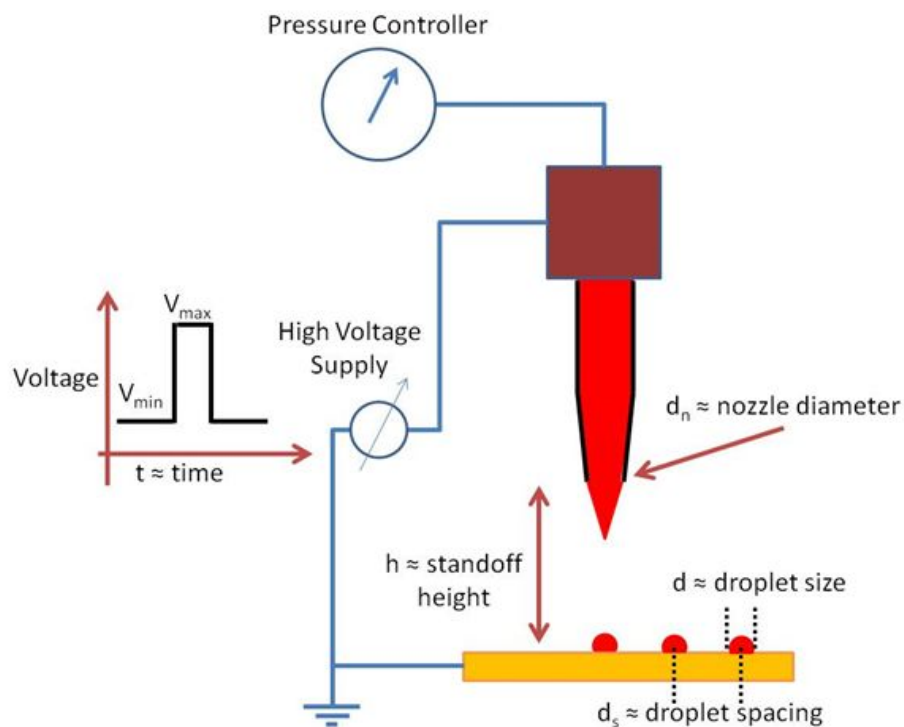
Figure 4.10Schematic diagram of Experimental setup used for Electrohydrodynamic drop-on-demand patterning by applying pulse voltage.
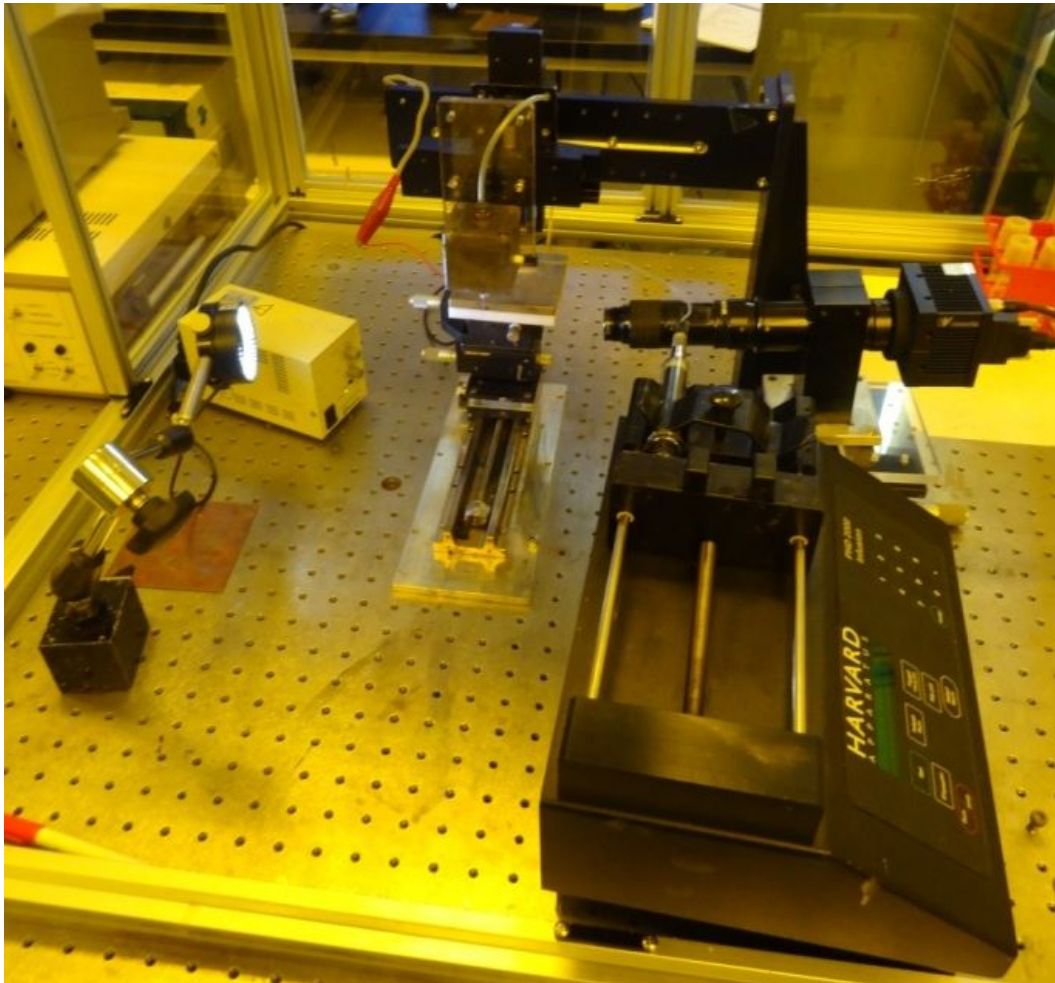
Figure 4.11Actual Experimental setup used for Electrohydrodynamic drop-on-demand patterning by applying pulse voltage.

4.2.2 Droplet Size and Operating Conditions.

Since the nozzle internal diameter is 10μm, it was difficult to observe the complete droplet generation phenomena from the nozzle tip. Therefore, for every experiment setup, the droplet generation frequency (f_d) is confirmed by measuring the center to center distance (d_s) between two consecutive droplets with respect to substrate velocity (V_s).

$$d_s = \frac{V_s}{f_d}$$

(4.1)

72

When the substrate velocity was kept at 25mm/sec, with applied frequency of 250Hz; the center to center distance between two adjacent droplets was calculated as 100μm.

Initially experiments were performed to investigate the minimum offset voltage (V_{min}) and amplitude voltage (V_{max}) by applying 250Hz frequency and 50% duty cycle with constant pressure of 1kPa for stable generation of droplet of Ag nanoparticles on glass substrate. The effect of the operating conditions was measured with the help of droplet diameter after sintering process. It was noted that minimum droplet diameter of 18μm with the deviation of ±0.5μm was measured at V_{min} of 1000V and V_{max} 1750V, with center to center distance of 100μm ± 5μm between two neighboring droplets, as shown in figure 4.12. With further increase in V_{min}, small droplets are ejected before ejecting the primary droplet as shown in figure 4.13. This is due to the high V_{min} causing the jetting in prior to application of droplet generation pulse voltage (V_{max}). As in case of increasing V_{max} from 1750V to 1800V and keeping the value of V_{max} at 1000V, irregular droplets surrounding with smaller atomized droplets were generated as shown in figure 4.14. In both the cases with high value of V_{max} and V_{min} droplets on the substrate were irregular due to disintegration of the droplet before reaching the substrate because of excess charges carried by droplets at high applied voltages(Yudistira et. al. 2010).

The droplet generation behavior and droplet diameter with respect to applied duty cycle is shown in figure 4.15. As shown in the graph, at same applied voltage the droplet size is proportional to the applied duty cycle. The droplet diameter measured by applying 25% duty cycle at V_{min} of 1000V and V_{max} of 1750V, was approximately 8μm and at 75% duty cycle, the droplet diameter is measured to be 37μm. This change in droplet diameter is related with ejection volume during the drop-on-demand jetting, the ejection volume increases with respect to increase in duty cycle or time of applied ejection voltage(Ganan et. al. 1997). However, change in the droplet diameter with respect to the applied voltage is approximately 15%. In electrohydrodynamic jetting the effect on size droplet of jet is less as compared to liquid flow-rate(Ganan et. al. 1997).
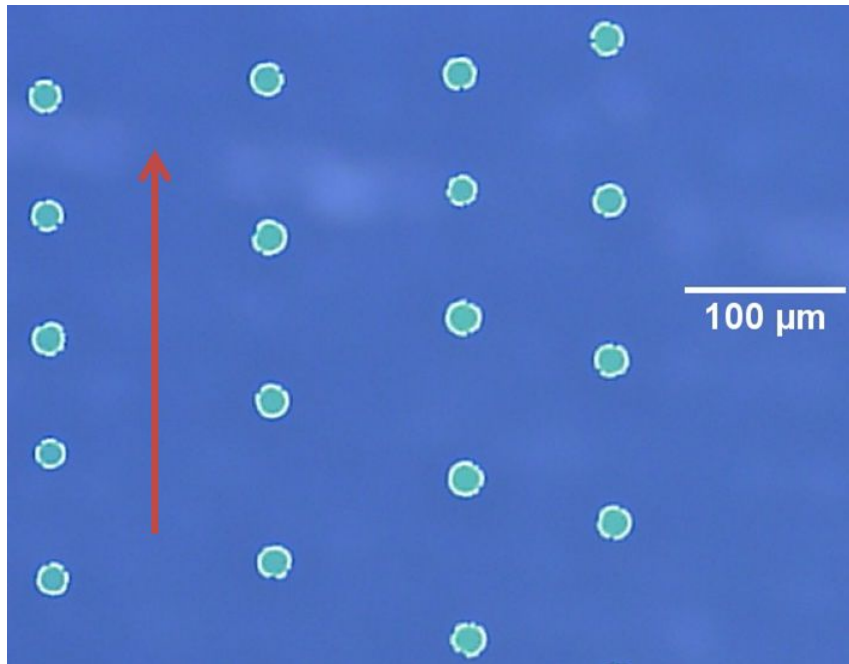
Figure 4.12Droplet diameter of 18 µm with the deviation of ±0.5 µm at V_{min} of 1000V and V_{max} 1750V, with droplet spacing of 100µm ± 5µm, where red arrow indicates the direction of printing
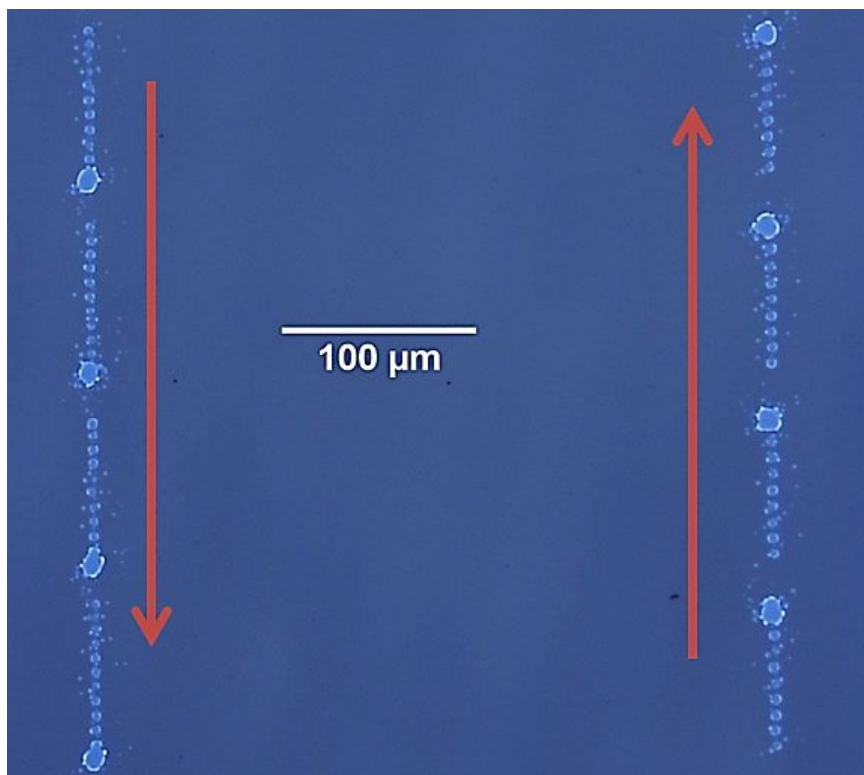
Figure 4.13Droplet generation when V_{min} of 1050 V, V_{max} 1750 V, 50% Duty-cycle and 1kPa of applied pressure, smaller size droplets were generated before main droplet generation due to high value of V_{min}, red arrows indicating direction of printing
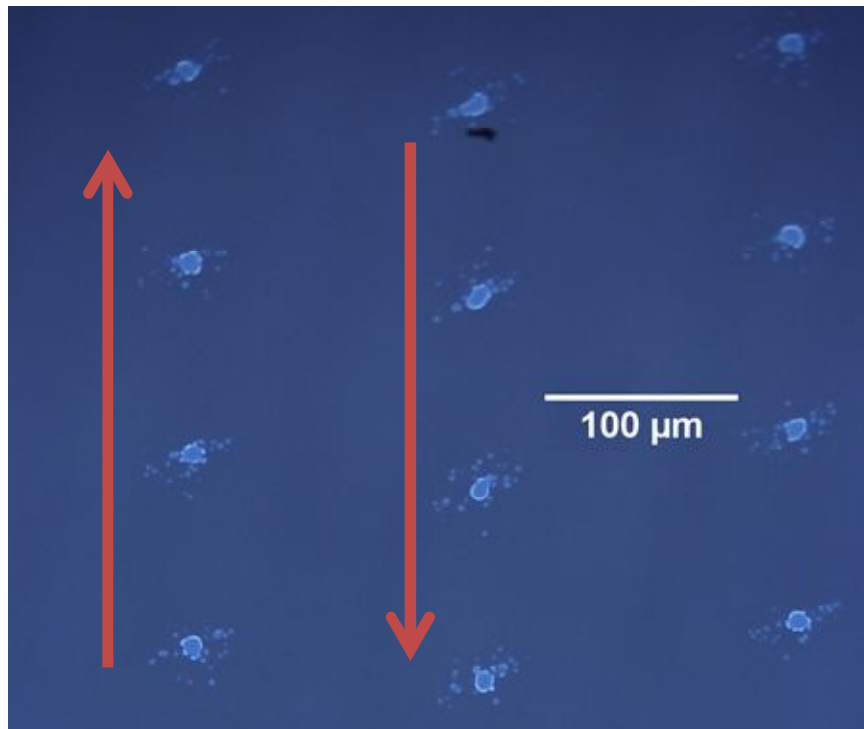
Figure 4.14Irregular droplet with smaller droplets surrounding the main droplet generation when V_{min} of 1000V, V_{max} 1800V, 50% Duty-cycle and 1kPa of applied pressure due to high value of V_{max}, red arrows indicating the direction of printing
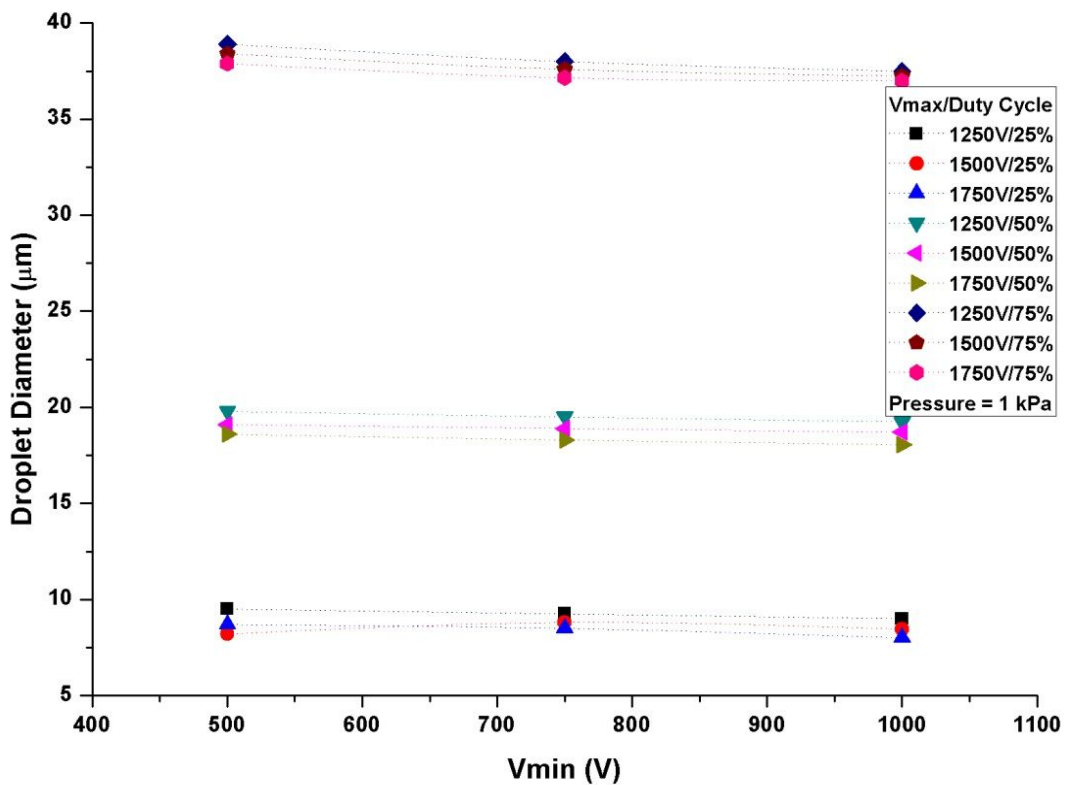
Figure 4.15Droplet diameter with respect to V_{min} at different V_{max} and duty cycle

After investigating the voltage range for stable deposition of Ag nanoparticles droplets, the effect of applied pressure is investigated by applying 250Hz frequency with V_{min} of 750 V and V_{max} of 1500V at 25, 50 and 75% duty cycle, as shown in figure 4.16. The minimum pressure at which steady drop-on-demand behavior observed was 0.5kPa. Under 0.5kPa applied pressure the droplet generation frequency was smaller than the applied voltage frequency. This behavior was due to insufficient supply of ink at the tip of the nozzle which affects the droplet generation frequency(Xu et. al. 2011). It was observed that the droplet diameter increases with increase in applied pressure due to increase in the liquid supply. This shows that the size of the droplet diameter is more depended on applied pressure as compared to applied voltage, which can be used for controlling the droplet size deposition on the substrate. In case of pressure effect on the droplet size the minimum droplet diameter achieved was 3.8μm at 0.5kPa, V_{min} 750V and V_{max} of 1500V at 25% duty cycle. At high pressure and duty cycle, the droplet frequency and size was difficult to measure because of the overlapping of the large diameter droplet at 25mm/sec substrate speed.
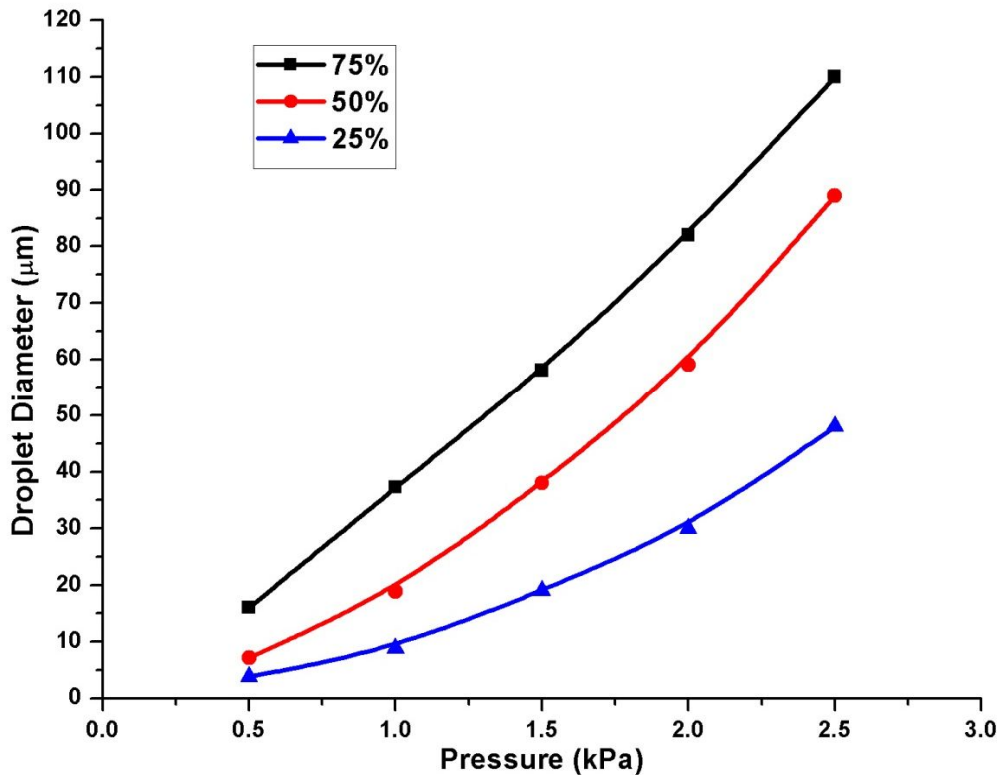
Figure 4.16Droplet size dependency on applied pressure at 250 Hz frequency with V_{min} 750 V and V_{max} 1500 V at 25, 50 and 75 % duty cycle

76

In order to minimize the droplet size at 0.5kPa applied pressure, the droplet diameter was measured by increasing the applied pulsed voltage at 250Hz frequency with 25% of duty cycle. The minimum droplet diameter of 3.6μm was measured after sintering process at V_{min} of 900V and V_{max} 1600V as shown in figure 4.17. The droplet diameter was also investigated by increasing the duty cycle and results are compared with the droplet diameter with V_{min} of 750V and V_{max} of 1500V at corresponding duty cycle, as shown in figure 1.18. As shown in graph at figure 4.18, the effect of the applied voltage is not significant as compared to duty cycle on droplet diameter. At V_{min} of 750V, V_{max} 1500V and 25% duty cycle the droplet diameter is 5.2times smaller than the droplet generated at same voltage but 75% duty cycle, However, when the . V_{min} of 950V, V_{max} 1600V and 25% duty cycle was applied the droplet size is only increased by approximately 0.6%.
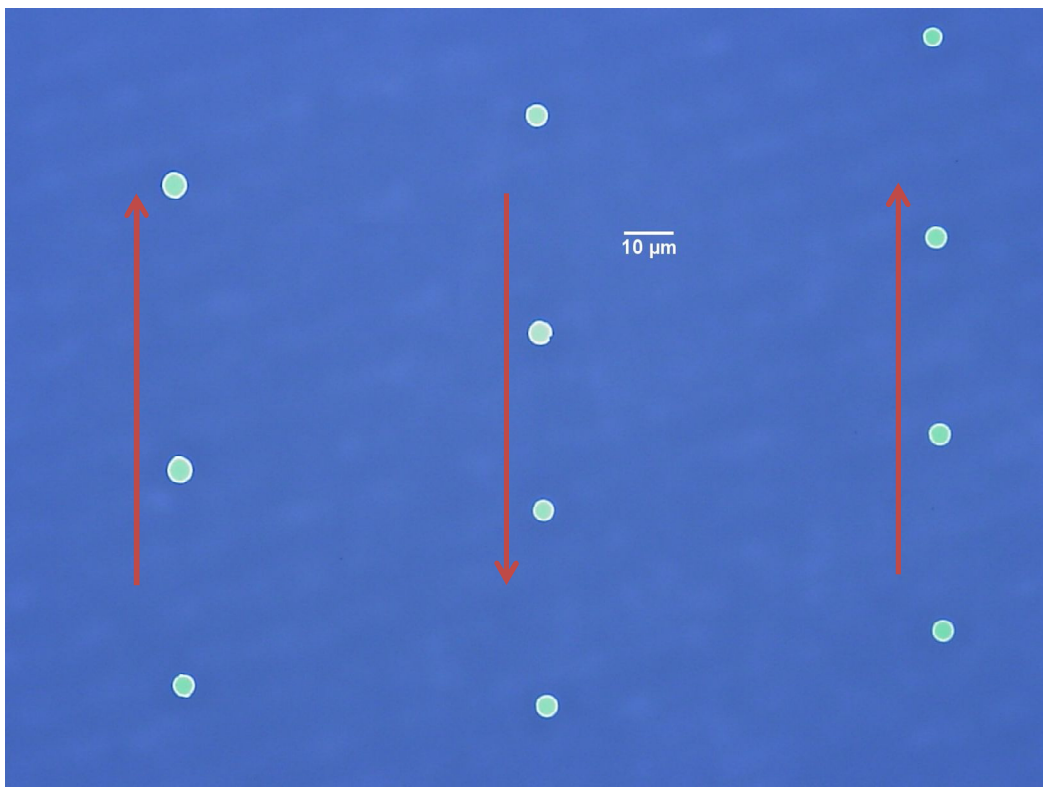
Figure 4.17Droplet diameter of 3.6μm (V_{min} 900V, V_{max} 1600V, duty cycle of 25% and applied pressure 0.5 kPa), red arrow indicating the direction of printing
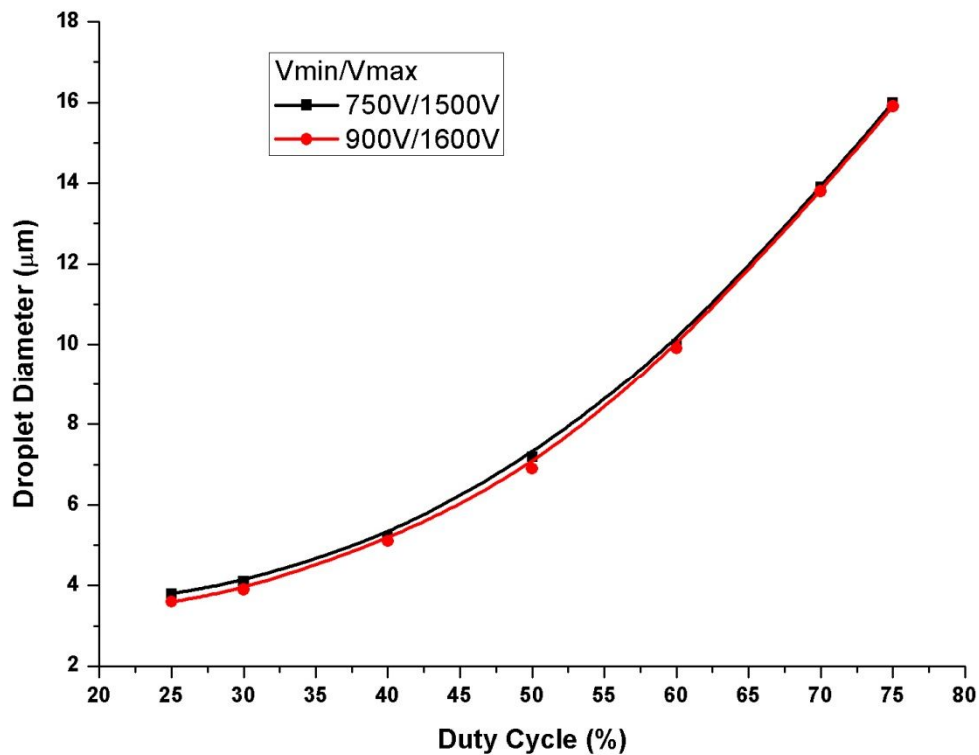
Figure 4.18Comparison of Droplet diameter between applied voltages at different duty cycle, red line V_{min} 900V, V_{max} 1600V and black line V_{min} 1750V, V_{max} 500V, constant pressure was kept at 0.5kPa

The experimental results indicate that in drop-on-demand phenomena, at any given frequency, the dependency of droplet size is more on applied pressure and duty cycle as compared to applied voltages

4.2.3 Patterning of continuous tracks

For direct deposition of Ag conductive tracks on the substrate, the patterns are formed by overlapping of the consecutive droplets by adjusting the substrate speed with respect to droplet frequency and size(Stringer and Derby 2010). Figure 4.19 shows the high speed image of the patterning process on the glass substrate. A number of experiments were performed to investigate the optimal substrate speed to produce smooth patterns of Ag nanoparticles, with droplet frequency of 250Hz by applying V_{min} of 900V and V_{max} of 1600V at 25% duty cycle with applied pressure of 0.5kPa, whereas the droplet diameter was 3.6µm on glass substrate.

제주대학교 중앙도서관
JEJU NATIONAL UNIVERSITY LIBRARY
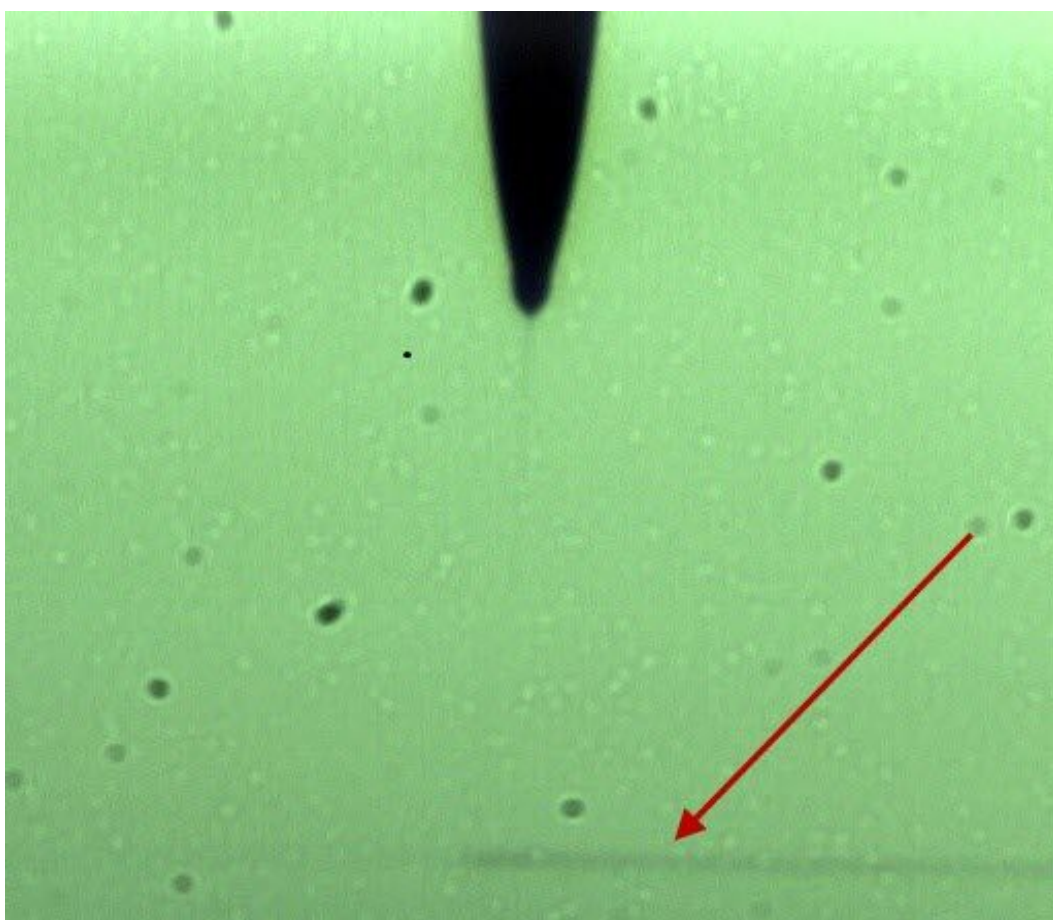
Figure 4.19Drop-on-demand patterining process of the continuous conducting pattern of Ag nanoparticles on glass substrate, where red arrow indicates the printing patterns

It was noted that when the substrate speed is relatively high and distance between the consecutive droplets is slightly smaller than the droplet diameter, the drop coalescence was observed, which caused irregular patterns with beads. However, at very low substrate speed, where the droplet spacing is relatively smaller, the patterns were formed with bulging instability. It was noted that, when the distance between consecutive droplets was approximately 70% of the droplet diameter, the smooth patterns with no beads or bulging were formed. Figure 4.20 shows the effect of substrate speed or distance between the consecutive droplets for 3.6μm droplet. As shown in figure 4.20(a) irregular patterns with beads are formed when distance between the consecutive droplets is 90% of the droplet diameter, when the distance was approximately 70% of the droplet diameter, smooth and regular patterns of 6.5μm approximate width (1.8 times larger than the printed droplet size) were

79

formed as shown in figure 4.20(b) and figure 4.20(c) shows patterns with bulging due to droplet spacing, which was 50% of the droplet diameter, which causes the accumulation of the ink on substrate. Based on the experiment results, for smooth patterns substrate speed (V_s) with respect to droplet size (d) and droplet generation frequency (f_d) can be predicted as:

$$V_s = 0.7d \cdot f_d \tag{4.2}$$

(a) (b) (c)
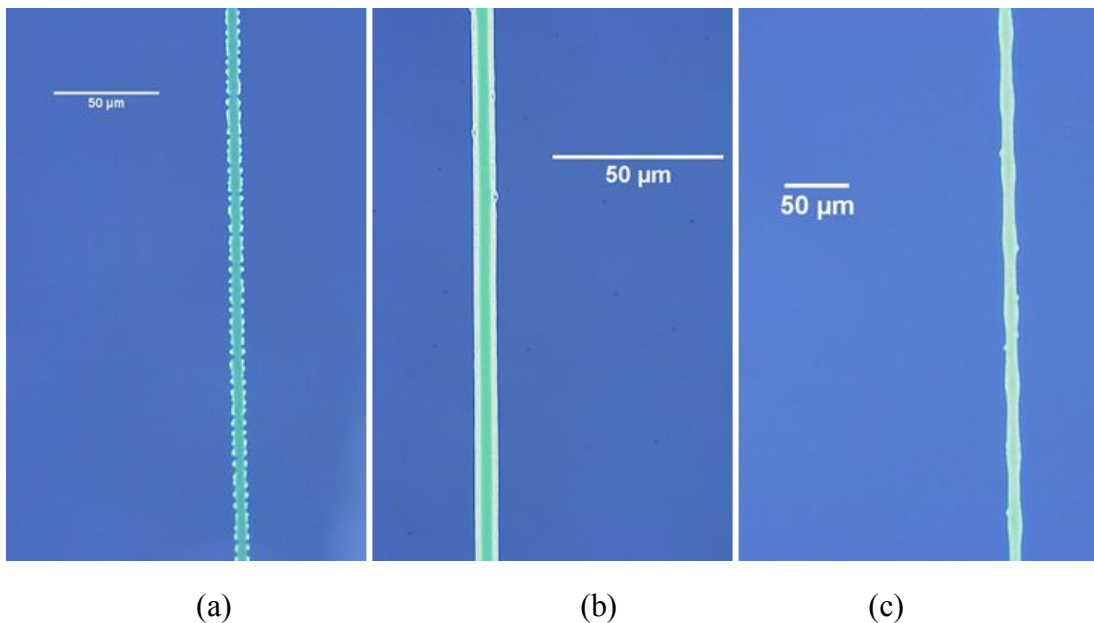
Figure 4.20Droplets over lapping by controlling substrate (droplet diameter 3.6μm), (a) irregular patterns with beads droplets spacing is 90% of the droplet diameter, (b) smooth pattern (6.5μm width) with droplet spacing is 70% of the droplet diameter (c) shows patterns with bulging due to droplet spacing was 50% of droplet diameter

However, experimental results also indicated that for stable and smooth pattern generation through larger droplets, the center to center distance between the consecutive droplets had to be kept larger than 70% of droplet diameter. The printed pattern width according to printed droplet size is shown in figure 4.21, where droplet frequency of 250 Hz by applying V_{min} of 900 V and V_{max} of 600 V with applied pressure of 0.5 kPa, by changing duty cycle from 25% to 75%.
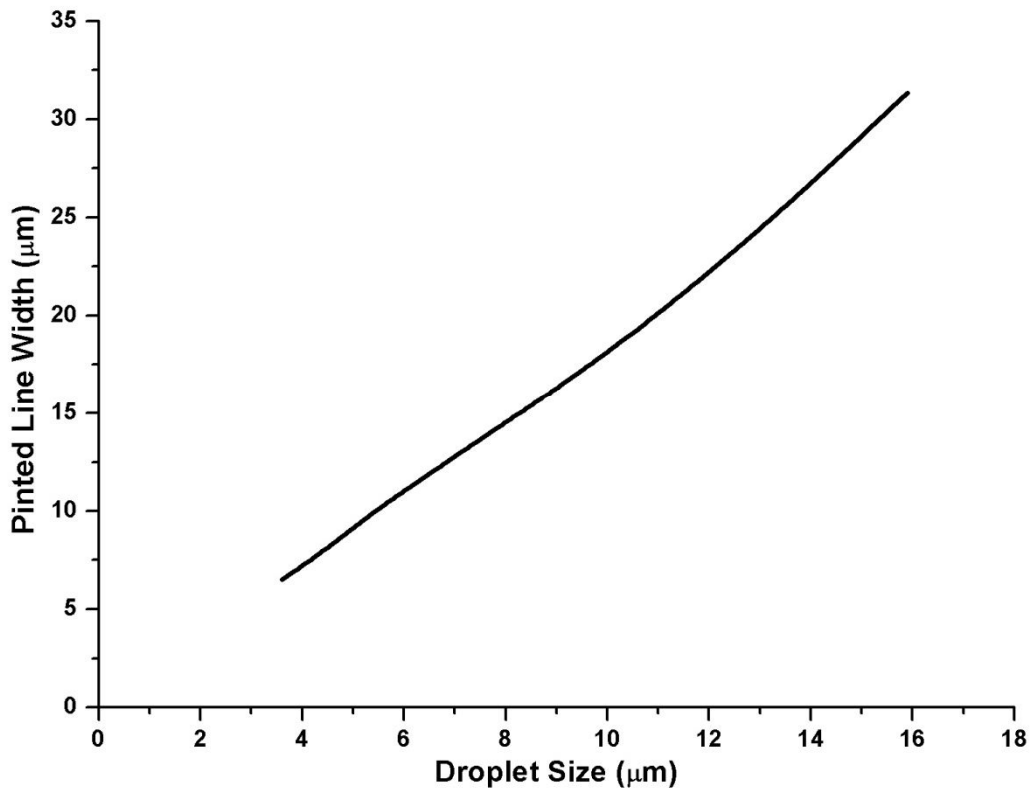
Figure 4.21Change in Pattern width with respect to droplet diameter; maintaining the droplet spacing of 70% of droplet diameter by applying V_{min} 900 V and V_{max} 1600 V with applied pressure of 0.5 kPa by changing duty cycle from 25% to 75%

The electrical characterization was measured through I-V curve, by connecting 2 probes on the sintered printed sliver patterns. The change in current was measured by increasing the voltage, which showed liner Ohmic behavior. Measured I-V curves of 6.5, 12.6 and 31.3μm patterns are shown in graph at figure 4.22. The resistance of 6.5, 12.6 and 31.3μm patterns were measured to be 111, 85, 62.5Ω respectively. The electrical characterization results shows that the fine resolution patterns printed through electrohydrodynamic printing can be used to fabricate conductive tracks for printed electronics application.
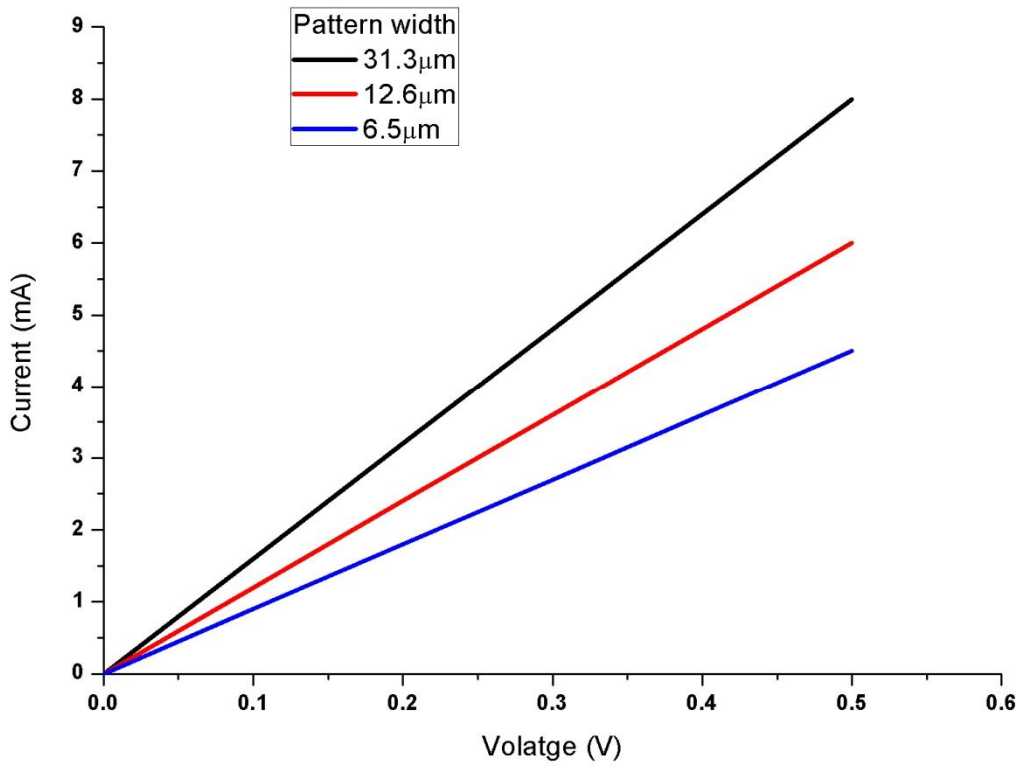
Figure 4.22 I-V curves of 6.5, 12.6 and 31.3µm patterns showing linear Ohmic behavior

5. Executive Summary

This chapter concludes the discussion of the thesis by providing the summary of the work presented in this thesis along with the guidelines and experimental issues related to electrohydrodynamic patterning in continuous mode as well as drop-on-demand mode.

5.1 Continuous EHD Pattering

This section will discuss the experimental investigation related to the formation of stable cone-jet and issues pertaining to pattern formation through stable and continuous cone-jet. The formation of con-jet has been studied and well known for almost a century(Zeleny 1914, 1916, Taylor 1964, and Hayati and Tadros 1987]; however, the process is not fully understood(Cloupeau and Foch 1994, Smith 1986, Jaworek and Krupa 1999, Hartman 1998, and Poon 2002). Different scaling models related to con-jet have been reposted(Chen and Pui 1997, Gana 1997, Mora and Loscertales 1994, and Cloupeau and Foch 1989), explaining the jet or droplet size dependency on various process parameters, but there are discrepancies due to variation in scaling model due to variations in experimental setups and also the limitation of the simplifying assumption in the scaling model and also all the scaling models are derived through chemicals not with the colloidal solutions or inks containing nanoparticles(Poon 2002). The other major challenge related to stabilization of a micron size jet under electric field, especially for a colloidal jet. Many researchers have demonstrated the continuous sub-micron jet over long distance producded through cone-jet mode using highly viscous polymeric fluids, which is also known as electrospinning. Compared to polymeric fluids, the colloidal jets are more difficult to control due to presence of charge. Controlled patterning is also an issue by impinging the micron size jet on surface of the substrate in continuous cone-jet mode(Saville 1971, and 1970).

5.1.1 Onset Voltage

Onset voltage can be defined as the minimum amount of voltage required to generate a stable cone-jet. Smith (Smith 1986)has purposed the formula for the onset voltage by taking the assumption of half cone angle of 49.8^O(Taylor 1964)as follows:

$$V_{on} = \frac{\sqrt{\frac{\gamma\, r_c cos\theta}{\varepsilon_0} \ln 4}}{r_c}$$

(5.1)

Where V_{on} is onset voltage, γ is surface tension of the liquid, θ is half cone-jet angle (49.8^O), ε_0 is permittivity of free space, r_c is radius of capillary and h is distance between nozzle and ground.

However, the above formula only provides the rough estimate of the onset voltage due to assumption of half cone-jet angle and also there is no non-conductive medium between nozzle and ground. The comparison between calculated value of onset voltage and experimental value for ethanol using 210μm metallic capillary is show in figure 5.1. The graph indicates that the experimental value of onset voltage is higher than the calculated values. In actual case, the patterning has to be perform on non-conductive surface (glass or polymer substrate) the experimental value of on-set voltage will different from the calculated value. However, the onset voltage strongly depends on the nozzle radius as well as the distance between nozzle and ground plate for any given liquid(Smith 1986).
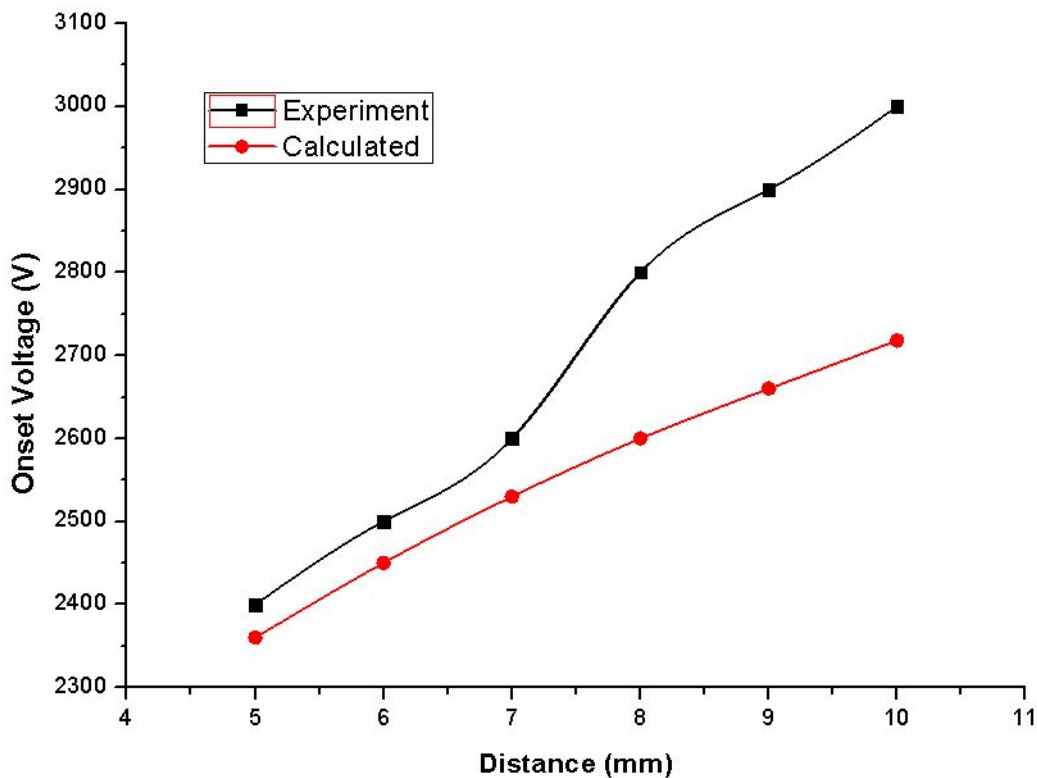
Figure 5.1 Comparison between calculated onset voltage and experiment on-set voltage for ethanol using 210μm metallic capillary

5.1.2 Flow-rate

Flow-rate is one of most important parameter for the formation of stable of cone-jet as well as controlling the pattern width. In cone-jet mode, the diameter of the jet depend two orders on magnitude on the flow-rate(Poon 2002). Flow-rate also affects the stability of the jet. For the patterning purpose, stable impinging jet is required, however, at high flow-rate the jet has more tendencies to break-up because of increased charge carries with jet which tends to destabilize it under electric field as shown in figure 2.3. Moreover, the applied flow-rate also dictates the jet diameter. In order to achieve smaller patterns size, the patterning process should be performed at low flow-rate of the operating envelop.

5.1.3 Ink Properties

Properties of ink containing nanoparticles play important role for the stable patterning process. Inks with high conductivity are difficult to stabilize due to high

charges on the jet. In order to investigate the effect of the ink conductivity, patterning was performed using Inktec-030 ink containing 40% wt Ag nanoparticles with the help of 110μm metallic capillary. The properties of the ink are given in table 5.1.

Density (kg/m^3)	Viscosity (cps)	Surface tension (N/m)	Conductivity (S/m)
1400	3~15	0.027~0.032	0.17

Table 5.1 Properties of inktec-030 Ag ink

During the experiment, the high speed camera revealed that the cone-jet produced by high conductive ink was not stable and also jet tends to disintegrate at shorter length as shown in figure 5.2. The reason of destabilization arises due to high conductivity of the ink(Smith 1986). The literature survey reveals that ink with intermediate range of conductivity (1e-2 to 1e-7 S/m) can produce stable cone-jet(Hayati and Tadros 1987). Moreover, the patterns formed were not smooth and uniform as shown in figure 5.3 as compare to other Ag and Cu ink as discussed in Chapter 2.

Figure 5.2High speed camera image cone-jet of Inktec-030 Ag ink at 2.5kV applied voltage and 150μl/hr flow-rate using 110μm internal diameter metallic capillary
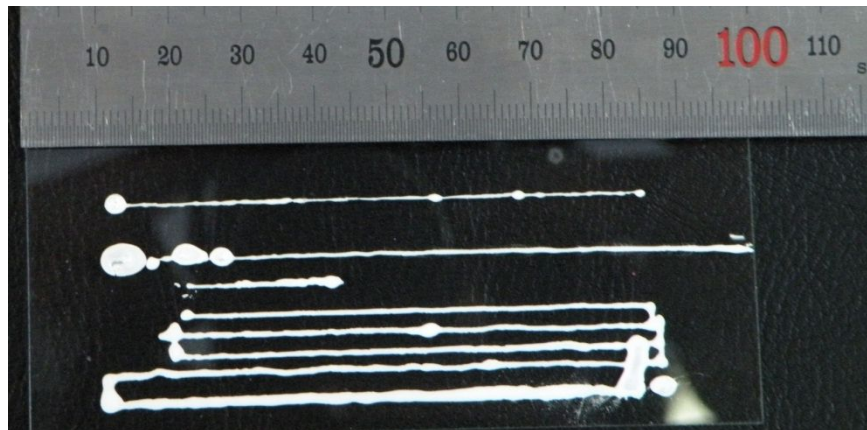
Figure 5.3Camera image of the pattern produce by Inktec-030 Ag ink

In order to stabilize the jet of high conductive ink, one method is to minimize the nozzle size(Poon 2002). The smaller nozzle diameter will help in reducing the required voltage to generate the stable cone-jet. In order to investigate the stable patterning of high conductive ink, the patterning was performed using 30µm internal diameter glass capillary. Due to reducing the nozzle diameter the required voltage for generating the stable cone-jet reduced to 1.25kV and also the minimum required flow-rate was 20µl/hr. The jetting behaviour was more stable which result in stable patterns. The high speed image of the patterning process is shown in figure 5.4. The minimum pattern achieved was approximately 75µm as shown in figure 5.5.
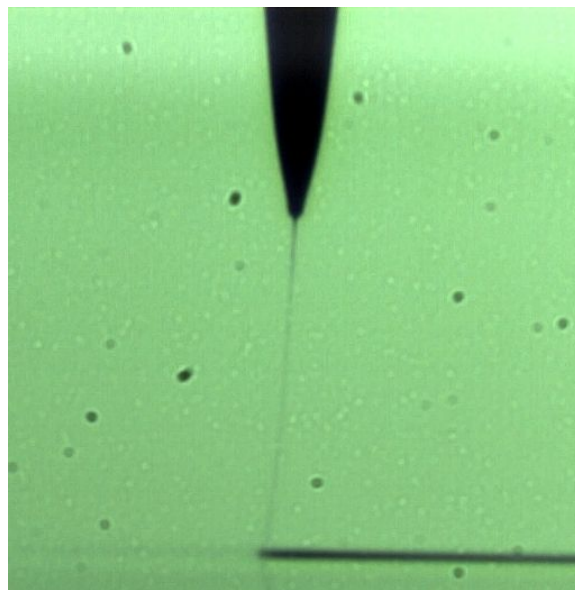
Figure 5.4High speed camera image of stable jetting of Inktec-030 ink and formation of pattern on glass substrate at 1.25kV and flow-rate of 20µl/hr using 30µm internal diameter glass nozzle

Figure 5.5Microscope image of Ag pattern using Intech-030, the pattern width is approximately 75µm

For generation of stable jet, many researchers have suggested (Poon 2002)to manipulate the viscosity of colloidal solution. There are three ways to increase the viscosity of colloidal solution as follows:

1. Replacing the dispersion medium with more viscous liquid
2. By increasing the concentration of nanoparticles
3. Adding traces amount of long chain polymeric thickeners

The number of experiments was performed using ParuMicroPE PG-007 silver nanopaste containing 80 wt% Ag nanoparticles, surface tension 40mN/m, viscosity of 1000cps and size of nanoparticles 80~100nm. However, the experimental results indicate that using the ink with high concentration of colloidal particles, the jet emerging from con-jet is not stable by using 110µm internal diameter metallic capillary. This is due to high voltage requirement to generate the stable cone-jet i.e. 5.8kV. Because of high voltage the jet destabilized as a resultant of high charge carried with thin jet emerging from cone-jet.The image of pattern on glass substrate by applying 5.8kV potential difference and flow-rate 50µl/hr is shown in figure 5.6. As shown in figure the patterns are irregular and no continuous.

Figure 5.6Irregular Ag patterns on glass substrate with ParuMicroPE PG-007 using 110μm metallic capillary by applying 5.8kV, after sintering process

For improving the quality of the patterning process, the stable impinging jet is required, by reducing the charge carried by the jet, for this 30μm internal diameter glass capillary was used. Due to smaller nozzle diameter the minimum required voltage for generating the stable cone-jet reduces from 5.8kV to 4.5kV and minimum required flow-rate of 0.5μl/hr, which result in stable impinging jet on the glass substrate, which result in smooth and continuous patterns. The analysis of the patterns with respect to surface treatment of substrate and substrate speed are discussed in section 5.14 and 5.15 respectively. The image of the patterns on hydrophobic treated glass substrateis shown in figure 5.7.

(a)
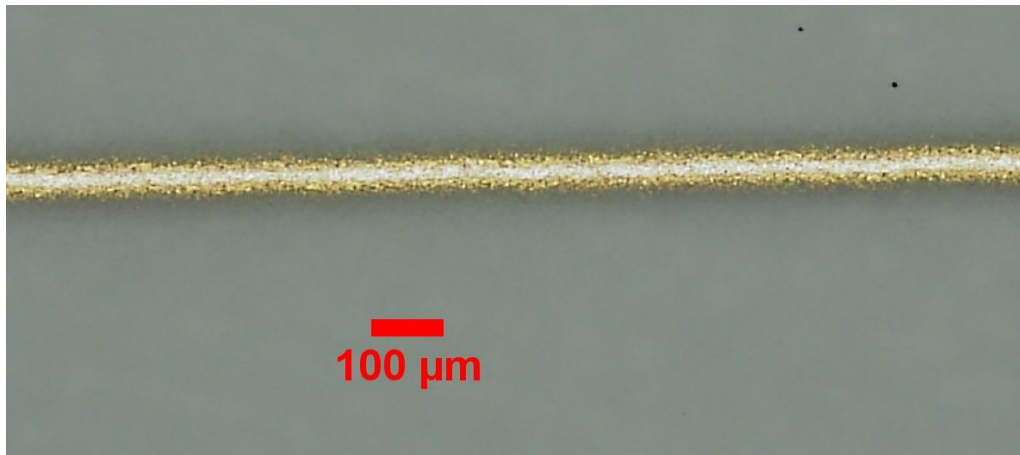
(b)

Figure 5.7Regular Ag patterns on hydrophobicglass substrate with ParuMicroPE PG-007 using 30µm internal diameter glass capillary by applying 4.5kV and substrate speed is 100mm/sec, after sintering process and (b) microscopic image of the pattern, where pattern size is approximately 50µm

5.1.4 Effect of Surface Treatment

For smooth patterns, interaction between impinging jet and substrate is very important. In order to investigate the effect of surface treatment, experiments were performed on both hydrophobic and hydrophilic substrates with the help of plasma treatment. The experiment results showed that with ParuMicroPE PG-007 silver nanopaste ink, the patterns are smooth on the hydrophilic substrate as compared the hydrophilic substrate. The patterns on hydrophobic substrate are shown in figure 5.7, whereas results on hydrophobic substrate with same operating conditions are shown in figure 5.8.

(a)

100 μm
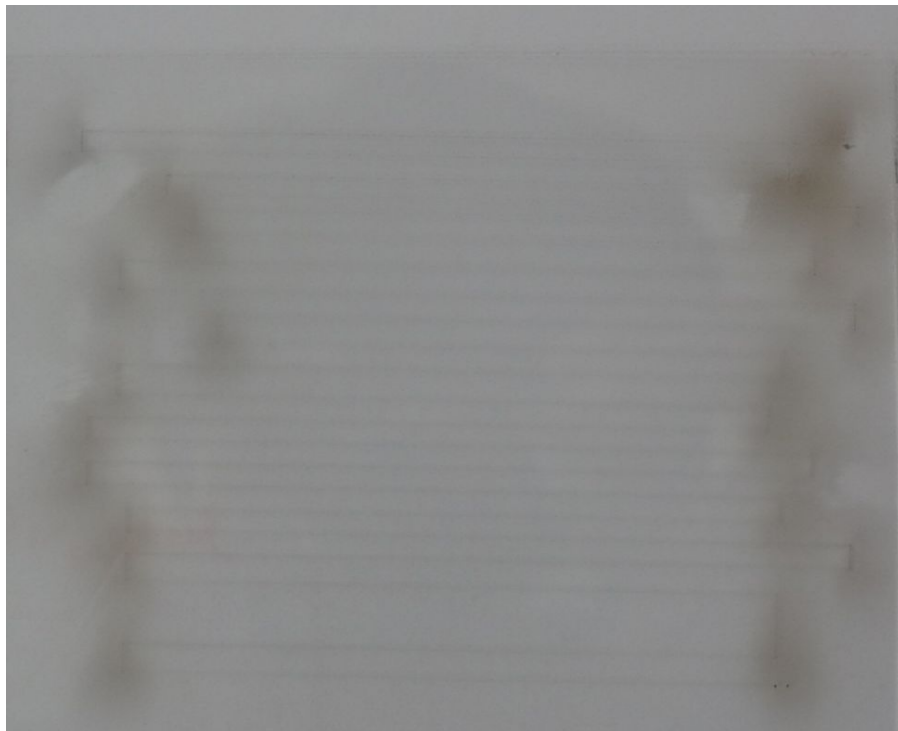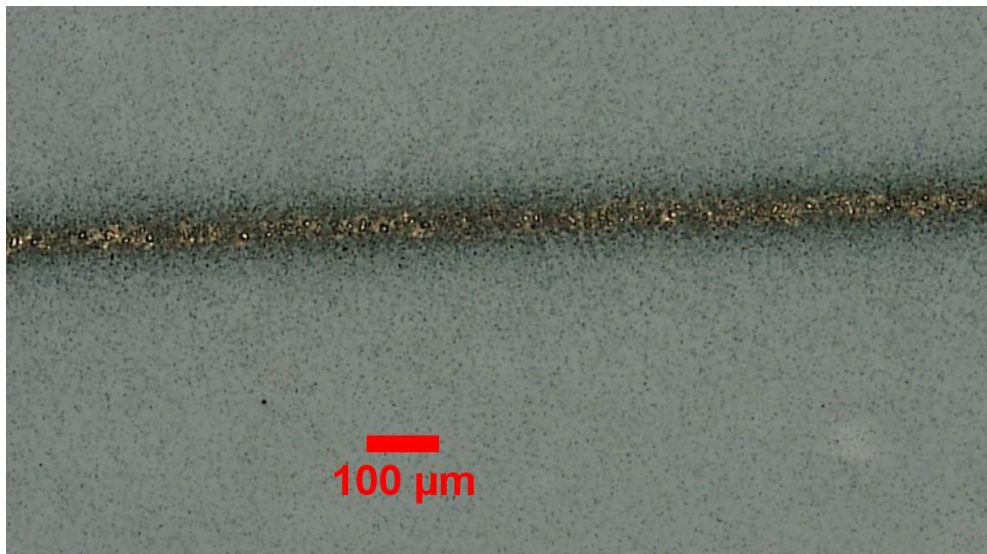
(b)

Figure 5.8Irregular Ag patterns on hydrophobic glass substrate with ParuMicroPE PG-007 using 30μm internal diameter glass capillary by applying 4.5kV and substrate speed is 100mm/sec, after sintering process and (b) microscopic image of the pattern, where pattern size is approximately 50μm

The morphology of the patterns can be adjusted through surface treatment of the substrate. However, this interaction varies with the properties of the ink used for the patterning, this phenomena needs to be further investigated.

5.1.5 Substrate Speed effect on pattern width

The other major challenge in electrohydrodynamic jet patterning is speed of the jet formed by cone-jet. For the formation of smooth and fine resolution patterns the substrate speed must be comparable with the jet speed to avoid the local mass accumulation. This local mass accumulation causes the increase in pattern width and also compromise the morphology of the patterns. Based on scaling law $(\gamma K/\rho\varepsilon\varepsilon_0)^{1/3}$ purposed by GananCalvo(Ganan 1997), the minimum jet speed scales as ~1m/sec for water jet. Number of experiments were performed by changing the substrate speed and measuring the pattern width after the sintering process.   The experiments were performed by applying electrical potential of 4.5kV and flow-rate of 1µl/hr and varying the substrate speed from 10mm/se to 150mm/sec, the pattern width with respect to substrate speed is shown in graph at figure 5.9.
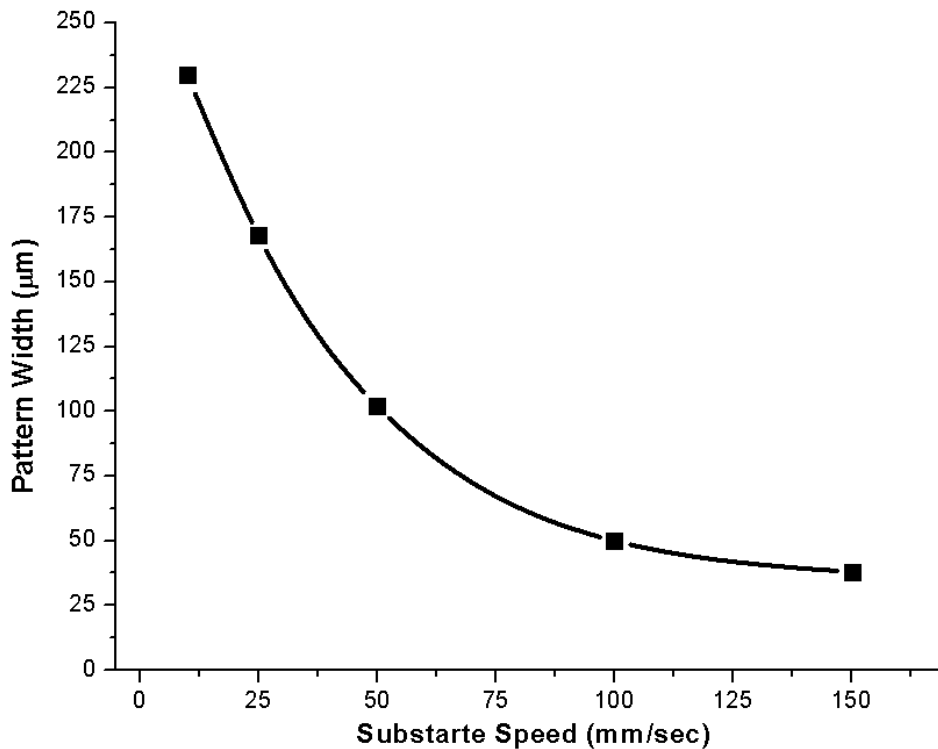
Figure 5.9Pattern width with respect to substrate speed

The microscope image of the patterns with change to substrate speed is shown in figure 5.10. As shown in microscope image the pattern width at 10mm/sec is approximately 230µm, this is due to very low substrate speed with respect to jet

speed, which causes accumulation of the colloidal ink on the substrate. Whereas, at substrate speed of 150mm/sec the pattern width is approximately 38μm with same operating conditions. As the substrate speed increases 15 times the pattern width decreases 6 times.
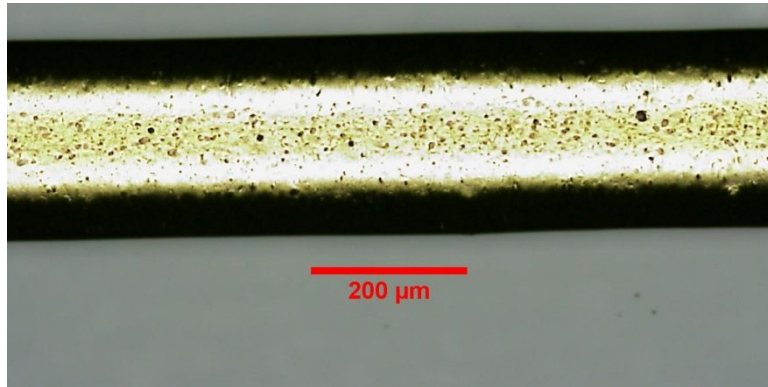
(a)
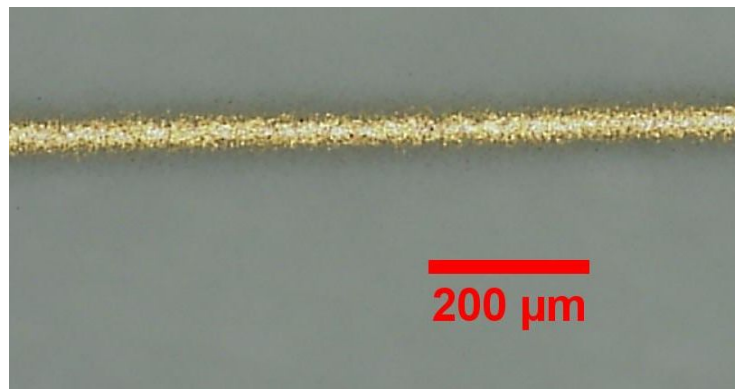
(b)

Figure 5.10Patterning of ParuMicroPE PG-007 using 30μm internal diameter glass capillary by applying 4.5kV and flow-rate 1μl/hr (a) pattern width of 230μm at substrate speed of 10mm/sec and (b) pattern width of 38 μm at substrate speed of 150mm/sec

However, high speed stage is still an issue because most translation devices have less than 1m/sec and also having relatively slow acceleration. This slow acceleration affects the sharp corner of the patterns. The other alternate solution is to reduce the speed of the jet from 1m/sec to 1cm/sec, by modifying the surface tension and conductivity of the ink. In order to reduce the jet speed to 1cm/sec scale the surface tension must be at order of 10^{-5}N/m and electrical conductivity of 10^{-3}μS/cm according to purposed scaling law. However, the effect of the liquid properties on jet

speed has to be verified experimentally and reducing the jet speed by manipulating the ink properties can be one of the major attentions of the future research.

5.2 Multi-nozzle EHD Patterning

Inkjet printing and thin film deposition for printed electronics is considered to be more promising applications. For large area and rapid printing a multi-nozzle setup is the suitable system (Ohigashi et. al. 2008). In case of the multi-nozzle system, the parameter affecting the dripping or jetting is the same as the single nozzle system, as mentioned above. However the stability of the jetting mostly depends on the electric field (Rulisona and Flagan 1993, and Tran et. al. 2009). Many researchers have studied the behavior of the multi-nozzle through linear arrays using the metallic capillaries as an emitter studying the stability of the electrohydrodynamics jetting. Previous studies are based on the systems in which the metallic capillaries are used with the voltage applied to each nozzle through a single source and common reservoir for liquid supply (Oh et. al. 2008, Tran et. al. 2009, and Tatemoto et. al. 2007). These studies are mainly focused on the effect on onset voltage, volumetric flow-rate, and droplet-size and nozzle-to-nozzle gap and minimizing the cross-talk effect. Study on the electric-field cross-talk which affects the printing position on the substrate is also reported by measuring the angle of the jetting and the position on the substrate, jetting through metallic capillary (Umezu et. al. 2006). In case of linear arrays of the nozzle the cross-talk effect is more significant at the end of emitters regarding the direction of the jet.

In this section the electric-field cross-talk effect on jetting angle is investigated on the glass capillary arrays by using three nozzles and keeping nozzle to nozzle gap 3mm and 5mm. Each nozzle is supplied with voltage and flow-rate through independent connection. Change in dripping and jetting angle by varying the applied voltage and flow-rate is reported in this study. Moreover, the effect of applied voltage on the jetting angle by operating two nozzles and keeping one nozzle off is also studied. For better understanding of the electric field interfacing numerical simulations are also performed and the results are elaborated on the basis of experimental data. Moreover, the cross-talk effect is minimized by reducing the

nozzle diameter for 5mm nozzle-to-nozzle gap. With 250μm nozzle diameter the cross-talk effect is negligible. The detail analysis of multi-nozzle electrohydrodynamic patterning has already been discussed by Arshad in his thesis work.

5.2.1 Experiment setup

A lab-made system is used for the experiments; the schematic of setup used is shown in figure 5.11. The DC voltage is supplied by the high voltage power supply (Trek Model 10/40A) which is connected to voltage distributor (HAN MAC HM10- 5) in order to provide the voltage to individual nozzle. Ink is supplied to each nozzle through multichannel peristaltic pump (ISMATEC-IP). The behavior of the system is monitored with the help of a high zoom camera (Sony, ST-404CD). A ground made of copper plate is used as counter electrode, which is mounted on moving stage; 0.5mm thick glass substrate is used on top of ground plate. Experimental setup consists of high voltage power supply, voltage distributor, multi-channel pump, camera, moving stage and movement of head (to adjust the distance between capillary array and ground) are connected through NI's PXI-1042Q hardware system which is controlled with lab-made software system based on LabView.
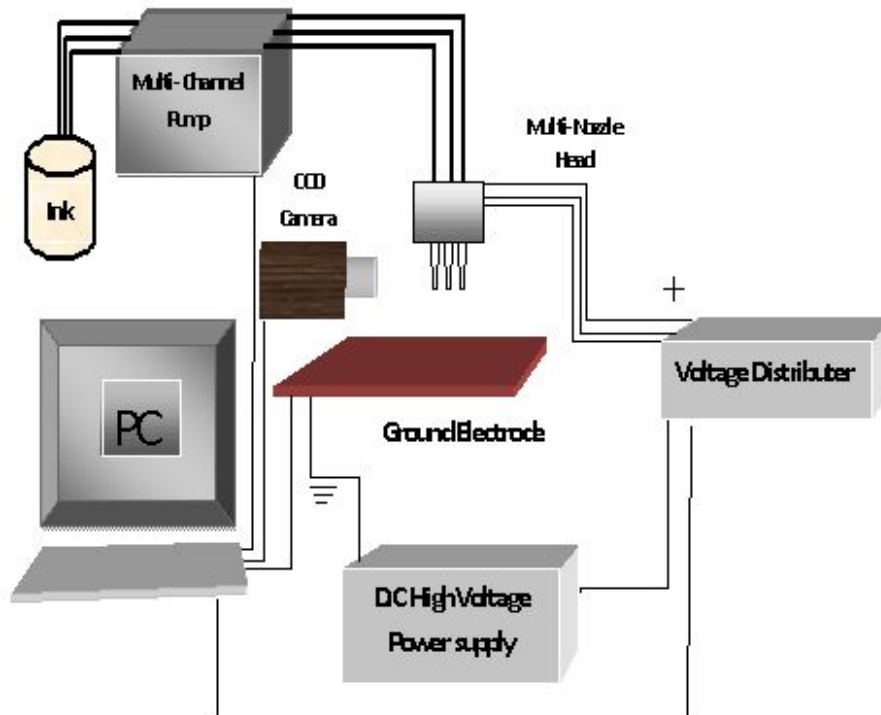
Figure 5.11 Schematic of experimental setup

Multi-nozzle array consists of glass capillaries fitted to the PDMS, through which individual channels are made to supply the ink to each capillary. The electrodes are inserted in PDMS to provide the high voltage to each capillary. Two types of arrays are constructed by keeping the capillary to capillary distance 3mm and 5mm. The schematic and PDMS based capillary arrangement for experiment are shown in figure 5.12. Thick wall glass capillaries are used with outer diameter of 1.5mm and inner diameter is 750μm. Copper wires having diameter of 650μm are inserted in PDMS structure to provide high voltage to the ink in capillaries. In all experiments, the distance between capillary tip and ground plate is kept at the distance of 4mm.Commercially available ink containing silver particles having viscosity of 39cps, surface tension of 5dyn/cm and conductivity of 9.5e-6S/cm is used for the experiment.
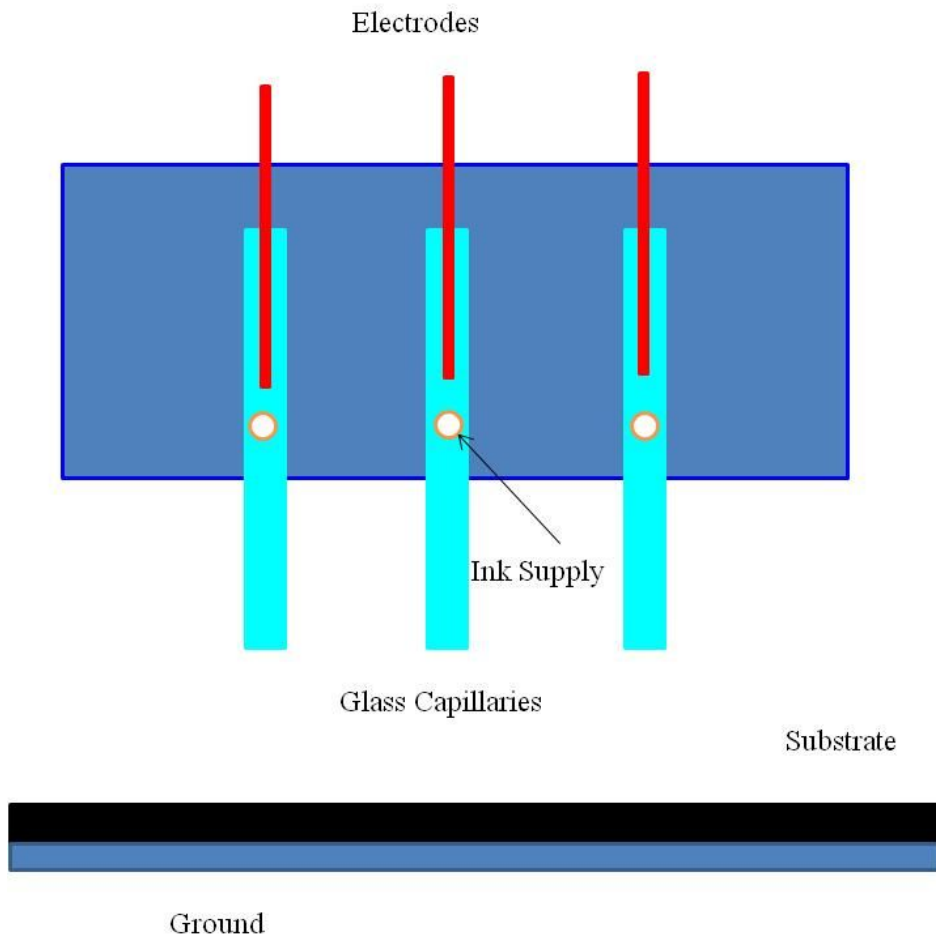
(a)
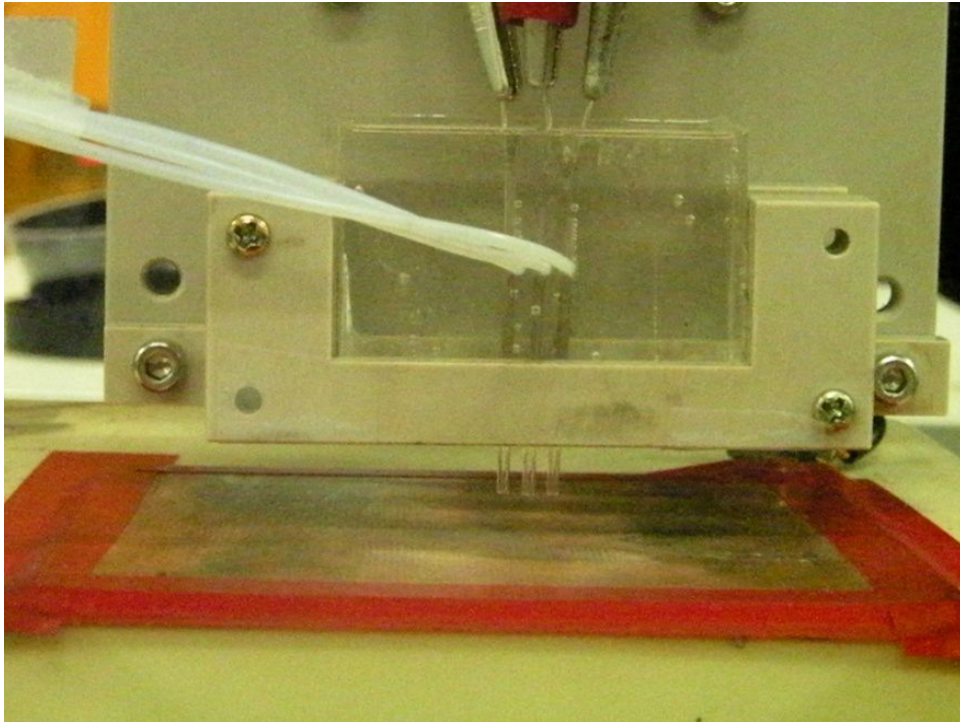
Figure 5.12Schematic arrangement of linear array of capillaries and (b) Image of the capillaries array used for experiment

5.2.2. Numerical Simulation

To understand the behavior of the multi-nozzle system, numerical simulation has been performed through commercially available software (COMSOL3.5a). The schematic of FEA model used for simulation along with sub-domain and boundary conditions is shown in figure 5.13.
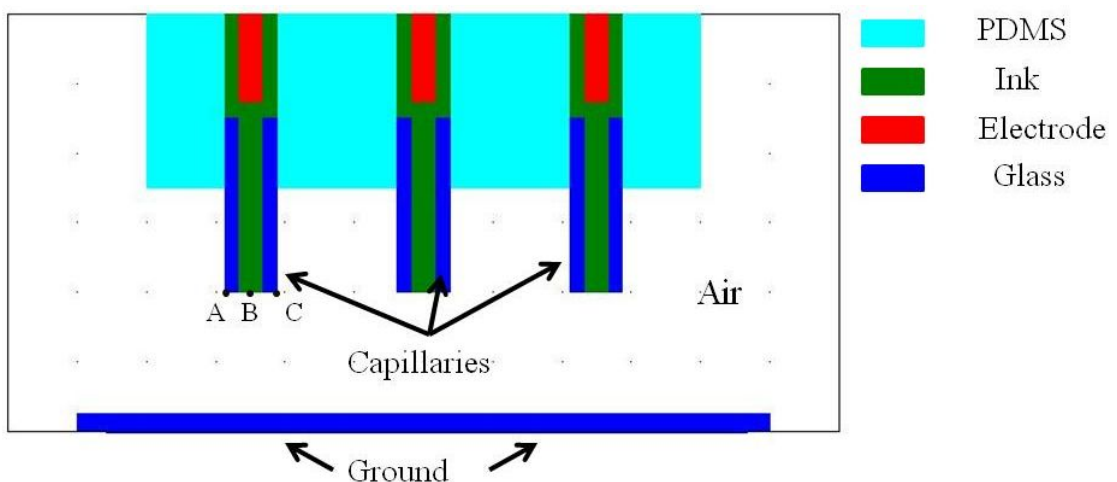
Figure 5.13 FEA model used to calculate electric-field

Two FEA models have been formulated by keeping the nozzle-to-nozzle distance 3mm and 5mm; electric field is calculated at points A, B and C at the tip of the each nozzle; the nozzles are marked 1, 2, and 3 from left to right as mentioned in figure 5.13. Electric-field simulation is performed by changing the applied voltage to all the nozzles simultaneously and also changing the operating conditions of the nozzles using different cases, for example nozzle-2 (i.e., middle nozzle) is "Off" and nozzle-1 and nozzle-3 (corner nozzles) are "On".

In case of multi-nozzle capillary array, the end effects are the prominent feature occurring at the corner nozzles in which the meniscus or jetting is deflected (Ohigashi et. al. 2008, and Rulisona and Flagan 1993). The major cause of this is asymmetric electric-field around the boundary of the meniscus or the jet, since the ejection occurs at the point of meniscus where the value of electric-field is at maximum. The asymmetric electric-field increases as an increase in applied voltage as shown in the numerical simulation for both the cases (nozzle-to-nozzle gap 3mm and 5mm). In case of 3mm gap simulation, the values of electric field at the tip of each nozzle are more as compared to 5mm gap and the value varies along the tip of corner nozzles. However, the middle nozzle has a symmetric electric field along the nozzle, which means that the jetting will be more stable and along the axis of the capillary (Ohigashi et. al. 2008). By looking the results of the electric-field simulation, it is observed that in all the nozzles, the value of the electric field is minimum at the center of the nozzle, point B. In corner nozzles the electric-field is maximum at the extreme end: point A in case of Nozzle 1 and point C in case of Nozzle 3. The results of the electric-field along the tip of the each nozzle for 3mm and 5mm gap (Nozzle-to-Nozzle) at different voltages are shown in tables 5.2 and 5.3, respectively.

3 mm Nozzle-to-Nozzle Gap									
Voltage (kV)	Nozzle-1			Nozzle-2			Nozzle-3		
	A	B	C	A	B	C	A	B	C
2.5	732	25	512	1161	23	1166	517	25	740
3	880	31	615	1400	28	1395	621	30	890
4	1172	40	820	1870	38	1860	830	41	1180
5	1470	51	1020	2330	47	2325	1030	52	1470
6	1760	61	1230	2798	56	2790	1240	62	1780
7	2050	71	1435	3260	66	3250	1450	71	2060
8	2345	81	1640	3730	75	3720	1650	81	2350
9	2637	92	1850	4195	85	4185	1860	92	2640

Table 5.2 Values of Electric field (kV/m) at the tip of each nozzle at different voltage and nozzle-nozzle gap of 3mm

5 mm Nozzle-to-Nozzle Gap									
Voltage (kV)	Nozzle-1			Nozzle-2			Nozzle-3		
	A	B	C	A	B	C	A	B	C
2.5	682	33	1220	1500	330	1300	1230	33	684
3	819	40	1470	1850	39	1560	1480	40	820
4	1090	53	1950	2470	53	2100	1980	53	1090
5	1360	67	2440	3100	66	2600	2470	67	1370
6	1640	80	2930	3710	79	3120	2960	80	1640
7	1910	98	3420	4320	92	3640	3470	94	1910
8	2180	107	3910	4950	105	4150	3950	107	2190
9	2450	120	4400	5560	119	4670	4450	120	2460

Table 5.3 Values of Electric field (kV/m) at the tip of each nozzle at different voltage and nozzle-nozzle gap of 5mm

5.2.3 Effect of applied voltage

To investigate the cross-talk effect, experiments are performed on 3mm gap and 5mm gap arrays; by increasing the applied voltage and keeping the flow-rate at 0.0025ml/min(minimum flow-rate can be achieved form the pump). Dripping and jetting angles are calculated from the picture taken during the experiments on different voltages at the corner nozzles, shown in figure 5.14. In case of 3mm gap the variation in jetting angle is greater as compared to the 5mm gap. Moreover, after 5kV and onward there is not much change in jetting angle; this is due to the change of dripping phenomenon to pulsating cone-jet. During the experiment the dripping is observed at 3kV till 5kV; after 5kV the dripping changes into pulsating cone-jet, and also the frequency of the cone-jet increases with increase in voltage. At 6kV and onward stable and continuous cone-jet is observed.
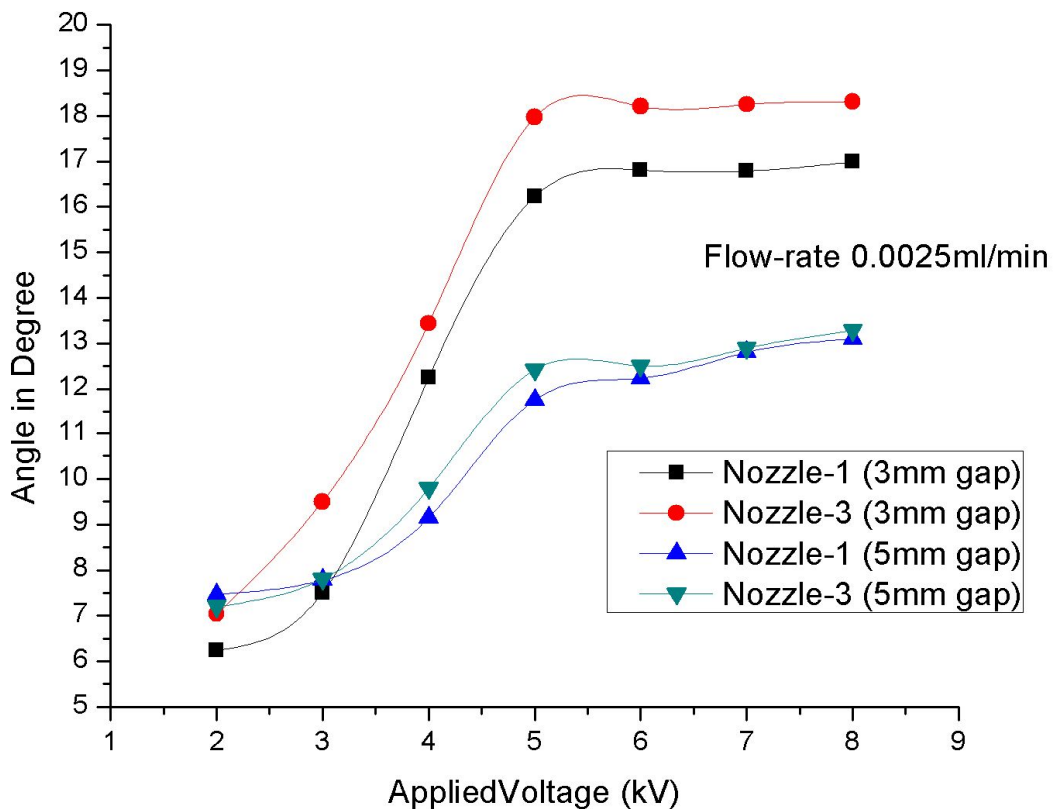
Figure 5.14Dripping and jetting angle at different applied voltage at flow-rate 0.0025ml/min

To verify this phenomenon of change in jetting angle, the same set of experiments is performed by increasing the flow-rate to 0.015ml/min (greater than the minimum achievable flow-rate through pump) shown in figure 5.15. The behavior in dripping and jetting angle is similar as compared to the previous case. However, there is sudden decrease in angle after 8kV; this is due to continuous cone-jet phenomena which are observed at 8kV and onward. This anomalous behavior is due to formation of a stable and continuous cone-jet. Experimental results show that the value of the dripping and jetting angle increases with increase in applied voltage; this effect is due to the asymmetric values of the electric field at the capillary tip, which is greater in case of 3mm gap. Images at figure 5.16 show the transition from pulsation cone jet to continuous cone-jet at different voltage and flow-rate. As observed during the experiment the value of dripping and jetting angle also depends on the mode of electrohydrodynamic jetting.
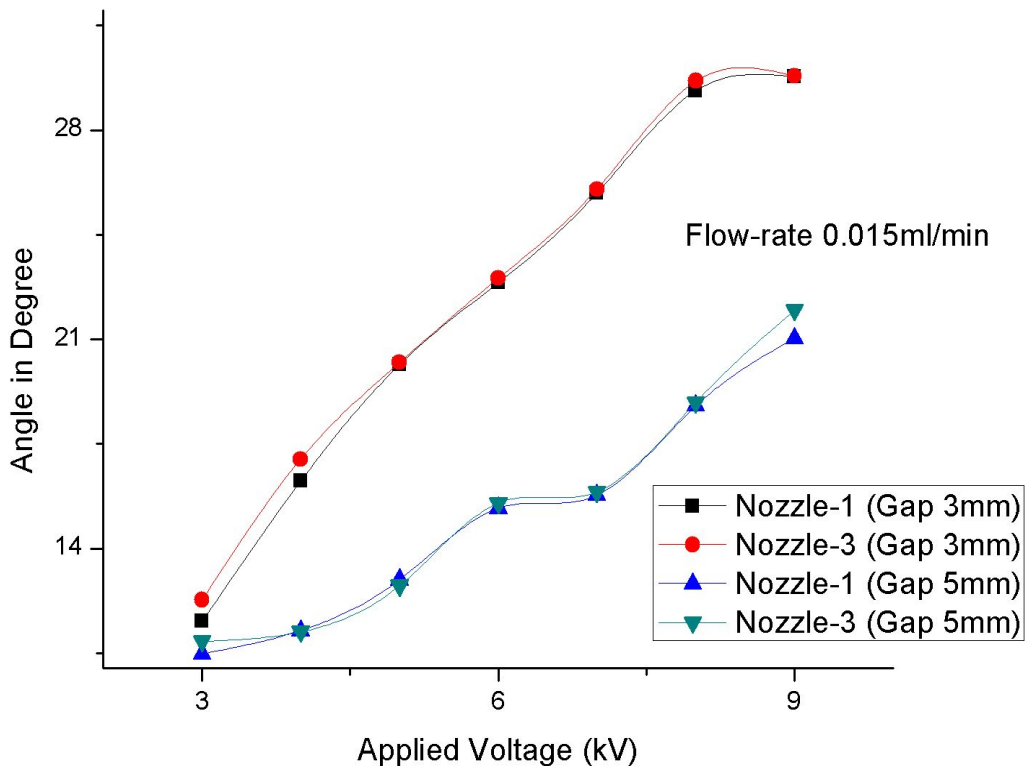
Figure 5.15 Dripping and jetting angle at different applied voltage at flow-rate 0.015ml/min
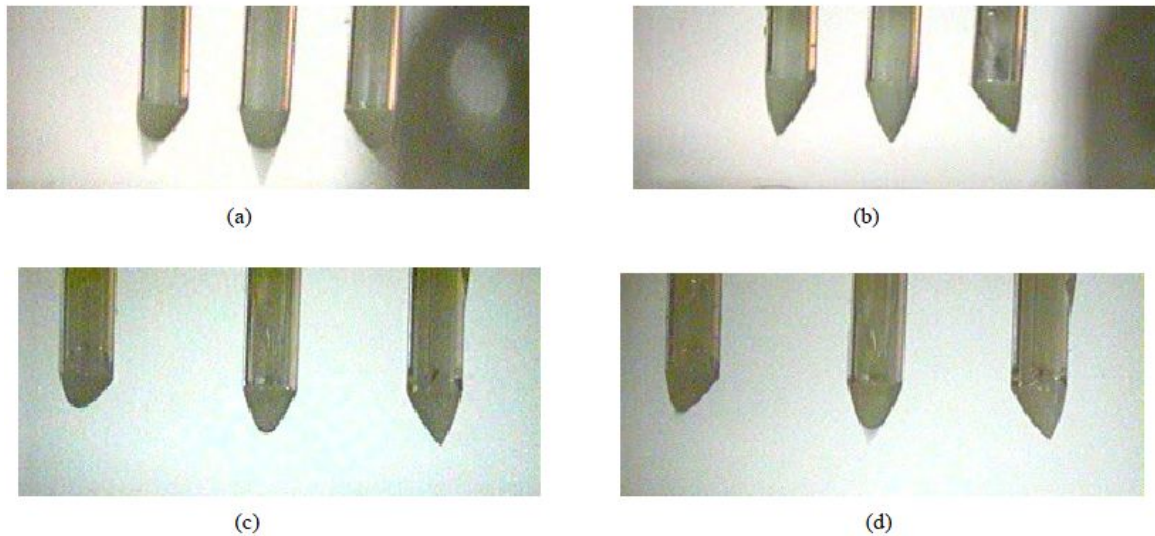
Figure 5.16Images showing the behavior of jetting with respect to applied voltage: (a) Gap 3mm, Applied Voltage 8kV and flow-rate 0.0025ml/min; (b) Gap 3mm, Applied Voltage 8kV and flow-rate 0.015ml/min; (c) Gap 5mm, Applied Voltage 8kV and flow-rate 0.0025ml/min; (d) Gap5mm, Applied Voltage 8kV and flow-rate 0.015ml/min

The effect of the applied voltage is also observed on the pattern position on substrate with respect to nozzle position. The deviation of pattern on the substrate with respect to applied voltage is similar as of the jetting angle as shown in graph at figure 5.17. As shown in the graphs the deviation in the position in case of high flow-rate is greater, because the charge carrying is increased in high flow-rate and causes the increase in radial component of the electric field, and more cross-talk effect is observed (Saville 1970, and 1971). Since the 3mm gap nozzle observed more cross-talk effect of the electric field as compared to 5mm, therefore, there is a larger deviation in the pattern position. The pattern on the glass substrate at 8kV and flow-rate 0.0025ml/min with nozzle to nozzle gap is shown in figure5.18; the average pattern width is 250μm approximately.
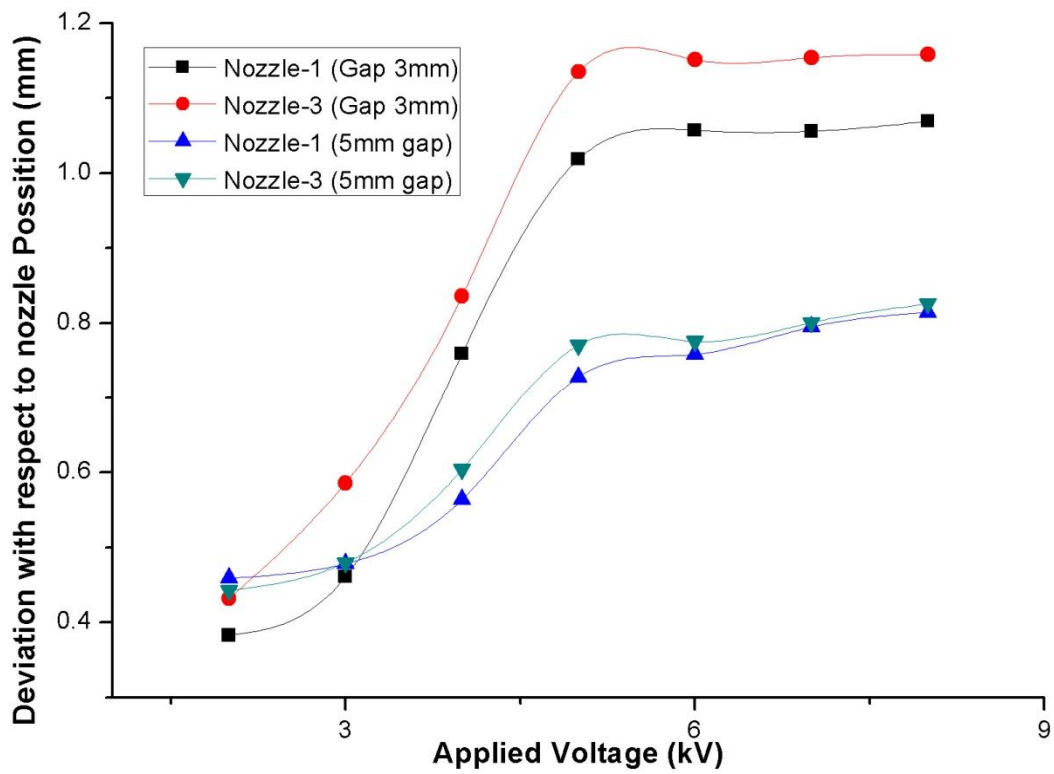
(a)
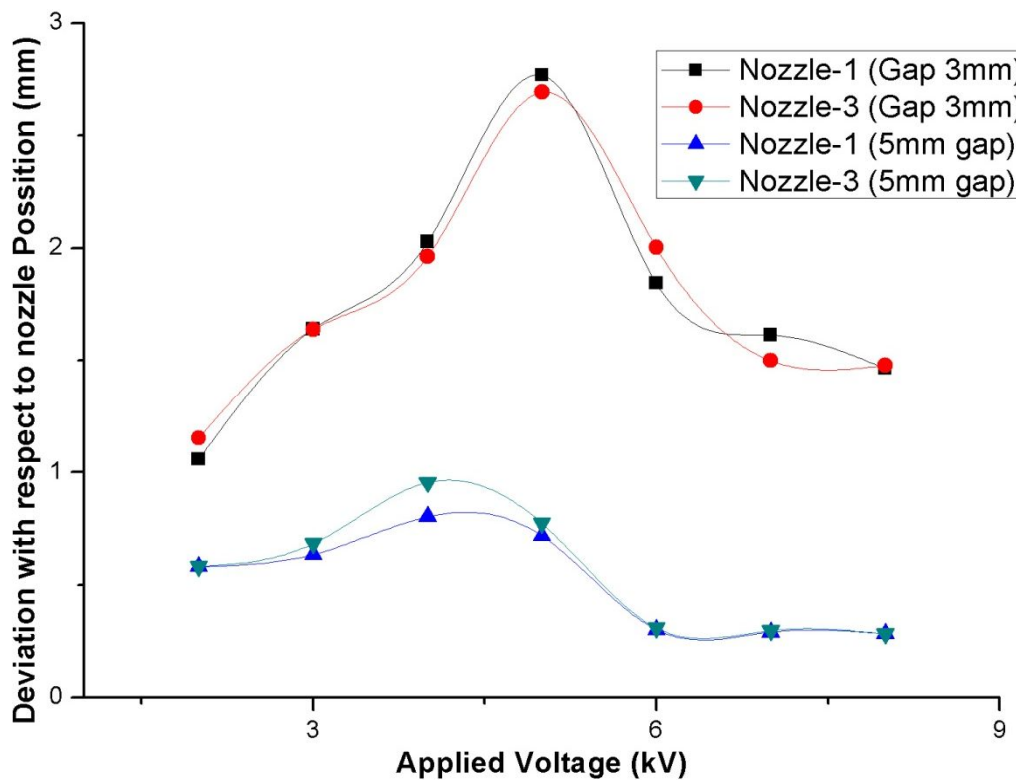
(b)

Figure 5.17 Deviation in pattern position with respect to nozzle position at different voltages and flow-rate (a) 0.0025ml/min and (b) 0.015ml/min
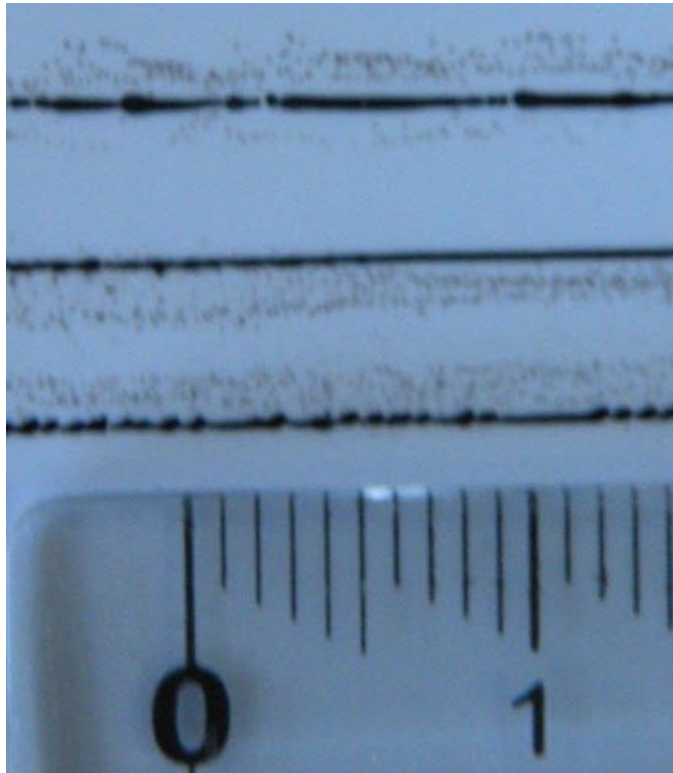
Figure 5.18 Multi-Nozzle patterns on glass substrate at 8kV and flow-rate0.0025ml/min

5.2.4 Effect of Flow-rate

The effect on the dripping and jetting angle is also investigated by changing the flow-rate while keeping the applied voltage at 6kV for both 3mm and 5mm nozzle-to-nozzle gap. The reason of taking this voltage is because the pulsatingcone-jet is formed after 5kV as observed in previous reportedexperiment. The jetting angle with respect to flow-rate at 6kVis shown in figure5.19. For a 3mm gap, the jetting angle increases when the flow-rate increases, but when the flow-rate reaches0.0195ml/min the angle of the cone-jet decreases till 0.025ml/min. Afterward the variation in jetting angle is insignificant;however, the height of the cone-jet increases with increasein flow-rate. This phenomenon is due to increase in jetdiameter at high flow-rate involved in case of stable cone-jetformation. A similar trend is observed for a 5mm gap. Asreported in different researches (Hartmann 1998, and Poon 2002), the cone-jet transitionis more dependent on the liquid flow rate as compared to appliedvoltage; this causes the decrease in jetting angle andincrease in height of the cone-jet. For a

104

5mm gap, the changein angle is not significant as compared to the 3mm gap due toless interfacing of the electric field at the tip of the nozzle.
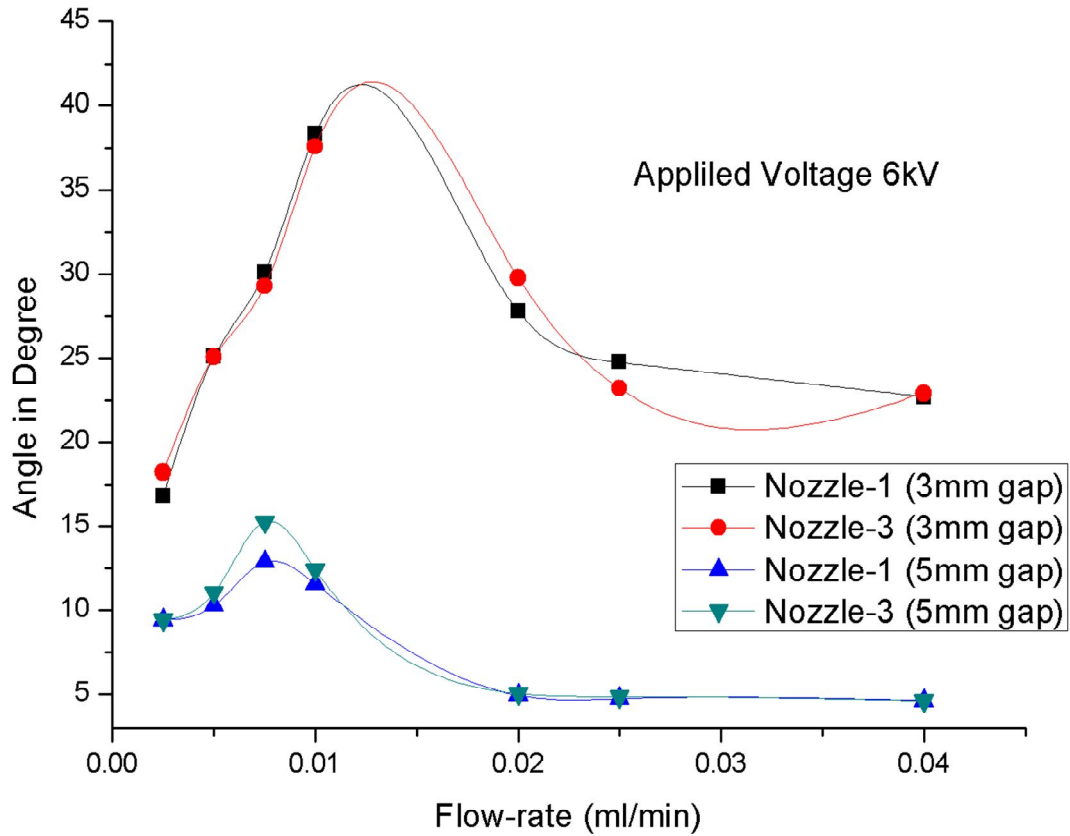
Figure 5.19 Dripping and jetting angle at different flow-rate and applied voltage 6kV

The transition of cone-jet at different flow-rates for 3mmnozzle-to-nozzle gap isshown in figure5.20. The deviation ofpattern on the substrate with respect to flow-rate is similar asof the effect of flow-rate on the jetting angle as shown ingraph at figure 5.21. The rapid decrease in the deviation is due tothe change in the jetting angle at higher flow-rate because ofmore inertial forces in the liquid due to the applied flow-rate.

(a)   (b)

(c)   (d)
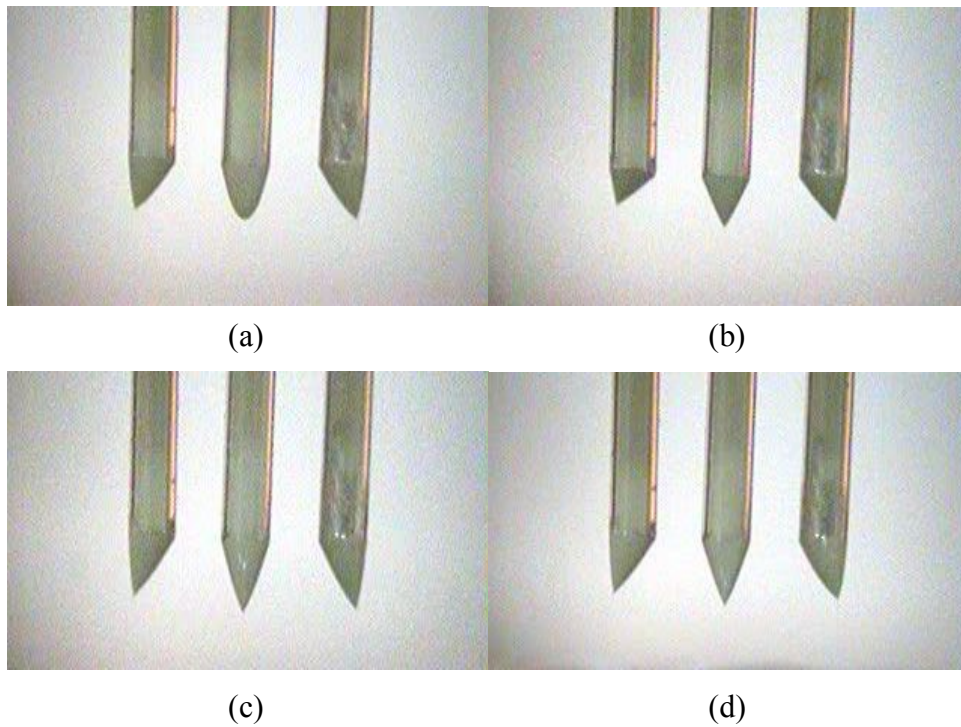
Figure 5.20 Images showing the behavior of jetting with respect to flow-rate (a) Gap 3mm, Applied Voltage 6kV and flow-rate 0.005ml/min – Cone-jet height 1mm (b) Gap 3mm, Applied Voltage 6kV and flow-rate 0.015ml/min – Cone-jet height 0.722mm (c) Gap 3mm, Applied Voltage 6kV and flow-rate 0.025ml/min – Cone-jet height 1.22mm and (d) Gap 3mm, Applied Voltage 6kV and flow-rate 0.04ml/min – Cone-jet height 1.35mm
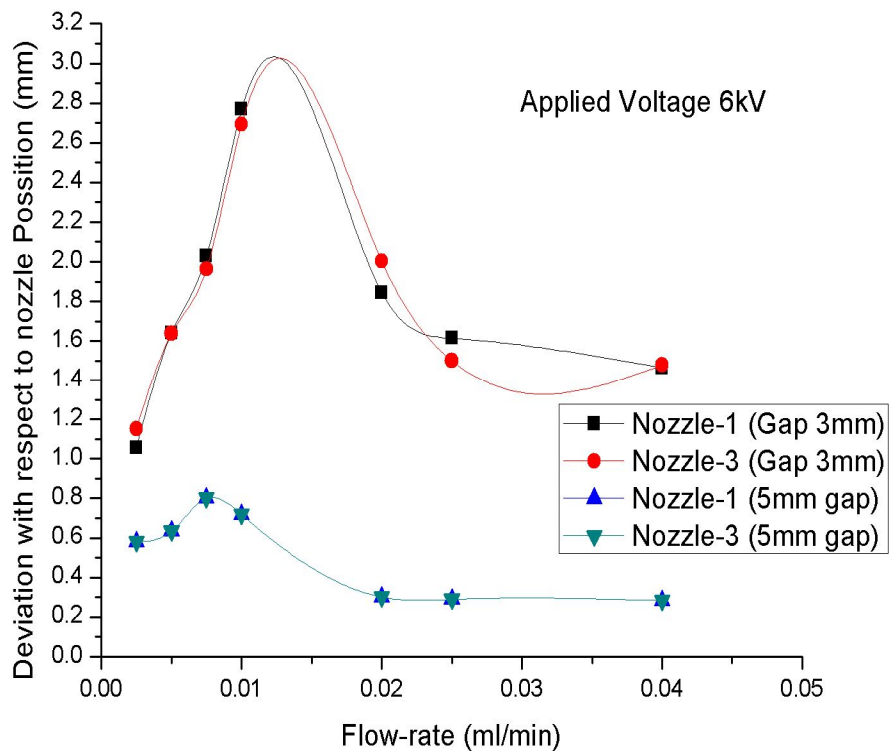
Figure 5.21 Deviation in pattern position with respect to nozzle position at flow-rate for applied voltage 6kV

106

5.2.5 Discrete operation of capillaries

In case of the multi-nozzle setup, for printing purposes,each nozzle is operating individually. In electrohydrodynamic multi-nozzle printing the electric-field plays an important roleby affecting the direction or position of the printing on thesubstrate. To study this phenomenon, experiments are performedby operating each capillary discretely, applying 9kVand 7kV on 3 mm and 5mm gap configuration, respectively,according to the cases as shown in Table 5.4.

Operating Case	Nozzle Number		
	1	2	3
1	On	Off	On
2	On	On	Off
3	Off	On	On

Table 5.4 Cases for discrete operation of applied voltage

To calculate theelectric field, numerical simulation has been performed foreach case. Electric field result at the tip of each nozzle at positionsA, B and C for 3 mm and 5 mm gap is reported in Table 5.5 and Table 5.6, respectively. In all the cases the electric field isminimum at the center of the nozzle, point B. The contour plotthrough numerical simulation of Case-1 by applying 9 kV fornozzle-to-nozzle gap 3 mm is shown in Figure 5.22.

3mm Nozzle-to-Nozzle Gap										
Voltage (kV)	Case	Nozzle 1			Nozzle 2			Nozzle 3		
		A	B	C	A	B	C	A	B	C
9	1	2600	91	1900	3850	81	3840	1925	90	2600
	2	2620	91.5	1920	3930	85.5	4700	1330	82	2320
	3	2314	82	1320	4710	86	3920	1940	91	2650
7	1	2020	70	1480	2980	62	29	1500	70	2030
	2	2040	71	1490	3060	66	36	1040	64	1800
	3	1800	66	1030	3660	66	30	1500	71	2040

Table 5.5 Values of Electric field (kV/m) at the tip of each nozzle at discrete operation of voltages and nozzle-nozzle gap of 3mm.

5mm Nozzle-to-nozzle Gap										
Voltage (kV)	Case	Nozzle 1			Nozzle 2			Nozzle 3		
		A	B	C	A	B	C	A	B	C
9	1	2400	119	4750	4680	103	3930	4650	119	2410
	2	2450	120	4480	5250	119	5150	2610	88.3	1830
	3	1830	88	2580	6080	119	4420	4530	120	2450
7	1	1870	92	3560	3640	80	3050	3600	92	1880
	2	1900	93	3490	4090	92	4010	2020	68	1430
	3	1420	68	2610	4730	92	3430	3520	93	1900

Table 5.6 Values of Electric field (kV/m) at the tip of each nozzle at discrete operation of voltages and nozzle-nozzle gap of 5mm
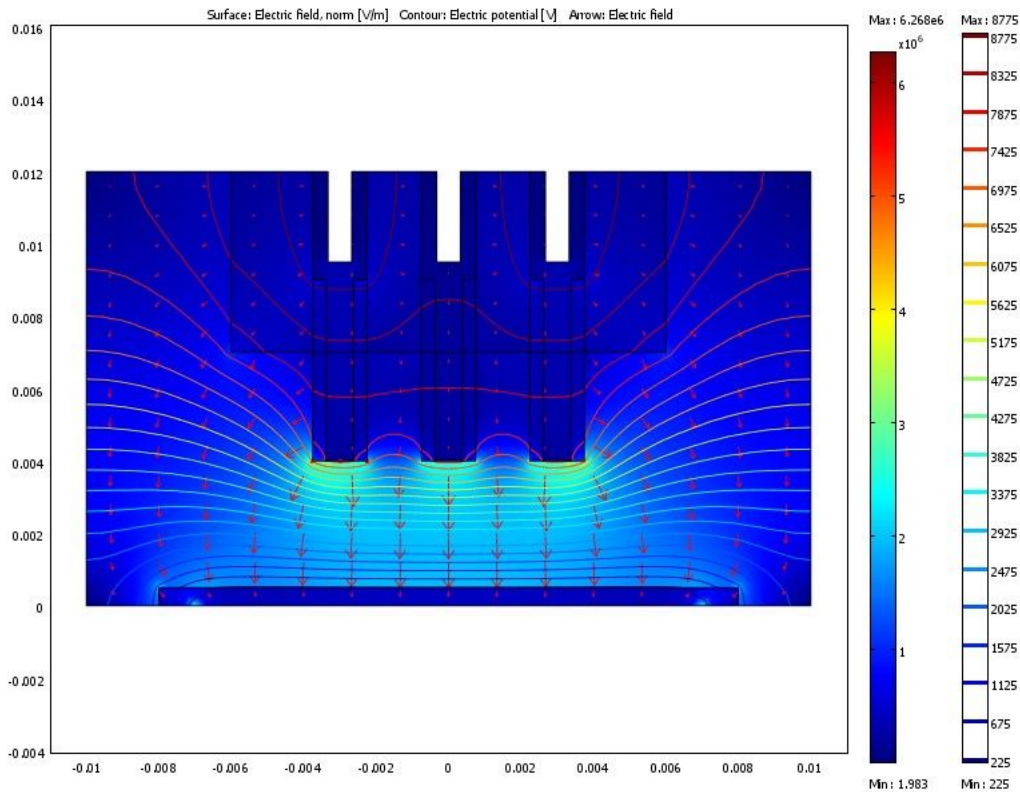
Figure 5.22 Electric field simulation results plotting electric-filed contours and arrows, nozzle-to-nozzle gap 3mm, applied voltage 9 kV. (Case-1)

The jetting angle for all the cases by applying 9kV and 7kV with flow-rate keeping 0.004 ml/min through experiment is reported in figure 5.23.
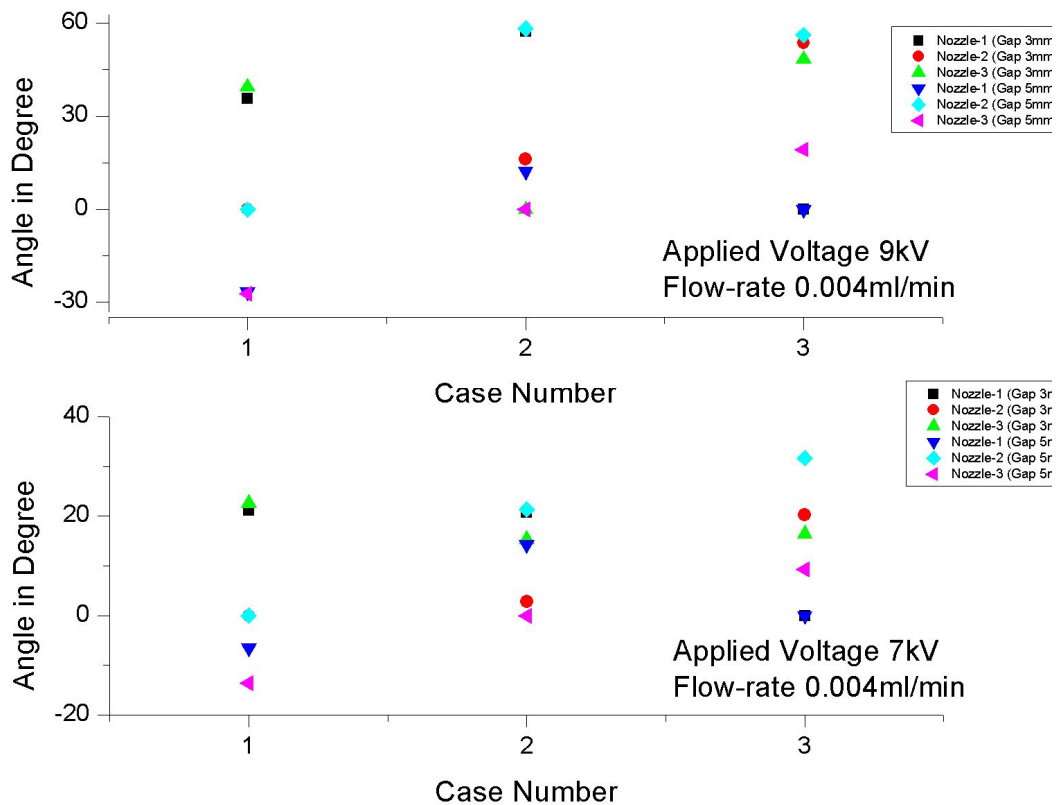
Figure 5.23 Jetting angle for discrete operation (Case-1, Case-2 and Case-3)

In 5mm gap setup, the direction of the jetting is towards the middle nozzle; this is due to the less cross-talk effect as compared to the 3mm gap and also due to the ground effect of middle nozzle; however, this phenomenon has to be investigated further. For 9kV applied voltage the value of the angles is more as compared to 7kV due to high electric field. As observed in the experiment, the wetting of non-operating capillary also affects the jetting angle; as in cases 2 and 3, the jetting angle has to be identical, but due to wetting effect the jet is attracted towards the non-operating wetted nozzle. This shows that the wetting effect has to be minimized during the discrete operation of the nozzles. Figure 5.24 shows the images of jetting at 9 kV for 3 mm and 5 mm gap for case 1 and 3. Figure 5.25 shows the pattern on the glass for cases 1 and 3 at 9 kV and 5 mm nozzle to nozzle gap at 0.004 ml/min flow-rate.
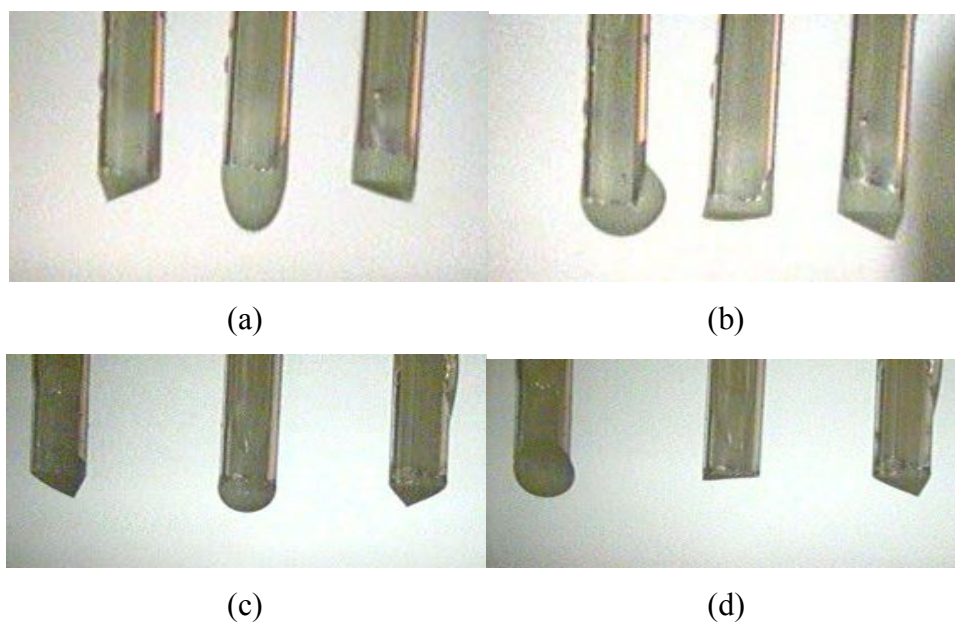
Figure 5.24 Images showing the behavior of jetting for Case 1 and Case 3, (a) Gap 3mm and flow-rate 0.004ml/min – Case-1, (b) Gap 3mm and flow-rate 0.004ml/min – Case-3, (c) Gap 5mm and flow-rate 0.004ml/min – Case-1 and (d) Gap 5mm and flow-rate 0.004ml/min – Case-3
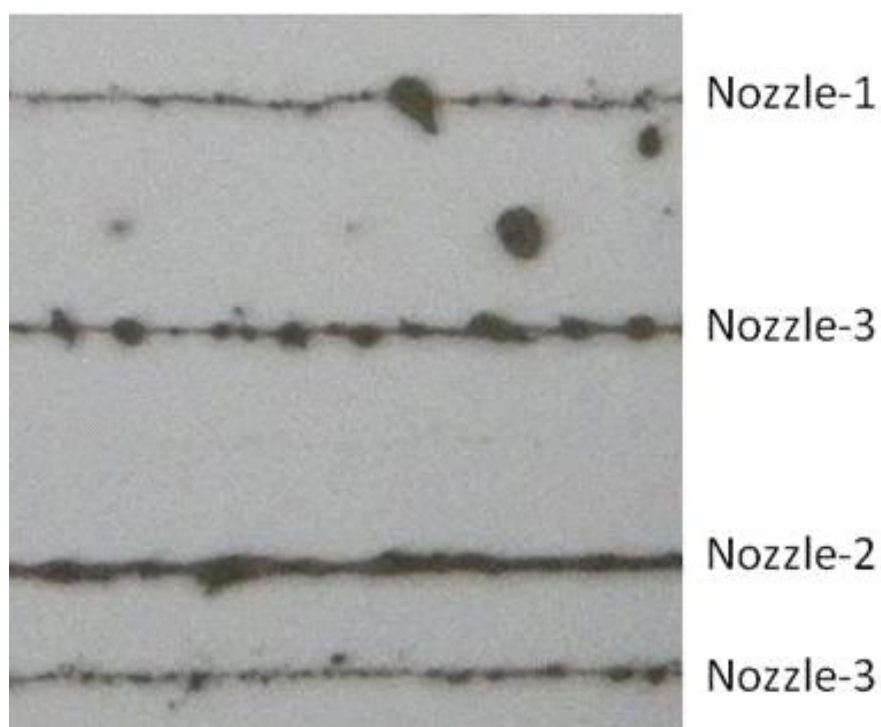
Figure 5.25 Patterns on the glass substrate, for case 1 and 3 at 9kV and 0.004ml/min with 5mm nozzle to nozzle gap

5.2.6 Minimizing cross-talk effect

To reduce the cross-talk effect, many researchers have studied to eliminate the effect by introducing the additional dummy nozzles on each end of the nozzles array (Umezu et. al. 2006, and Deng et. al. 2009). Electric potential is applied to end dummy nozzles in order to eliminate the cross-talk effect at end jetting nozzles. Some researchers performed multi-nozzle jetting using circular or triangular array configurations (Choi et. al. 2011 and Lee et. al. 2011). The cross-talk effect can also be reduced by introducing extractor electrode between nozzle array and the substrate (Choi et. al. 2011 and Lee et. al. 2011). This extractor electrode is used to lower the applied voltage requirement for jetting and reducing the electric field cross-talk by reducing the distance between nozzle and ground. However, the crosstalk effect can be minimized by reducing the nozzle diameter.In this section, the cross-talk effect is investigated by reducing the nozzle diameter to 250μm using 5mm nozzle to nozzle gap. The value of 250μm nozzle diameter is investigated through electric field simulation by reducing the nozzle diameterfrom 750μm, by finding the diameter at which crosstalk is negligible, which means the values of electric field at points A and C are equal. The electric field simulation with respect to nozzle diameter at 5kV of applied voltage is shown in table 5.7. As shown in the table, as the nozzle diameter decreases, the value of electric field is increased at the tip of the nozzle due to decrease in the smaller diameter nozzle.

Nozzle Diameter	Nozzle 1			Nozzle 2			Nozzle 3		
	A	B	C	A	B	C	A	B	C
750μm	1470	51	1020	2330	47	2325	1030	52	1180
500μm	3260	86	3050	3180	65	3190	3100	87	3290
250μm	3750	245	3760	3650	240	3650	3750	246	3740
200μm	3800	260	3810	3780	258	3790	3800	260	3800

Table 5.7 Values of Electric field (kV/m) at the tip of each nozzle with respect to nozzle diameter and nozzle-nozzle gap of 5mm

Moreover, the difference between the value of electric field atpoint A and C also decreases at Nozzle-1 and Nozzle-2, whichshows that the cross-talk effect is minimized by reducing thenozzle diameter. The simulation results also reveal that

thecross-talk is minimized when the nozzle diameter is 250μmand less. For nozzle diameter of 250μm and smaller the crosstalkis negligible for nozzle to nozzle gap of 5mm. To verify the cross-talk effect experiments are performed by using an internal diameter of 250μm and outer diameter of300μm glass capillaries nozzle. The glass capillaries of innerdiameter of 750μm and outer diameter of 1.5mm are pulledby using micro-pipette puller (P-97, Shutter Instrument). The250μm pulled glass capillaries are then fitted to PDMS nozzleholder by maintaining the 5mm nozzle-to-nozzle gap asshown in figure 5.26
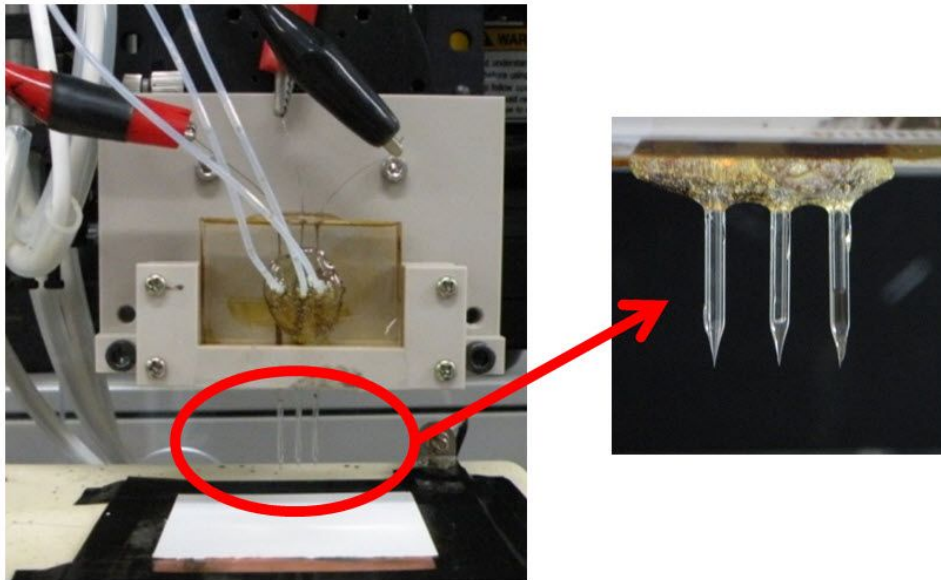
Figure 5.26250μm multi-nozzle array mounted to PDMS with 5mm nozzle to nozzle gap

For 250μm diameter nozzle the jetting behavior is observedwith help of a high speed camera (X3, 5000 fps, Motion Pro).The experiments are performed by applying 2 to 6kV andflow-rate of 0.0025ml/min to 0.015ml/min. With 250μmdiameter nozzle, stable dripping and jetting is observed from 2to 6KV, after 6kV multi-jet is observed, because appliedvoltage for stable jetting is reduced when the nozzle diameteris decreased (Poon 2002). The axisymmetric jetting is observed atindividual nozzle with no sign of deflection or cross-talk indripping or jetting behavior. Figure5.27 shows the high speedcamera images of the stable and axisymmetric jetting at individualnozzles by applying 4kV of applied potential and at0.002 ml/min.
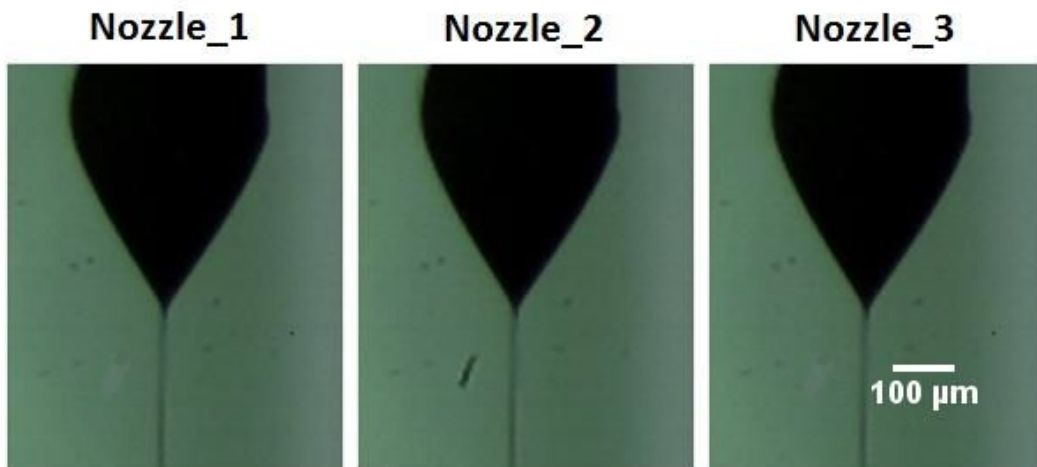
Figure 5.27High speed camera of axisymmetric jetting on each nozzleusing 250µm nozzle diameters with no sign of cross-talk effect

The pattern on the glass substrate at 4 kV and 0.0025ml/min is shown in figure 5.28. The minimum pattern widthachieved is approximately 185µm with no deviation in patternposition on glass substrate with respect to nozzle position.
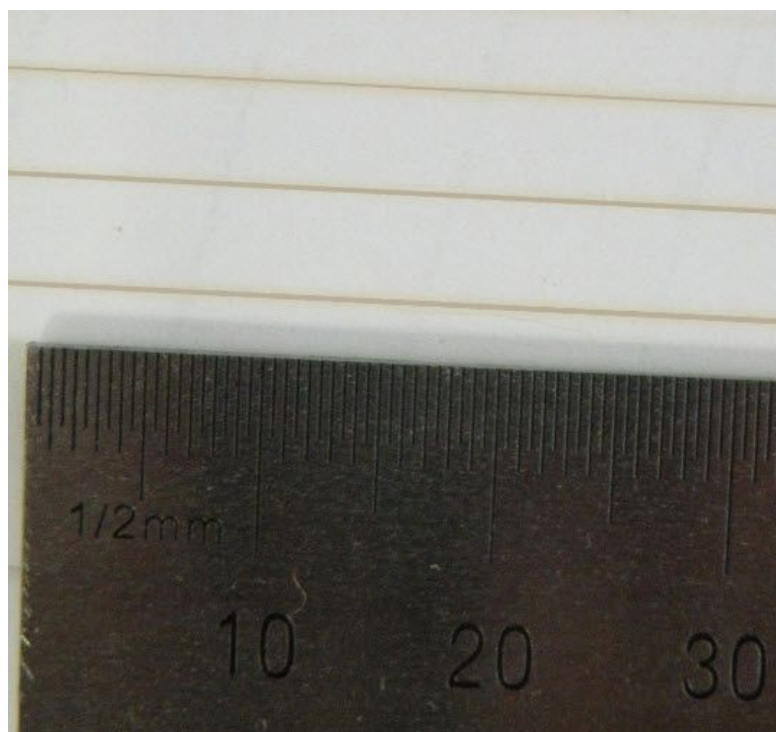
Figure 5.28Multi-Nozzle patterns on glass substrate using 250µm nozzle diameter at 4kV and flow-rate 0.0025ml/min

5.2.7 Conclusions

The cross-talk effect is evaluated with the help of jetting angle by keeping 3mm and 5mm nozzle-to-nozzle gap and varying the applied voltage and flow-rate. The jetting angle is also evaluated through discrete operation of nozzles. In case of varying the applied voltage, the angle of the jetting depends on the applied voltage. As the voltage increases, the dripping angle also increases, but the value of the angle also depends on the jetting behavior. The value of the angle is more for 3mm gap as compared to 5mm gap. However, the effect of the change in angle with respect to system behavior from dripping to cone-jet needs further investigation.

By increasing the flow-rate, the jetting angle is also increased, but when the flow-rate reaches a critical point where the pulsation phenomenon transient to continuous stable cone-jet the angle of the jetting starts decreasing. However, the cone-jet length increases with increase in flow-rate. When the nozzles are operated discretely, the direction of the jet is towards the center nozzle in Case 1, for 5mm gap; this is due to the ground effect on the middle nozzle and less cross-talk effect due to larger gap. However, in the case of 3mm gap the angle of jetting is away from middle nozzle. The wetting of the non-operating nozzle also affects the jetting angle.

The cross-talk effect can be minimized by reducing the nozzle diameter. For 5mm nozzle to nozzle gap, the cross-talk effect is negligible with 250µm nozzle diameter. For nozzle-to- nozzle gap of 3mm, jetting without observing cross-talk effect has been reported in our previously published article (Khan et. al. 2011). For decreasing the nozzle-to-nozzle gap, smaller diameter capillaries have to be used, which reduces the value of operating voltage. The transition effect from dripping to cone-jet in multi-nozzle case also affects the angle of dripping and jetting, but this is a matter for further investigation.

5.3 DOD EHD patterning

There are two modes of electrohydrodynamic jetting: Continuous and drop-on-demand. In continuous mode DC voltage is used to achieve continuous printing and is most suitable direct writing approach of colloidal solutions for low resolution patterning. The speed and high velocity of the jet enables it to travel larger distance to the substrate. In continuous EIP the scattering masses are significantly less for the submicron resolution printing and also the continuous flow of the ink through nozzle minimize the risk of clogging it in EIP. Continuous mode only forms continuous lines and therefore use of the continuous mode eliminates the requirement of overlapping of successive ink droplets to produce a continuous line. Both modes are capable of producing high resolution patterns but the control and stabilization of the high speed jet in continuous mode is very difficult and can lead to unreliable printing. In case of drop-on-demand mode the pulse voltage is applied to the capillary for liquid charging instead of continuous DC voltage, which causes the meniscus to deform into a cone and forms a droplet rather than continuous jet and can provide greater control over the size and interval of the drop ejection.When the drop is ejected, the surface tension forces dominate and the charges around the surface of the nozzle tip is decreased, due to which the meniscus is pulled back and when the next voltage pulse is applied then another drop is produced.

This section will present the relationships and the effects of the various operating parameters for the drop-on-demand phenomena. The experiments are performed using glycol. Different sets of experiments are performed by varying various process parameters, i.e. voltage, duty cycle, pressure and frequency. The results of this section can be used as the guideline by the EIP operators and are useful for electronic industry by achieving more controlled EIP operations for the fabrication of electronic devices.

5.3.1 Experiment Setup

Metallic capillary having an internal diameter of 110μm and 210μm of external diameter (World Precision Instruments) was connected with an ink reservoir. The ink reservoir was mounted on Z- axis stage to adjust the gap between the nozzle and substrate. The ink reservoir was then connected to the pressure regulator in order to supply the ink to the tip of the nozzle with a constant flow rate. The voltage was supplied through the metallic wire which was connected to the high voltage power amplifier (Trek 610E) and controlled multifunctional signal synthesizer (HP 33120A). To control the substrate speed during the process, the ground plate was mounted on X-Y motorizes stage (SURUGA SEIKI DS102). The process was monitored with high speed camera (Motion Pro X3), which was connected to the PC controller.

For the analysis of drop-on-demand phenomena experiment of ethanol also been discuss in chapter 3, however, in this section detail analysis of drop-on-demand phenomena will be discussed using glycol. The properties of ethylene-glycol are given in table 5.8.

Surface Tension γ (mN/m)	Viscosity μ (cps)	Density ρ (g/m^3)	Conductivity S (μS/m)	Dielectric constant
48	19.83	1.1135	10	37

Table 5.8Physical properties of ethylene-glycol

5.3.2 Relaxation time related to DOD

In order to explain the drop-on-demand phenomena, the relaxation time related to electrohydrodynamic jetting has to be considered. Electrohydrodynamic drop-on-demand is combination of electrical and hydrodynamic phenomena:

116

a) Charge relaxation

b) Hydrodynamic relaxation

c) Natural vibration of pendant drop volume

d) charging the capacitance between the tip of the nozzle and the grounded plate over theresistance of the fluid between the tip of the electrode in the capillary and the meniscus

The charge relaxation time is given by(Marginean et. al. 2006):

$$\tau_c = \frac{\varepsilon}{4\pi K} \qquad (5.2)$$

Where K is conductivity of liquid, ε is permittivity of liquid. To calculate the RC time of the electrical circuit consisting of the capacitance between the tip of the nozzle and the grounded plate over the resistance of the fluid between the tip of the electrode (in this case tip of capillary) and the meniscus following has to consider. The resistance between the tip of the electrode (nozzle) and the meniscus is given by(Creemers et. al. 1989):

$$R_M = \frac{l}{K A_L} \qquad (5.3)$$

with$l$is the distance between tip of electrode and meniscus (which is considered as outer diameter of the capillary) and $A_L$is the cross section of the fluid volume between the tip of the electrode and the meniscus. To estimate the capacitance of the meniscus and the ground plate we take the formula of the capacitance of two parallel plates with air in between (S_M - the surface area of the meniscus, ε_{air} - the permittivity of air and h- the distance between tip of the nozzle and grounded plate)(Creemers et. al. 1989):

$$(5.4)$$

In our set-up we have $l = 210\mu m$, $d = 1mm$, $A = \pi(i.d.)^2/4 = 9.5e\text{-}9m^2$, $S_M = \pi(o.d.)^2/4 = 4.46e^{-8}m^2$,. $C = 3.94e^{-16}F$ and $R = 1.15e^9\Omega$, leading to a RC time $\tau_{RC}=RC=0.45\mu s$. To calculate the natural frequency of a pending droplet we use Rayleigh'sformula (Rayleigh 1896):

$$(5.5)$$

With r - the radius of the pending droplet (approximately equal to o.d./2), γ - surface tension of liquid and ρ - the density of the fluid of the pending drop. The damping can be estimated by thehydrodynamic relaxation time (Marginean et. al. 2006):

$$\tau_H = \frac{\mu r_c}{\gamma} \tag{5.6}$$

Where,$r_c$is radius of the capillary (o.d./2) and μ is viscosity of liquid. All characteristic times constants for ethylene glycol are shown in table 5.9.

Charge Relaxation Time (τ_c) sec	Hydrodynamic Relaxation Time (τ_H) Sec	$1/f_{Rayleigh}$ sec	RC Time sec
2.6e-6	4.54e-5	3.9e-4	0.45e-6

Table 5.9Electrical and hydrodynamic relaxation time of Ethylene Glycol with 110µm capillary

Calculated results indicate that hydrodynamic relaxation times and Rayleigh time are the most important factor for drop-on-demand process.

5.3.3 Experimental results

In order to analyse the drop-on-demand behaviour, initially minimum jetting voltage was determined by applying the DC voltage at 0.1kPa of applied pressure, using the same experiment as reported in section 4.2.1. Metallic capillary of internal diameter 110µm and external diameter of 210µm was used for the studying of drop-on-demand phenomena with the help of high speed camera, where capillary to ground distance was kept at 1mm. The minimum voltage at which stable con-jet was observed was 2kV. Based on the minimum voltage the square pulse voltage with bias voltage of 1.75kV was selected, whereas for ejection voltage 2.5kV was used. Numbers of experiment were performed at different frequency and keeping the ejection voltage time as 50% of applied pulse width. Pulsed time with respect to applied frequency is given in table 5.10.

118

Applied Frequency Hz	Pulse Times (Ejection Voltage Time) sec
100	0.005
200	0.0025
300	0.00167
400	0.00125
500	0.001
600	8.33e-4
700	7.142e-4
800	6.25e-4
900	5.5e-4
1000	5e-4
1100	4.454e-4
1200	4.16e-4
1300	3.84e-4
1400	3.57e-4
1500	3.33e-4

Table 5.10Ejection voltage time with respect to frequency as 50% of duty cycle

Experiment results revealed that up to applied frequency of 800Hz, a stable drop-on-demand phenomenon was observed. With each pulse following sequence of events were observed as shown in figure 5.29:

1. After the ejection voltage applied, the hemispherical meniscus deformed into cone.
2. A thin micron size jet was emerged from the apex of the cone
3. The jet breaks up just after the end of the ejection voltage
4. After that the meniscus returns to its stable hemispherical position
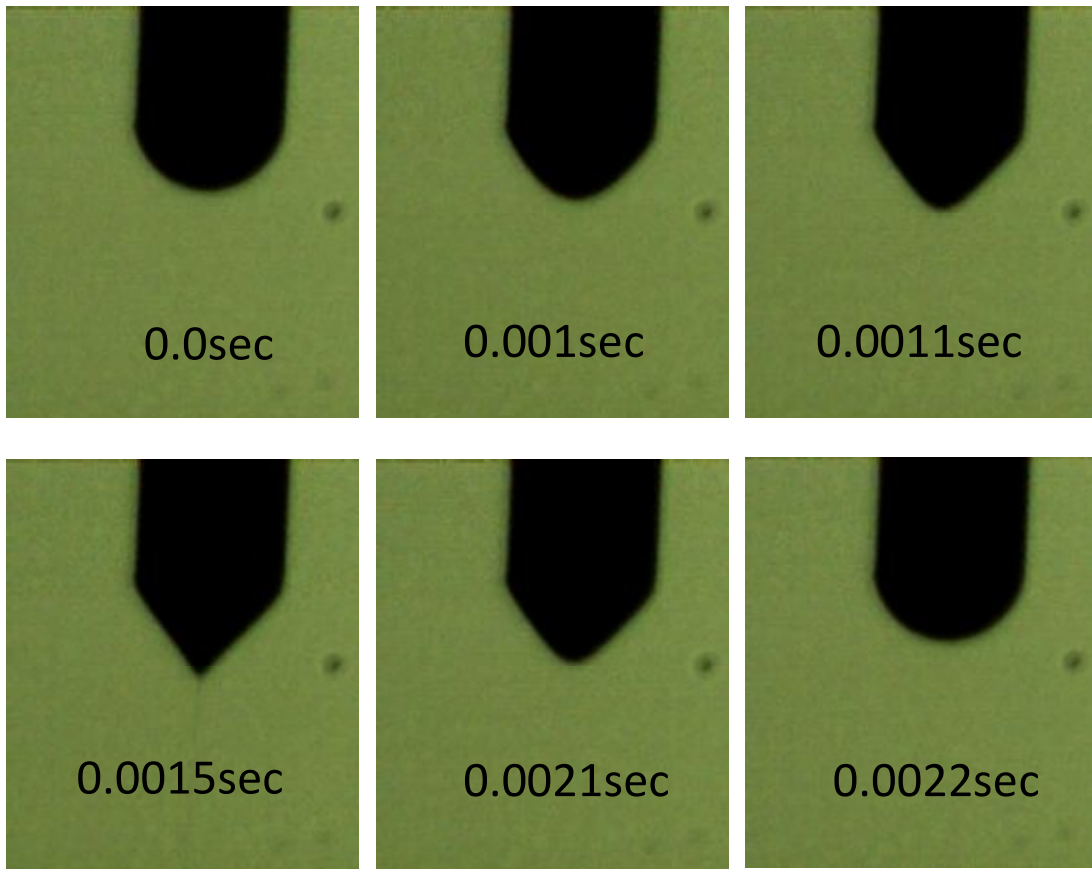
Figure 5.29 High speed camera image of the drop-on-demand phenomena using ethylene glycol by applying bias voltage of 1.75kV, ejection voltage of 2.5kV, pressure of 0.1kPa and duty cycle of 50%

At applied frequency of 900Hz till 1200Hz a stable drop-on-demand phenomena was not observed, due to ejection voltage time, which reduces with increase in applied frequency. Instead of single event per pulse behaviour, intermittent jetting was observed. At 1300Hz frequency and above, no ejection was observed and only vibration of meniscus was observed. At very high frequencies, there is less time for the ejection voltage as compared to hydrodynamic relaxation time, due to this meniscus only showed vibration behaviours instead of ejection of any liquid jet. The relationship between stable drop-on-demand behaviour, with respect to ejection time and applied frequency is shown in table 5.11.

Applied Frequency (Hz)	Approximate Ejection Time (sec)	Behaviour
100	0.005	DOD
200	0.0025	DOD
300	0.00167	DOD
400	0.00125	DOD
500	0.001	DOD
600	8.33e-4	DOD
700	7.142e-4	DOD
800	6.25e-4	DOD
900	5.5e-4	Intermittent Jetting
1000	5e-4	Intermittent Jetting
1100	4.454e-4	Intermittent Jetting
1200	4.16e-4	Intermittent Jetting
1300	3.84e-4	No ejection
1400	3.57e-4	No ejection
1500	3.33e-4	No ejection

Table 5.11Relationship between ejection time and applied frequency

Experimental results also revealed that at lower frequency the ejection of the liquid is greater than the ejection at higher frequencies, due to the time of the ejection pulse. Moreover, in order to control the ejection volume of the liquid, the ejection time has to be controlled at any given frequency with respect to relaxation time.

For drop-on-demand patterning the major issues arises with high viscosity liquid. Since viscosity of the liquid dictates hydrodynamic relaxation times, hence high viscosity liquids are difficult to pattern through electrohydrodynamic drop-on-demand technology. At larger nozzle diameter, the drop-on-demand phenomena is stable at very low frequency, less than 100Hz, in some cases less than 50Hz with high viscous polymers with viscosity of 2500cps. In order to increase the deposition frequency, nozzle diameter has to be decreased.

5.3.4 Visualization of DOD

For study of fine resolution electrohydrodynamic drop-on-demand patterning, currently there is limitation with respect to visualization of the phenomena with the help of high speed camera. For detailed study, the applied pulse voltage must be synchronized with the capture mechanism of the camera. This synchronization will help in detail analysis of drop-on-demand phenomena and behaviour of ejection. The other issue is the resolution of the camera, currently 10μm feature size can be analyse with the help of high speed camera. In order to study the patterning behaviour at submicron level high resolution camera with high magnification is required. The sequential image of the drop-on-demand behaviour using 30μm glass capillary is shown in figure 5.30.
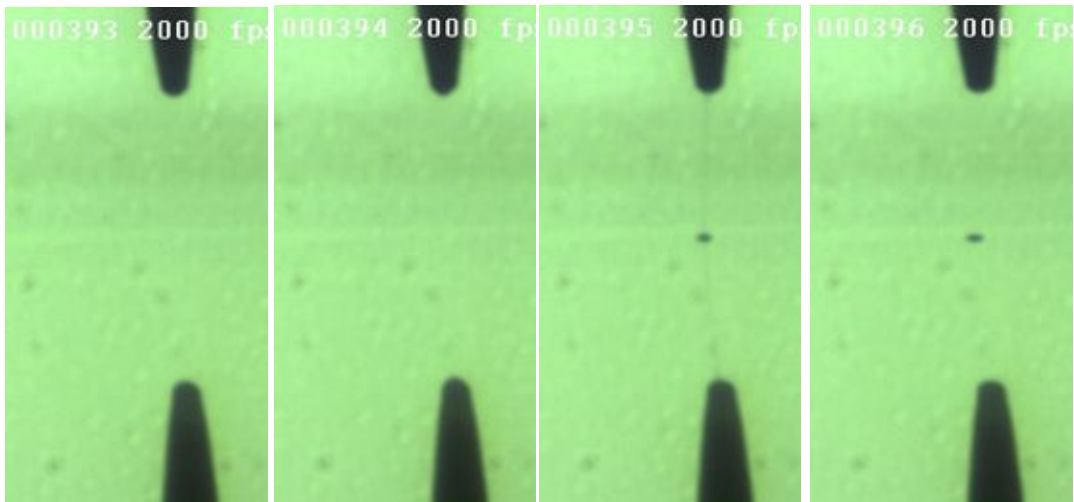
Figure 5.30Patterning of single droplet of Ag nanoparticles using 30μm internal diameter nozzle, with applied frequency of 1000Hz, sequential images shows the deformation of the meniscus as well as ejection of single droplet

6. Conclusions and Future Work

Following is the conclusion of this thesis work:

Chapter 2

- Chapter 2 successfully demonstrates the direct patterning of copper nanoparticles and silver nanoparticles on a glass substrate through electrohydrodynamic printing using continuous cone-jet mode. The patterning is performed on glass substrate at different flow-rates and applying maximum value of applied voltage. The minimum pattern width achieved is 32μm in case of copper nanoparticle ink through 110μm capillary which is 3.125 times smaller than nozzle diameter, whereas, in case of silver nanoparticle ink the minimum pattern width achieved in 80μm through 210μm capillary which is 2.65 times smaller than the nozzle diameter. This neck-down feature of Electrohydrodynamic pattering the smaller pattern width as compared to nozzle diameter is major attraction.

- The XRD analysis and electrical resistivity measurement of the pattern shows the functionality of the copper nanoparticles after direct deposition through electrohydrodynamic printing. As demonstrated in this chapter the electrohydrodynamic printing can be the alternative direct fine resolution patterning method for low-cost copper nanoparticles for printed-electronics applications.

Chapter 3:

- Chapter 3 presents the novel technique of electrohydrodynamic DOD by applying multi-step voltage. The results show that electrohydrodynamic DOD phenomena could be achieved through multi-step voltage, which provided stable and controlled process as compared to square pulse voltage. The experimental data shows that, the multi-step voltage at optimal values gives stable DOD jetting. The low value of bias-voltage causes more movement in meniscus, and also required higher value of ejection-voltage, due to this the phenomenon was not smooth. The other effect on the DOD phenomena is due to frequency and flow-rate.

- For the first time electrohydrodynamic drop-on-demand inkjet printing of copper colloidal conductive ink on glass substrates has been demonstrated. A novel forward multi-step waveform superimposed on bias dc voltage has been applied to generate uniform, controlled and reproducible colloidal droplets containing copper nanoparticles. Tests have been performed with different pulse frequency (10Hz, 25Hz, 50Hz, and 100Hz), biased voltage (2.5kV, 3.5kV) duty cycle (50%, 75%). This drop-on-demand printing method (using forward multi-step waveform) shows promising results in controlled deposition i.e. with each pulse a single drop has been generated. Uniform and very small drops i.e. 110 ±2μm compared to nozzle orifice i.e. 750μm are generated by increasing the magnitude of biased voltage, while decreasing the magnitude of multi-step pulsed voltage. However due to hydrophilic nature of glass substrate the generated droplets spread after deposition resulting in larger sizes than the original size of generated droplet. The minimum average size of deposited droplets and continuous lines on substrate are 500 ±10μm and 450 ±10μm respectively.

- The DOD patterning was also performed through silver ink on glass substrate. The experimental result showed that the droplet size is depended on different values of the applied multi-step voltage. The applied frequency had direct effect on the droplet size. As the frequency is increased the droplet size is decreased due to the short duration of the applied multi-step voltage.

Chapter 4

- This Chapter successfully demonstrates the fine resolution patterning of the conductive tracks through electrohydrodynamic printing in continuous as well as drop-on-demand mode, which can be an alternative process for the deposition of low cost functional material such as copper and silver conductive tracks. In continuous mode of electrohydrodynamic patterning of copper nanoparticles, the minimum pattern width printed on the silicon substrate is approximately 12μm with 148nm of maximum height; the minimum pattern width is five times smaller than the nozzle internal diameter, which is the major benefit of electrohydrodynamic printing to produce a pattern size smaller than the nozzle size. The patterns with different width are printed on the substrate through the

stable cone-jet by changing the flow rate. The result shows that the size of the patterns can be controlled by changing the operating parameters such as flow rate. In order to check the functionality, the resistivity of the patterns is measured; this is 3.5–14 times higher than the bulk, depending on the pattern width and average thickness.

- Fine resolution Ag nanoparticles patterns are successfully deposited on untreated thick glass substrates using electrohydrodynamic jet printing in drop-on-demand mode. The experiment results indicate that printed droplet size at any given frequency is depended on the operating conditions; applied voltage, duty cycle and pressure. However, the applied pressure and duty cycle has more prominent effect on the droplet size as compared to applied voltage. Continuous patterns were fabricated by overlapping consecutive droplets by adjusting the substrate speed with respect to droplet diameter. For smooth and continuous patterns, the experimental results revealed that 70% of droplet spacing is sufficient, for given experimental setup. I-V curves of the sintered printed patterns showed linear Ohmic behaviors. The minimum droplet diameter achieved 3.6µm, whereas the pattern width was approximately 6.5µm, which is 2.7 and 1.53 times smaller than the nozzle internal diameter respectively, which highlights the main advantage of electrohydrodynamic printing to produce smaller pattern size as compare to nozzle diameter. This feature of electrohydrodynamic printing of conductive patterns can help in miniaturizing the electronics devices using non-contacting direct printing technology.

6.1 Future Work

For the fabrication of electronic devices, patterning has to perform on pre-deposited layers, which is still an issue for electrohydrodynamic patterning technology due to charges on the jet. These accumulated charges on the substrate generates an electric field with effects the deposition process and also affects the morphology of the patterns. Some researcher suggested the electrically discharge of jet before imping on the substrate. Detail study of this problem can be interesting topic for future research.

One of the interesting applications of electrohydrodynamic drop-on-demand patterning is formation of 3D structure or micro-pillar. However, for the formation of micro-pillar modified ink with high rate of evaporation is required, which helps in rapid drying of the deposited nanoparticles. The formation of Ag micro-pillar using 5µm nozzle is shown in figure 5.31. This deposition of micro-pillar can be interesting topic for future research. But high rate of evaporation causes nozzle blockage due to accumulation of nanoparticles at the tip of the nozzle opening.
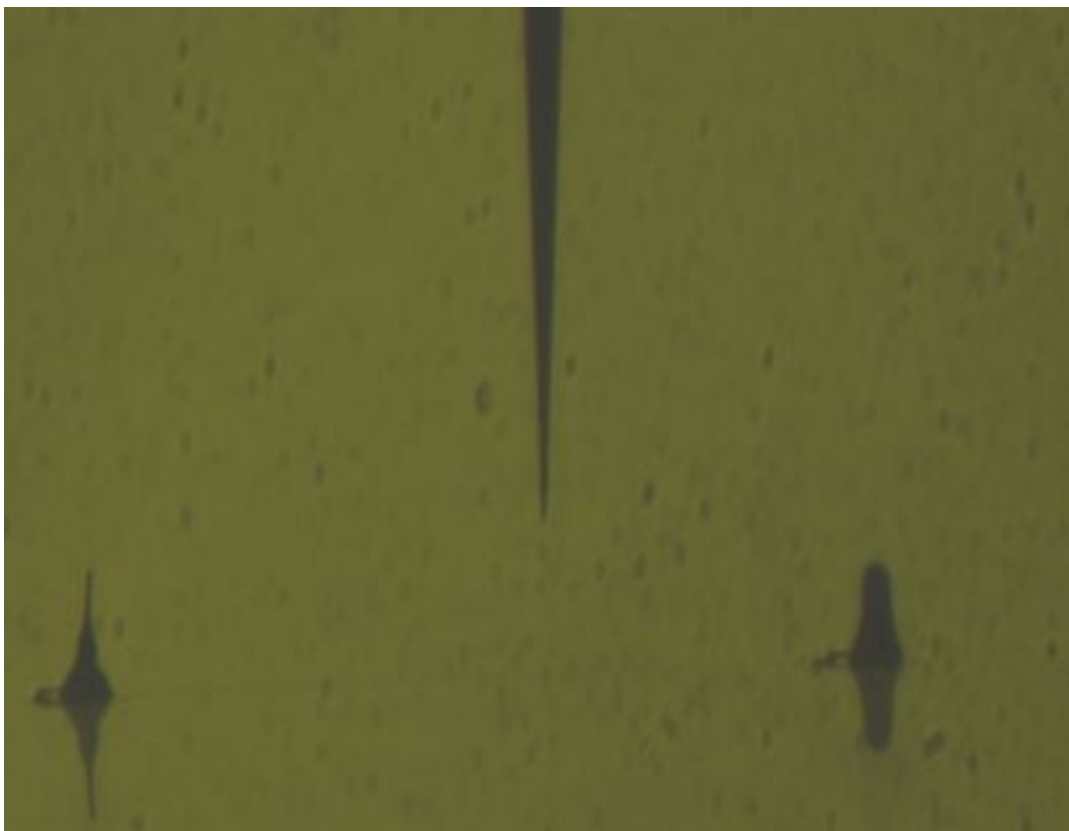
Figure 6.1Ag micro-pillar deposited through electrohydrodynamic drop-on-demand patterning

The other major challenge is deposition at subs-micron level. In order to achieve sub-micron size feature, nozzle size has to be miniaturized. But this miniaturization of nozzle size causes blockage problems. In order to address this issue, inks has to be modified, by reducing the wt% of nanoparticles, reducing the size nanoparticles, homogenous dispersion of nanoparticles and also replacing the high-rate evaporation solvent with the suitable solvents. Moreover, high speed camera with high resolution will be required for the study of sub-micron patterning.

126

References:

Ahmad et. al. N. J. Biomed. Nanotechnol., 4, 185– 195 (2008)

Arias et. al. Applied Physics Letters, 85, 15, 3304-3306 (2004)

Balachandran et. al. Industry Applications Society Annual Meeting, Vol. 2, pp. 1369-1373 (1992)

Bietsch et. al. Langmuir, 20 (12), 5119-5122 (2004)

Bisht, et. al.. Nano Lett., 11 (4), 1831-1837 (2011)

Tran et. al.Aerosol Science 38, 924-934 (2007)

Calvert, Chem Mater., 13, 3299-3305 (2001)

Chen et. al. J. Mater. Sci. 31 5437–42 (1996)

Chen et. al.Aerosol Science and Technology 27 367-380 (1997)

Cheng K., et al. Macromol. Rapid Commun. 26, 247-264 (2005)

Choiand Kim, Int. J. Precis. Eng. Manuf., Vol. 12, No. 1, pp. 165-168, (2011)

Choi et. al. Applied Physics Letter, Vol. 93, No. 19, Paper No. 193508 (2008)

Choi et. al.Journal of Electrostatic, 69, 380-387 (2011)

Chrisey, Science, 289, 879-881 (2000)

Cloupeauand Foch, J. of Electrostatics, 22, (2) 135-159 (1989)

Cloupeauand Foch, J. Aerosol Sci. 25, 1021-1036 (1994)

Cloupeau and Foch, J. Aerosol Sci., 25 (4), 1143-1157 (1994)

Creemerset. al. 1989 Poly-technischzakboekjeElektronica (Koninklijke PBNA BV ed) p H3

Deng et. al.Aerosol Science 40, 907-918 (2009)

Derby, Annu. Rev. Matter. Res. 40, 395-414 (2010)

Mora and Loscertales, J. Fluid Mechanics, 260, 155-184 (1994)

Forrest, Nature, 428, 911-918 (2004)

Fuller et. al. J. Microelectromechanical Syst. 11 54–60 (2002)

Ganan et. al. J Aerosol Sci., 28 (2), 249-275 (1997)

Gamotaet. al.. ISBN 1-4020-7707-6, Massachusetts, USA (2004)

Gana andBarrero, J. Aerosol Sci., 27 (1), S179-S180 (1996)

Ganan, Physical Review Letters,79, (2) (1997)

Gans et. al. Advanced Materials, 16, 203–213. (2004)

Goldmann and Gonzalez, Journal of Biochemical and Biophysical Methods, 42, 105-110 (2000)

Griss et. al. Journal Micromechanics and Microengineering, 12, 682–687 (2002)

Hartman, PhD Thesis, TU Delft (1998)

Hayati andTadros, J. Colloid Interface Sci. 117 (1) 205-221 (1987)

Hohman et. al. Phys. Fluids, 13, 2201-2220 (2001)

Huneiti et. al. IEEE 31th IAS Annual Meeting, San Diego, Vol 3, p p 1768 1774. (1996)

Ishida,et. al. Japanese Journal of Applied Physics, Vol. 47, No. 6, pp. 5281-5286 (2008)

Jaworekand Krupa,J. Aerosol Sci. 30 (7), 873-893 (1999).

Jaworek, Powder Technology, 176, 18–35 (2007)

Jaworek andKrupa, Exp. Fluids, 27 (1), 43-52 (1999)

Jaworek, et. al. Czech, T. Bulletin of the Polish Academy of Sciences – Technical Sciences, 57 (1), 63-70 (2009)

Jeonget. al. Langmuir 27 3144–9 (2011)

Jung, et. al. Japanese Journal of Applied Physics, 49, 5, 05EB03-05EB03-5 (2010)

Juraschek andRollgen, Int. J. Mass. Spectrom., 177 ,1–15. (1998)

Kang et. al. Mater. Sci.-Mater. Electron. 21 1213–20 (2010)

Kawamoto, Proc. of International Conference on Digital Printing Technologies and Digital Fabrication, pp. 961-964 (2007)

Khan et. al. Applied Physics A: Materials Science & Processing, 104 (4), 1113-1120, (2011)

Kim et. al. Mater. Manuf. Process. 26 1196–201 (2011)

Kimand Lee, Int. J. Precis. Eng. Manuf., Vol. 12, No. 1, pp. 161-164, (2011)

Kim et. al. Mater. Manufac. Process., 26 (9), 1196-1201 (2011)

Kim et. al. Journal of Aerosol Science, Vol. 39, No. 9, pp. 819-825 (2008)

Kim et. al. Analytical Chemistry, Vol. 82, No. 5, pp. 2109-2112 (2010)

Kim et. al. J. Micromech. Microeng., 20, 55009 (2010)

Korkut et. al. Langmuir, 24, 12196- 12201 (2008)

Korkut et. al. A. Phys. Rev. Lett., 100 (3), 034503 (2008)

Krpoun and Shea, J. Micromech. Miroeng., 19, 045019-045028 (2009)

Kuil et. al. Journal of Biotechnology, Vol. 1, No. 9, pp. 969-975 (2006)

Law et. al. R. Anal. Chem., 82, 4494-4500 (2010)

Le, The Journal of Imaging Science and Technology, 42, 1, 49-62 (1998)

Lee et. al. Appl. Phys. A 82 671–4 (2006)

Lee, ISBN 0-8493-1559-X, Florida USA (2003)

Lee et. al. Applied Physics Letter 93, 243114 (2008)

Liand Zhang, Journal of Electrostatic, Vol. 67, No. 4, pp. 562-567, (2009)

Li, Journal of Electrostatic, Vol. 65, No. 12, pp. 750-757 (2007)

Li, Journal of Electrostatic, Vol. 65, No. 4, pp. 251-255 (2007)

Li et. al. J. R. Soc. Interface, 5 (19), 253-257 (2008)

Ling and Bao, Chem. Mater. 16, 4824-4840 (2004)

Margineanet. al., Phys. Rev. Lett. 97, 064502 (2006)

Menard E., Meitl M.A., Sun J., Park J.U., Jeon S., Nam Y., Rogers J.A. Chem. Rev. 107, 1117 (2007)

Muhammad et. al. Current Applied Physics, 11 (1), 68-75 (2011)

Nuret. al. J. Mater. Sci.-Mater. Electron. 13 213–9 (2002)

Oh et. al.Aerosol Science, 39, 801-813 (2008)

Ohigashiet. al., Journal of Microelectromechanical Systems, 17 (2) (2008) .

Parashkovet. al. Proceedings of IEEE, 93, 1321-1329 (2005)

Park et. al. Thin Solid Films 515 7706–11 (2007)

Park et. al. Nature Materials, 6, 782-789 (2007)

Park et. al. Nano Letters, 8 (12), 4210-4216 (2008)

Perelaeret. al. Nanotechnology, 20, 165303 (2009)

Pique andChrisey, ISBN 978-0121742317, San Diego, USA (2001)

Poon et. al. Applied Physics Letters , 93 (133114) (2008)

Poon, PhD Thesis, Princeton University **(2002)**

Raghunath, et. al.Biotechnol. Appl. Biochem.**,** 52, 1-8 (2009)

Rahman et. al. Int. J. Prec. Eng. Manufac., 12 (4), 663-669 (2011)

 Rayleigh, Theory of Sound (New York: Macmilllan and Co.) (1896)

Rulisonaand Flagan, Rev. Sci. Instrum. 64 (3), (1993).

Sanauret. al. Organic Electronics, 7, 423-427 (2006)

Saville, Journal of Fluid Mechanics, 8 (4) (1971) 815-827.

Saville, Physics of Fluids, 13, 2987-2994. (1970)

Saville, Physics of Fluids 14, 1095-1099 (1971)

Shimoda,et. al. Nature, 440, 783–786 (2006)

Sirringhaus, et al. Science, 290, 2123-2126 (2000)

Smith, IEEE. Trans. Ind. Appl., IA-22 (3), 527–535 (1986)

Stachewicz, et. al. Journal of Physics: Conference Series, Vol. 142, No. 1, pp. 012043-012046 (2007)

Stachewicz et. al. Applied Physics Letters, Vol. 95, No. 22, Paper No. 224105 (2009)

Stachewicz et. al. Langmuir, 25, 2540- 2549. (2009)

Stachewicz et. al.Microfluid. Nanofluid. 9, 635-644. (2010)

Stringer and Derby, Langmuir, 26 (12), 10365–10372 (2010)

Stutzmann et. al. Science, 299, 1881-1885 (2003)

Szczechet. al. IEEE Transactions on Electronics Packing Manufacturing, 25, 26-33 (2002)

Tatemoto et. al.Chem. Eng. Technol., 30, (9) 1274-1279 (2007)

 Taylor, Royal Soc Series A MathematPhysSci280 (1382) 383-397 (1964)

Tran et. al.Journal of Electrostatics xxx. 1-7, (2009)

Umezu et. Al.Proc. Of International Conference on Digital Printing Technologies, 22, 66-68 (2006)

Vela et. al. Journal of Microelectromechnical System, Vol. 15, pp. 1272-1280 (2006)

Wang et. al. Appl. Phys. Lett. 88, 133502 (2006)

Wangand Stark, Journal of Nanoparticle Research, Vol. 12, No. 3, pp. 707-711 (2010.)

Wang and Stark, Appl. Phys. A: Mater. Sci. Process., 99, 763-766 (2010)

Wang et. al. Journal of Applied Physics, 106, 024907 (2009)

Xu et. al. Langmuir, 27 (10), pp 6541–6548 (2011)

Yang et. al. IEEE Transactions on Microwave Theory and techniques, vol. 55, no. 12 (2007)

Yin et. al. Chin. Sci. Bull. 55 3383–407 (2010)

Yudistira et. al.Appl. Phys. Lett., 96, 023503 (2010)

Zeleny, The physical review 3, 69-91 (1914)

Zeleny, The physical review second series 10(1) 1 1-7.

List of Related Publications

PUBLICATIONS (Book Chapter):

1. K.H. Choi, **K. Rahman,** N. M. Muhammad, A. Khan, K.R. Kwon, Y.H. Doh and H.C. Kim (2011). Electrohydrodynamic Inkjet – Micro Pattern Fabrication for Printed Electronics Applications, Recent Advances in Nanofabrication Techniques and Applications, Bo Cui (Ed.), ISBN: 978-953-307-602-7, InTech.

PUBLICATIONS (Journals):

1. **K. Rahman**, A. Khan, M.N. Muhammad, J. Jo and K.H. Choi, "Fine Resolution Patterning of Copper Nanoparticles through Electrohydrodynamic Jet Printing", Journal of Micromechanics and Microengineering, **22, (2012) 065012.**

2. **K. Rahman,** A. Khan, N.M. Nam, K.H. Choi and D.S. Kim, "Study of Drop-on-Demand Printing Through Multi-Step Pulse Voltage", International Journal of Precision Engineering and Manufacturing, **12(4) (2011) 663-669**.

3. K.H. Choi, **K. Rahman**, A. Khan, D.S. Kim, "Cross-talk Effect in Electrostatic Based Capillary Array Nozzles", Journal of Mechanical Science and Technology, **25 (12) (2012) 3053-3062**.

4. D.S. Kim, **K. Rahman**, A. Khan, and K.H. Choi, "Direct Fabrication of the Copper Nanoparticles Patterns through Electrohydrodynamic Printing in Cone-jet Mode", Materials and Manufacturing Processes **(DOI:10.1080/10426914.2012.663121– in press).**

5. **K. Rahman**, J.B. Ko, S. Khan, D.S. Kim and K.H. Choi, "Simulation of Droplet Generation Through Electrostatic Forces", Journal of Mechanical Science and Technology, **24(1) (2010) 307-310**.

6. K.H. Choi, A. Khan, **K. Rahman**, Y.H. Doh, D.S. Kim and K.R. Kwan, "Effects of Nozzles Array Configuration on Cross-Talk in Multi-Nozzle Electrohydrodynamic Inkjet Printing Head", Journal of Electrostatics, **69 (2011) 380-387.**

7. A. Khan, **K. Rahman**, M.T. Hyun, D.S. Kim and K.H. Choi, "Multi-Nozzle Electrohydrodynamic Inkjet Printing of Silver Colloidal Solution for the

Fabrication of Electrically Functional Microstructures", Applied Physics A: Material Science and Technology, **104 (2011) 1113–1120.**

8. D.S. Kim, A. Khan., **K. Rahman**, S. Khan, H.C. Kim and K.H. Choi, "Drop-on-Demand Direct Printing of Colloidal Copper Nanoparticles by Electrohydrodynamic Atomization", Materials and Manufacturing Processes, **26(9) (2010) 1196-1201.**

9. A. Khan, **K. Rahman**, D.S. Kim, and K.H. Choi, "Direct printing of copper conductive micro-tracks by multi-nozzle electrohydrodynamic inkjet printing process", Journal of Materials Processing Technology **212 (2012) 700-706.**

10. K.H. Choi, M. Mustafa, **K. Rahman**, J.B. Ko and Y.H. Doh, "Cost-effective Fabrication of Memristive Devices with ZnO Thin Film using Printed Electronics Technologies" Applied Physics A: Materials Science & Processing **(DOI 10.1007/s00339-011-6670-z).**

11. A. Rahman, A. Ali, **K. Rahman**, H.C. Kim, Y.H. Doh, D.S. Kim, and K.H. Choi "Influence of Electrode Position and Electrostatic Forces on the Generation of Meniscus in Dielectric Ink", Japanese Journal of Applied Physics, **49 (2010) 05EC02.**

12. K.H. Choi, A. Ali, A. Rahman, N. M. Mohammad, **K. Rahman**, A. Khan, S. Khan and D.S. Kim, "Electrode configuration effects on the electrification and voltage variation in an electrostatic inkjet printing head", Journal of Micromechanics and Microengineering, **20 (7) (2010) 075033.**

PUBLICATIONS (Conferences):

1. **K. Rahman**, J.B. Ko, S. Khan, K.H. Choi and D.S. Kim, "Simulation of Droplet Generation Through Electrostatic Forces", The 3rd International Conference on Manufacturing, Machine Design and Tribology, Jeju Island, South Korea, July 2009.

2. **K. Rahman**, A. Rahman, A.A. Gohar, S. Khan, J.B. Ko and K.H. Choi, "Analysis of Electro-Static Drop-on-Demand Patterning of Conductive Lines and CNTs for Printed Electronics Applications", Large-area, Organic and Printed Electronics Convention, Frankfurt, Germany, June 2009.

3. **K. Rahman**, K.H.Choi and D.S. Kim, "Multiphysics Numerical Simulation of Drop Generation Through Electrostatic Force", The 1st International Symposium on Hybrid Materials and Processing, Busan, South Korea October 2008.

4. K.H. Choi**, K. Rahman** and D. S. Kim, "Simulation of Ejection of Silver Nano-Particles Through Electrostatic Forces", The 5th International Conference on Advanced Materials and Processing, Harbin, China, September 2008.

5. K.H. Choi, **K. Rahman**, and D.S. Kim, "Simulation of drop-on-demand electrostatic inkjet printing for printed electronics", Asia-Pacific Conference On Transducers and Micro-Nano Technology, Tainan, Taiwan, June 2008.